社 団 法 人

日本造船研究協会報告

第 25 号

昭和 34 年 3 月

船舶の波浪中における復原性に関する研究 ……第 17 研究部会

Investigations on the Stability of Ships in Rough Seas

…… The 17th Research Committee

The Report

of the

Shipbuilding Research Association

of Japan

Tokyo, JAPAN

No. 25

March 1959

第 17 研究部会委員名簿

委員長	加藤　弘	顧問	横山　渉
幹事	井上正祐	内田　守	佐藤美津雄
	桝田吉郎	真鍋大覚	元良誠三
	山内保文		
委員	秋葉芳雄	荒稲蔵	伊田力
	泉晃	出淵巽	岩田秀一
	稲村桂吾	内田勇	菅四郎
	川島栄一	蒲田利喜蔵	木下昌雄
	北川次郎	桑野研一	見学道彦
	小柳雅志郎	佐藤正彦	佐藤茂
	佐野桂	志波久光	篠田寅太郎
	篠原資八	菅井和夫	杉田松次
	首藤保文	高橋幸伯	谷口中
	田宮真	田崎亮	土田陽
	土田達夫	塚本裕四郎	富武満
	遠山伝蔵	中西久	中田富次郎
	永島雄吉	原田久明	原田敏
	埴田清勝	林達夫	橋本進
	菱田敏男	牧山幸弥	松本武一
	水品政雄	山県彰	山県昌夫
	山上直人	横田利雄	渡辺恵弘
	渡辺俊道		

Membership of the 17th Research Committee

Chairman	Hiroshi KATŌ	Adviser	Wataru YOKOYAMA
Secretaries	Masasuke INOUE	Mamoru UCHIDA	Mitsuo SATŌ
	Yoshirō MASUDA	Taikaku MANABE	Seizō MOTORA
	Yasuhumi YAMANOUCHI		
Members	Yoshio AKIBA	Inezō ARA	Chikara IDA
	Akira IZUMI	Tatsumi IZUBUCHI	Shuichi IWATA
	Keigo INAMURA	Isamu UCHIDA	Shirō KAN
	Eiichi KAWASHIMA	Rikizō KAMATA	Masao KINOSHITA
	Jirō KITAGAWA	Kenichi KUWANO	Michihiko KENGAKU
	Masashirō KOYANAGI	Masahiko SATŌ	Shigeru SATŌ
	Kei SANO	Hisamitsu SHIBA	Toratarō SHINODA
	Sukehachi SHINOHARA	Kazuo·SUGAI	Matsuji SUGITA
	Yasuhumi SUDŌ	Kōhaku TAKAHASHI	Kaname TANIGUCHI
	Makoto TAMIYA	Riyō TAZAKI	Kiyoshi TSUCHIDA
	Tatsuo TSUCHIDA	Yushirō TSUKAMOTO	Takemitsu TOMI
	Denzō TOYAMA	Hisashi NAKANISHI	Tomijiro NAKATA
	Yūkichi NAGASHIMA	Hisaaki HARADA	Takashi HARADA
	Kiyokatsu HANITA	Tatsuo HAYASHI	Susumu HASHIMOTO
	Toshio HISHIDA	Kōya MAKIYAMA	Buichi MATSUMOTO
	Masao MIZUSHINA	Akira YAMAGATA	Masao YAMAGATA
	Naoto YAMAGAMI	Toshio YOKOTA	Yoshihiro WATANABE
	Toshimichi WATANABE		

CONTENTS

Introduction

1. History

There have been a number of attempts to developing an adequate standard of stability of ships so that they can withstand the sea conditions they may encounter during their service, with a view to protecting them against the casualties caused by the insufficient stability and at the same time preventing them to have surplus stability which often necessitate the adoption of such uneconomic forms of the ship as may cause the deterioration of ship's speed, operation efficiency, etc. Though, however, the necessity to establishing the standard of stability has long been recognized, definite conclusion has not been arrived at up to the present.

This may be due to the fact that little progress has been made as to the investigations of sea conditions the ship may encounter, particularly waves and winds in stormy weather, as well as that few experiments in a large scale have been carried out to measure the actual ship motion when they are running among waves and winds in stormy weather. Such experiments would not be accomplished without enormous amount of funds and joint work of experts under a large organized body.

In 1953, the Japanese Ministry of Transportation planned to make a thorough revision of the Ship Safety Law in the light of various circumstances. In particular regarding the stability, they decided on a policy to establish a standard of stability with a view to legislating it, and in 1953 took their first step to developing the standard of stability for small ships of less than 5 tons gross. In September, 1953, when they finished to draw up a draft for this standard, they subsequently took to make out the standard for ships engaged in coasting service or more which possibly encounter stormy weather.

As mentioned in the foregoing, however, in order to clarify the stability of ships, comprehensive investigations by a large organized body is necessary. In 1954, therefore, the 17th research committee, consisting of the members listed in the foregoing part, was organized in the Shipbuilding Research Association of Japan, and subsidized by the Ministry of Transportation, they conducted various kinds of investigation for subsequent 3 years.

On the other hand, the activities of the Ministry of Transportation

toward the revision of the Ship Safety Law were unexpectedly progressed. In January 1954, a draft for the standard for ships engaged in smooth water service was drawn up, and in June 1955 a draft for ships engaged in coasting service or more was completed. Through reviews from various angles, both standards were put into force from February 1st, 1957. During the period, the interim results of the investigations undertaken by this research committee were adopted to the draft of the standard whenever they were obtained, thus their work acted as a driving force to draft the standard.

This investigation, participated by a number of experts, took 4 years until its completion including the time for the analysis and the preparation of the report. The complete text of the report is voluminous, exceeding 1,000 pages. but owing to limited space, this pamphlet merely refers to the outline of the investigations.

PART I

Investigation into the Damping Coefficient of Rolling

Chapter 1 Effect of Bilge Keels upon Actual Ships

This chapter refers to the results of a series of rolling experiments conducted as to ships both with and without bilge keels in order to examine the effect of bilge keels upon actual ships.

For this purpose bilge keels were newly attached in several ships and moreover the sizes of bilge keels were varied in two ships. The experiments also included those for three ship in which, by making them roll over 10 degrees, damping angles were measured.

1.1 Rolling Experiments on 23 m Type Coast Guard Ships both with and without Bilge Keels.

1) Particulars.

Item	Loa	Lpp	B	D	d	Rise of floor	Bilge circle
Actual ship	23.000 m	22.000 m	4.600 m	2.400 m	0.947 m	0.500 m	0.710 m
Model ship	2.091	2.000	0.418	0.218	0.086		

2) Conditions (without bilge keels).

Item Name of the ships	Displacement	Mean draft	Trim	GM	Period of roll
Akizuki	57.90 t	1.360 m	0.400 m	1.258 m	3.44 sec
Fuyuzuki	51.00	1.260	0.450	1.464	3.42
Mochizuki	52.90	1.338	0.560	1.212	2.90
Yamazuki	62.43	1.410	0.688	1.124	3.41
Okinami	48.87	1.245	0.550	1.355	3.33
Isonami	56.00	1.340	0.365	1.234	3.42
Model ship	37.10 kg	11.450 cm	4.090 cm	13.310 cm	1.032

(with bilge Keels)

Item Name of the ships	Displacement	Mean draft	Trim	GM	Period of roll	Size of the bilge keels
Akizuki	58.00 t	1.360 m	0.405 m	1.147 m	3.500 sec	6.800×0.30m
Fuyuzuki	52.43	1.271	0.487	1.398	3.600	Do.
Mochizuki	55.80	1.345	0.585	1.126	3.410	Do.
Yamazuki	58.83	1.368	0.610	1.235	3.420	Do.
Okinami	53.37	1.295	0.500	1.305	3.530	Do.
Isonami	56.90	1.355	0.400	1.218	3.500	Do.
Model ship	38.43 kg	11.550 cm	4.420 cm	12.710 cm	1.086	

3) The Body plan and bilge keel are shown in Fig. 1.1.

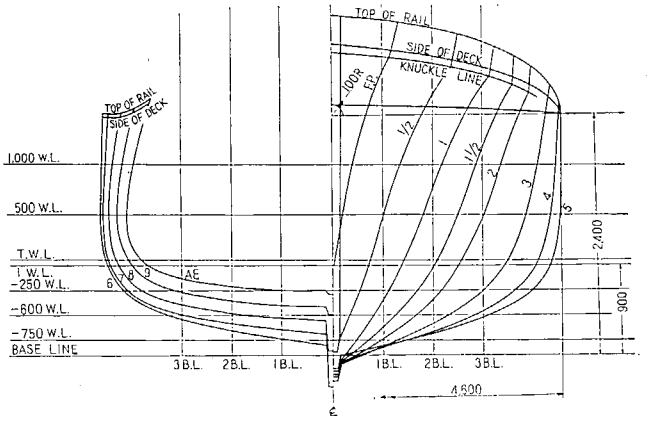

Fig. 1.1 (a)

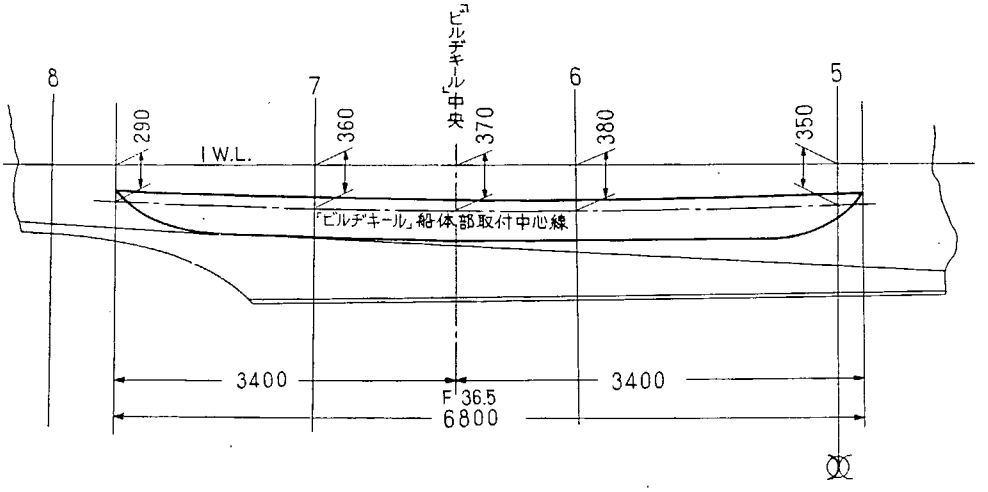

Fig. 1.1 (b)

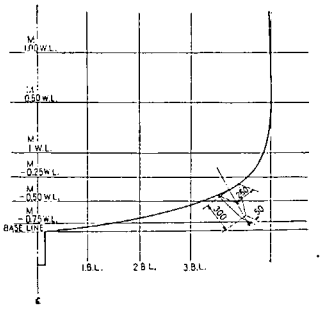

Fig. 1.1 (b′)

4) Results. The curves of extinction without bilge keels are shown in Fig. 1.2, and those with bilge keels are shown in Fig. 1.3.

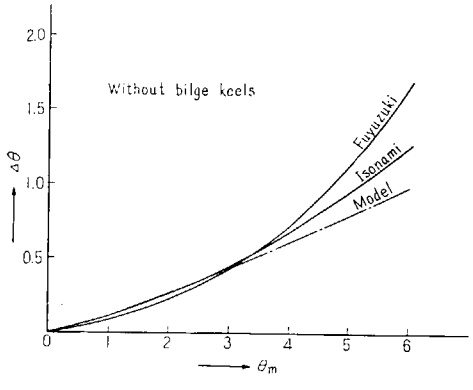

Fig. 1.2

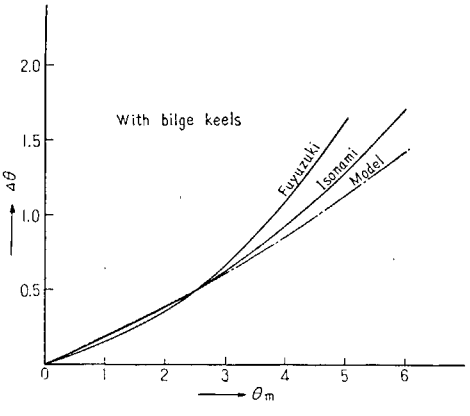

Fig. 1.3

1.2 Rolling Experiments on a Passenger Ship U-Maru.

In this case, the experiments were done on the occasion of a reformation of bilge keels from small size to a large size.

1) Particulars.

Item	Loa	Lpp	B	D	d	Rise of floor	Bilge circle
Actual ship	62.350 m	57.000 m	9.300 m	4.300 m	3.000 m	0.500 m	1.800 m
Model ship	2.188	2.000	0.326	0.151	0.105	0.017	0.063

2) Conditions.

Item	Displacement	Mean draft	Trim	GM	Period of roll	Size of bilge keels
Before the bilge keels reformed	596 t	2.480 m	0.605 m	1.034 m	7.86 sec	23.40×0.35 m
After the bilge keels reformed	619	2.540	0.720	1.128	7.74	25.80×0.65 m

3) Results. The curves of extinction of both before and after the reformation of the bilge keels are shown in Fig. 1.4, in which block lines show those for the actual ship while chain lines show those for the model.

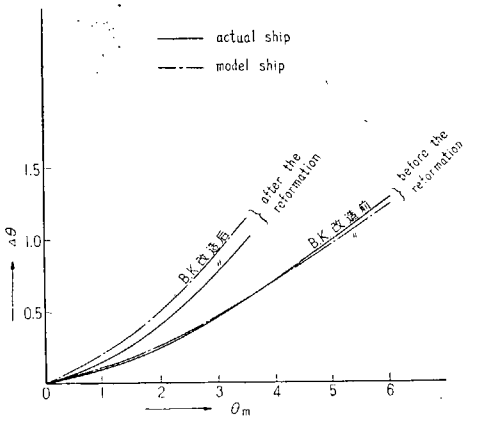

Fig. 1.4

1.3 Rolling Experiments on a Passenger Ship O-Maru.

This experiment was done to get the curve of extinction through large angle.

1) Particulars.

Item	Loa	Lpp	B	D	d	Rise of floor	Bilge circle
Actual ship	33.120 m	29.400 m	5.400 m	2.750 m	2.000 m	0.280 m	0.500 m
Model ship	2.253	2.000	0.367	0.187	0.135	0.019	0.034

2) Conditions (with bilge keels).

Item	Displacement	Mean draft	Trim	GM	Period of roll	Size of the bilge keels
Actual ship	185.100 t	1.955 m	1.53 m	0.201 m	9.030 sec	7.50×0.12 m
Model ship	52.236 kg	13.300 cm	10.40 cm	1.370 cm	2.355 sec	51.02×0.99 cm

3) Results. The curve of extinction both for the actual ship and the model are shown in Fig. 1.5, where the block line shows that of the model, and ·plots show those for the actual ship.

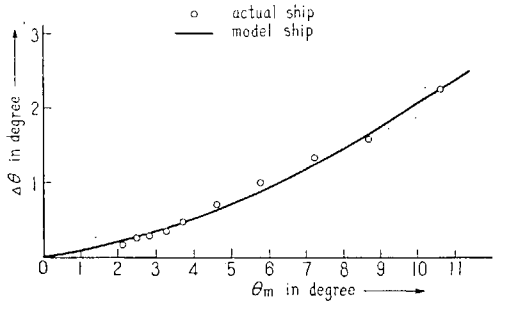

Fig. 1.5

1.4 Rolling Experiments on a passenger ship K-Maru.

The purpose of this experiment is the same as 1.3.

1) Particulars.

Item	Loa	Lpp	B	D	d	Rise of floor	Bilge circle
Actual ship	31.890 m	28.000 m	5.700 m	2.600 m	2.000 m	0.350 m	0.760 m
Model ship	2.200	2.000	0.393	0.179	0.138	0.024	0.052

2) Conditions.

Item	Displacement	Mean draft	Trim	GM	Period of roll	Size of the bilge keels
Actual ship	152.130 t	0.706 m	1.343 m	0.488 m	8.000 sec	11.66×0.23 m
Model ship	48.681 m	11.770 cm	9.290 cm	3.040 cm	2.100 sec	80.4×1.59 cm

3) Results. The extinction curve for both actual and model ships are shown in Fig. 1.6, where block line shows that of the model and plots show these for the model.

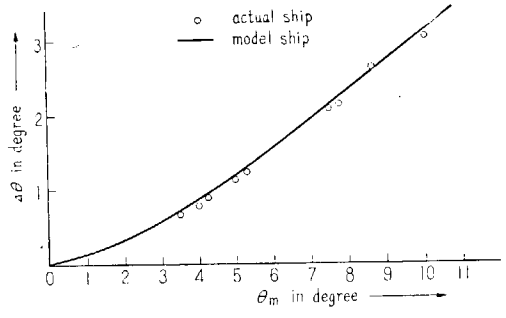

Fig. 1.6

1.5 Rolling Experiments on a Fisher boat.

The purpose of this experiment is the same as 1.3 and 1.4.

1) Particulars.

Item	Loa	Lpp	B	D	d	Rise of floor	Bilge circle
Actual ship	30.940 m	27.500 m	5.450 m	2.650 m	2.150 m	0.250 m	0.650 m
Model ship	2.250	2.000	0.396	0.193	0.156	0.018	0.047 m

2) Conditions.

Item	Displacement	Mean draft	Trim	GM	Period of roll	Size of the bilge keels
Actual ship	152.130 t	1.706 m	1.348 m	0.488 m	8.000 sec	11.66×0.23 m
Model ship	48.681 kg	11.770 cm	9.290 cm	3.040 cm	2.100 sec	80.4×0.15 cm

3) Results. The curves of extinction both for the actual ship and the model are shown in Fig. 1.7, where plots show those for the actual ship and the block line shows that for the model ship.

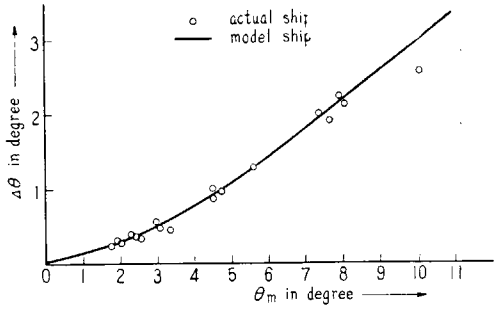

Fig. 1.7

1.6.1 The Effect of Bilge Keels.

Most of the investigations into the effect of bilge keels made in the past were based on the model experiment. Since, however, a lot of data on actual ships were obtained by this experiment, an attempt was made to develop a more specific method to estimate the rolling resistance of bilge keels.

For this purpose, bilge keels were fitted to a ship model of cylindrical form. As suggested by Bryan, the increase in the resisting moment of rolling due to fitting of bilge keels m was divided into the resisting moment of bilge keel plates themselves m_F and that due to the change of dynamical pressure acting to the ship's surface m_S, and as a first step both moments were measured separately. Then the approximate formula to estimate the latter was developed.

Nextly, the resisting moment of bilge keel plates themselves M_F was obtained by the rolling experiment of bilge keels of actual size, and thus the method to estimate the increase in the resisting moment for actual ship M was developed.

(1) Experiment as to ship model of cylindrical form.

Let the work-done of resisting moment in one roll :

a	a_F	a_S	in ship model,
A	A_F	A_S	in actual ship.

As it was difficult to measure a_s (dynamical pressure) directly, total work-done a and the work-done by bilge keels a_F were measured, and a_S was obtained as their difference. As to ship model, the models with 4 different bilge circles were used as shown in Fig. 1.8.

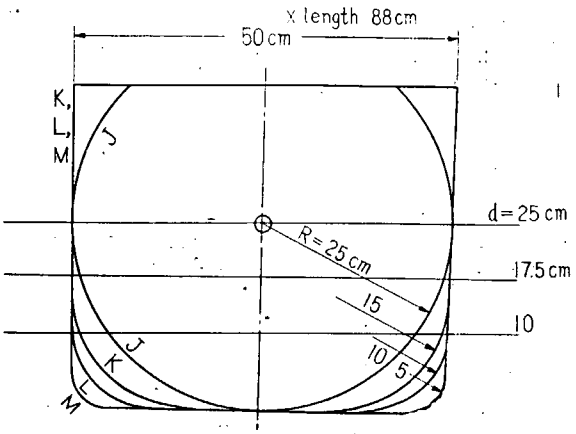

Fig. 1.8

The experiment was made as to conditions of 3 different draughts, 3 KG, 3 breadths of bilge keels and 3 rolling periods, thus aggregating to approximately 2,000 conditions as their combinations.

As a result of experiment, a_F was obtained as:

$$a_F = 5.23 \times 10^{-9} l \cdot b^{1.3} \cdot \theta_0^{2.46} \cdot T^{-1.8} \cdot r^{2.8} \quad \text{(in kg, cm, sec, deg.)}$$

where: r=Distance from the centre of gravity G to the centre of breadth of bilge keel.

θ_0=Rolling amplitude.

The followings are deduced from the above:

(a) a_F is almost independent of aspect ratio,

(b) a_F is almost independent of d, where $d > B/4$,

(c) Radius of bilge circle does not affect a_F appreciably.

On the other hand it was found that a_S was in fair consistency with the actual value when their distribution was assumed to be as given in Fig. 1.9

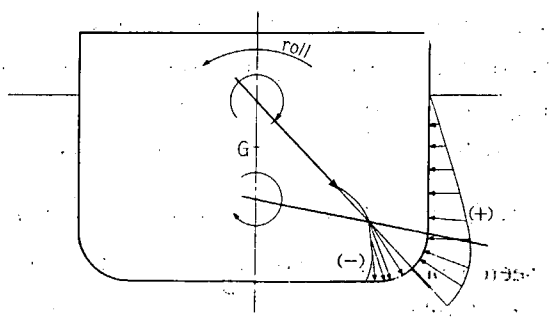

Fig. 1.9

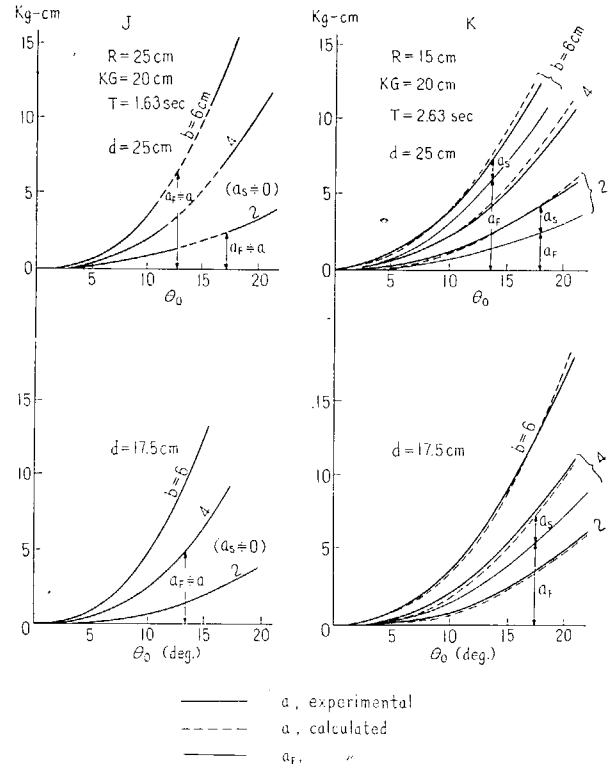

Fig. 1.10

and the pressure on the surface of bilge keel (at the direction of movement) was given by :

$$P_m = \frac{a_F}{2\theta_0 rbl}$$

Fig. 1.10 shows the comparison between measured and calculated values.

(2) Experiment as to bilge keels of actual size.

The bilge keels of actual size were fitted to the cylinder surface as shown in Fig. 1.11, and forced rolling was applied thereto. The work-done was obtained by measuring the applied force.

As a result the following formula was obtained.

$$A_F = 0.384 b \cdot l \cdot \theta_0^{2.5} \cdot T^{-1.6} \cdot r^{2.6} \quad \text{(in m, kg, sec, deg.)}$$

It may be seen from the above formula that A_F is proportional to :

(a) The area of bilge keel plates,

(b) 1.6-th power of the absolute velocity of bilge keel.

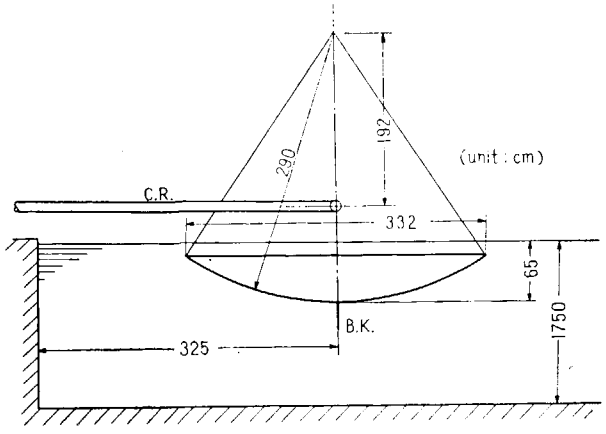

Fig. 1.11

(3) Application to actual ships.

As A_F for actual bilge keel has been obtained by the foregoing analysis, let us now estimate A by adding a_S in the same way as in the case of ship model.

The results are exemplified in Figs. 1.12 and 1.13. Fig. 1.12 indicates the results for Revenge, and 1.13 for passenger ship of 800 tons gross (U-Maru) on which the experiment was carried out. As Fig. 1.13 was the case where the size of bilge keels was varied, the differences between the total extinction angles obtained by the experiment and the extinction angles for bilge keels alone were computed. These are as shown in ①—② and ③—④ respectively, which coincide well with the calculated value ④.

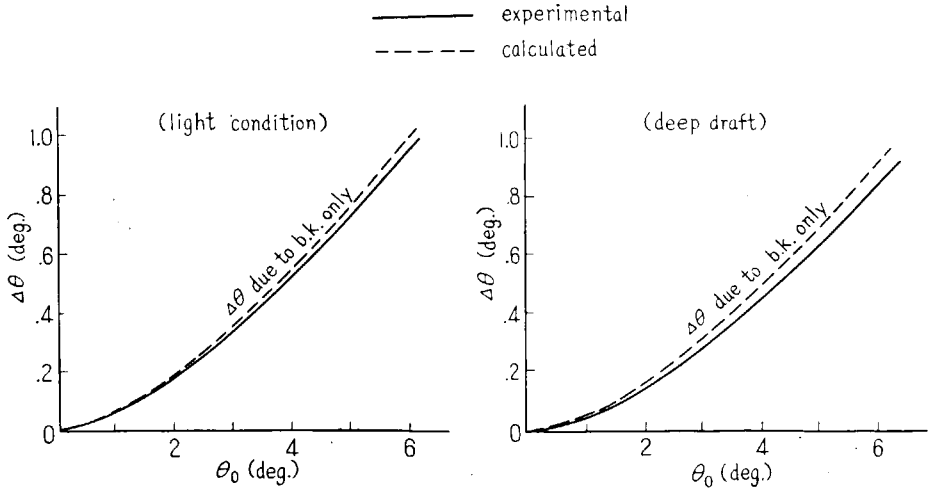

Fig. 1.12

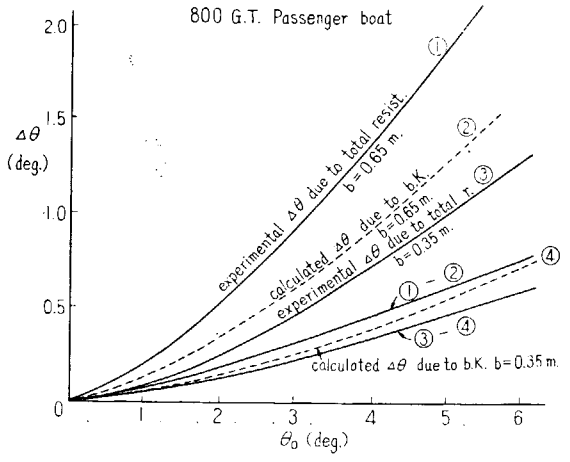

Fig. 1.13

1.6.2 Law of Similarity.

In the investigations of the rolling of ships, we must base to some extent upon the results of experiments conducted by small model even in case of theoretical investigations. Accordingly, in applying these results to actual ships, consideration of scale effect would be required.

In considering a scale effect, the characteristics of free rolling, in particular resistance against rolling, is important. In conducting rolling experiment as to two ships of different size but geometrically similar form, it is necessary to carry out the experiment according to the Froude's law, i.e. $T_s \propto \sqrt{L}$. In order that there exists no scale effect between these two ships, extinction coefficient should be equal.

Although discussions have been made as to which resistance, wave-making, eddy-making or frictional, affects the extinction coefficient most appreciably, it would be difficult to give a definite conclusion to this problem. Of these resistances, however, it would be sufficient to consider the frictional resistance. The different Reynold's number causes the different value of the frictional resistance, and whether or not the scale effect may be neglected would be determined according to the proportion of frictional resistance to the total resistance. Accordingly, fitting of bilge keel has close connection with the scale effect.

Fig. 1.14 and 1.15 indicate the results of experiments conducted with round- and box-shaped models of 0.9 m and 1.8 m in length. It may be noted from these figures that scale effect is conspicuous in models without bilge keel,

while it is slight in box-shaped model with bilge keel and almost inappreciable in round-shaped model with bilge keel. As the form of actual ship is the midway between those of the above two models, scale effect is considered very small, though it might be perceptible in case of rolling of small angle.

Nextly, in order to examine the scale effect between actual ships and the model, rolling test for actual ship is necessary. Figs. 1.16, 17, 18, 19 and 20 show the comparison of N-coefficient between models (2 m in length) and actual ships. N is almost coincidental except in case of rolling of small angle, and therefore the scale effect is considered negligible.

In Fig. 1.20, however, which shows the results of experiment in small angle, scale effect can be recognized. In this case, increase in the resistance

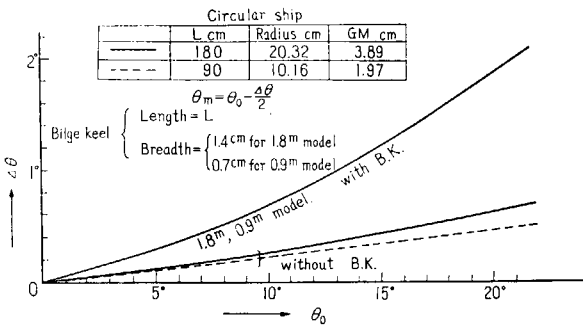

Fig. 1.14

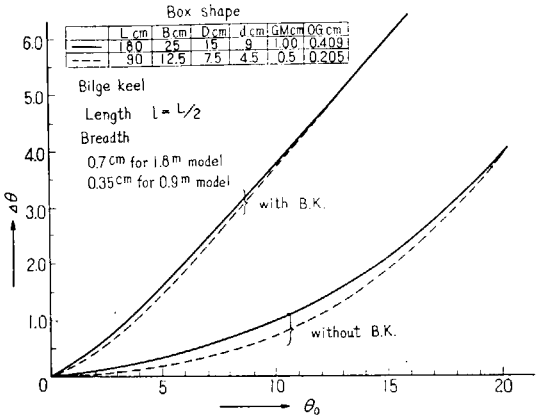

Fig. 1.15

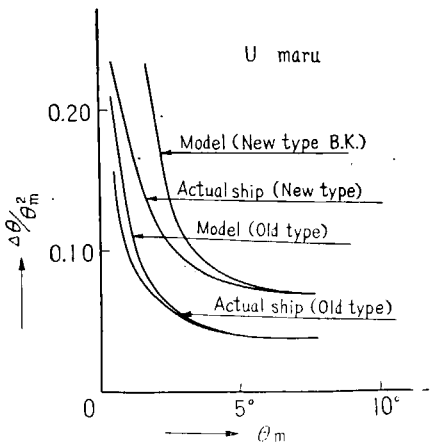

Fig. 1.16

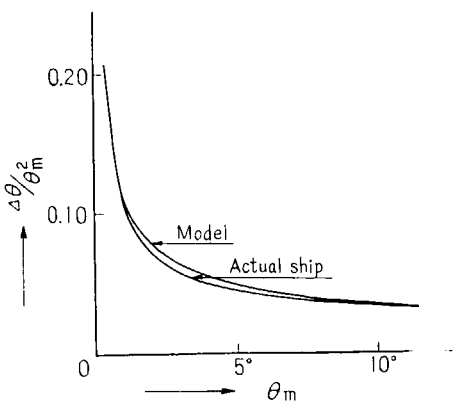

Fig. 1.17

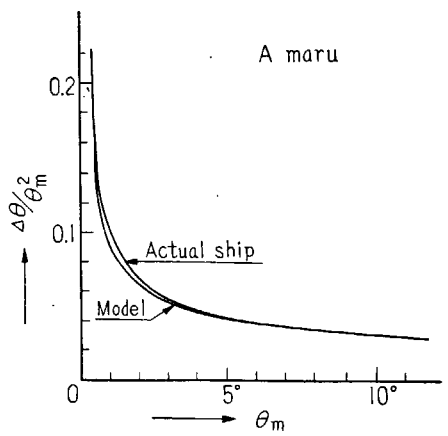

Fig. 1.18

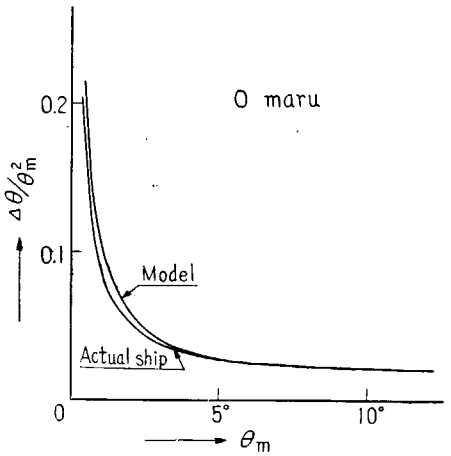

Fig. 1.19

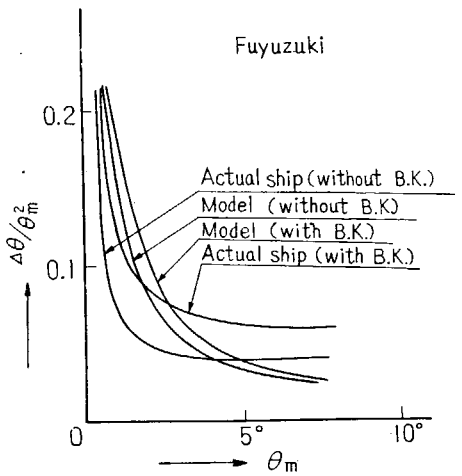

Fig. 1.20

due to bilge keel is small, i.e. N with bilge keel is 1.4 times N without bilge keel, as compared with the case of ordinary ships, in which the resistance would increase to 2.5 to 4 times. It is therefore considered that, if the resistance increases to about 2.5 times that in case of ships without bilge keel, scale effect can be neglected within the range of angles large enough to cause rolling of ship.

Chapter 2 Method of Estimation of the Extinction Coefficient of Rolling

2.1 General.

The estimation of the resistance against rolling of ships in still water is one of the important subject of the investigation of rolling, and it is usually attained by means of model experiment. If, however, it can be estimated by calculation, the determination or improvement of ship's form may be eased in the early stage of design, and moreover the investigations on the improvement of ships having insufficient stability may be expedited. In this paper, the investigation as to ships of ordinary form and having bilge keel is dealt with.

2.2 Ship's Form and Resistance against Rolling.

When an experiment is conducted as to ships having same form under waterline and different forms above waterline, that is, flare, wall-side and tumble home, it may be found that wall-sided ships have the smallest resistance and are in the safest side in the viewpoint of stability. We therefore consider in this paper the waterline form of wall-sided ship.

According to the investigations by Bertin and by Serat[1], the effect of rolling period of ship T_s, length L, breadth B, displacement W, metacentric height m, height of the centre of gravity, midship section coefficient, etc. upon the resistance against rolling has been clarified. As to the effect of fineness,

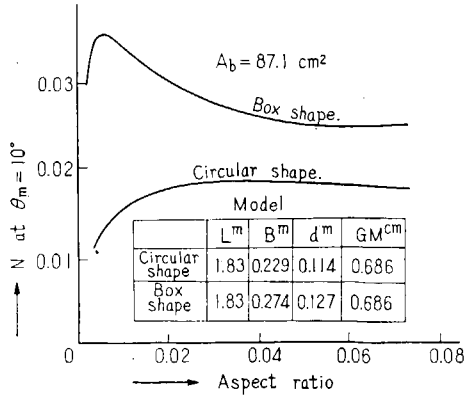

Fig. 1.21

1) M. E. Serat: "Effect of Form on Roll", T.S.N.A. & M.E., 1933.

it is known that in ships without kilge keel the resistance increases as the ship's form becomes full. On the other hand, it has been found that in ships with bilge keel the effect of aspect ratio of bilge keel (with constant area) upon the resistance is quite contrary between box- and round-shapes as shown in Fig. 1.21, and furthermore that the similar results can be obtained in the models of full cargo ship and of fine warship. It may be derived from the foregoing that, if the area of bilge keel is same, aspect ratio should be made small and the interference with the hull should be considered primarily in case of full ships, while aspect ratio should be made big and fin action should be considered primarily in case of fine ships.

In addition, it has been found that the resistance is proportional to the area of bilge keel Ab; the most favourable position of bilge keel along the girth of ship is the bilge part, and the resistance is the greatest at the position of the bilge keel slightly aftward from midship.

2.3 Development of Calculation Formula.

As shown in Fig. 1.22, if the ship is subjected to the water pressure on her sides and bottom proportional to the square of linear velocity when she rolls with an angular velocity $\dot{\theta}$ about the centre of gravity, the moment calculated from this water pressure becomes the resistance against rolling.

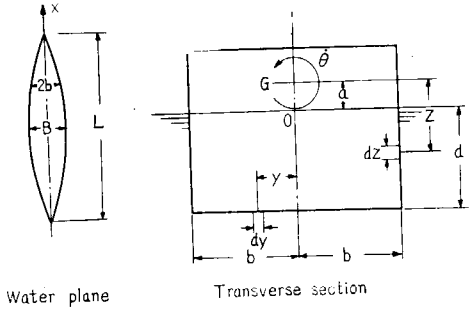

Fig. 1.22

Now, expressing the extinction curves by Bertin's form, i.e. $\Delta\theta = N\theta_m^2$, N is calculated as:

$$N = n\frac{Ld}{WmT_S^2}\left\{l^3\left(1+\frac{1}{4}\frac{d^2}{l^2}\right)+\frac{f(C_W)}{64}\frac{B^4}{d}\right\}$$

Where $\quad l = \frac{d}{2} + \overline{OG}$

$$f(C_W)=1-\frac{1}{m+1}+\frac{6}{2m+1}-\frac{4}{3m+1}+\frac{1}{4m+1}$$

$$m=\frac{C_W}{1-C_W}$$

C_W = Waterplane area coefficient.

As n relates to the area of bilge keel, aspect ratio and fineness, and is given by the linear function of Ab, it is expressed as:

$$n=n_0+\sigma\frac{d}{L}\frac{Ab}{L^2}$$

If Cb is taken as the value representing the fineness of ship, n_0 is considered as the function of Cb d/L, and σ as the function of Cb and the aspect ratio of bilge keel. The form of these functions can be determined from a series of model experiment, and their results are given in Figs. 1.23 and 1.24. These figures indicate the results where θm is 10°. Where $\theta m=20°$, it becomes:

$$n=n_0+\frac{2}{3}\sigma\frac{d}{L}\frac{Ab}{L^2}$$

On the other hand, observation as to the section of bilge keel has disclosed that no difference is seen where the bilge keel is of ordinary form.

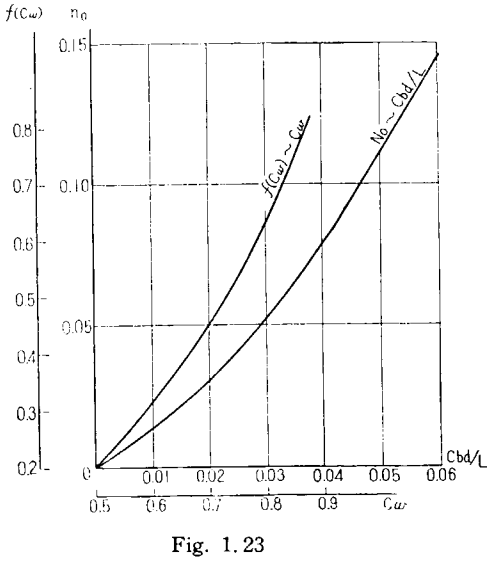

Fig. 1.23

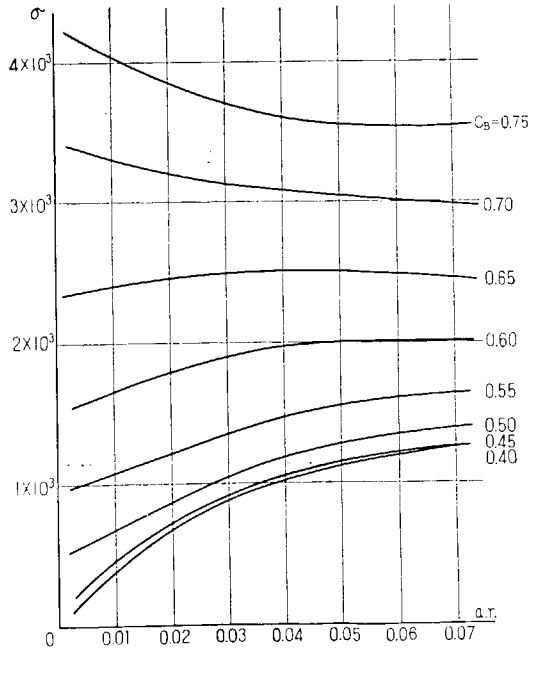

Fig. 1.24

Chapter 3 Damping Coefficient in the Inclination of Large Angle

3.1 Introduction.

The resistance against rolling is usually obtained from the decrease of rolling angle within one roll or damped angle. It is, however, impossible to obtain its value by this method when the ship rolls to the angle beyond the deck edge. On the other hand, in case of considering the capsizing of the ship, it is necessary to asses the value when the ship rolls beyond the deck edge. In this paper we attempted to obtain this value by forced rolling method.

3.2 Method of Experiment.

When the external rolling moment is applied to ship, the sum of the kinetic energy due to the inertia moment and the potential energy due to stability in one roll becomes zero, and therefore the energy of external moment supplied becomes equal to the energy dissipated as the damping resistance. When the simple harmonic motion caused by the shift of weight W applied through a pulley is transmitted to the ship, thus causing her rolling, work-done by the resistance of ship $R=2\alpha I\dot{\theta}+\beta I\dot{\theta}^2$ equals the work-done by the weight, that is:

$$Wh=\int Rd\theta=\frac{4\pi^2 I\theta_0^2}{T}\alpha+\frac{32\pi^2 I\theta_0^3}{3T^2}\beta$$

Accordingly, when α and β are estimated from the experiments carried out by varying W, extinction curve can be drawn as there is a known relation between the extinction a, b or N and α and β.

3.3 Results of Experiment.

The principal particulars of the models employed in the experiment are given in the following table.

	Hokuto Maru	Box-shaped Model I (without Bulwark)	Box-shaped Model II (with Bulwark)
Length	2.000 m	1.000 m	1.000 m
Breadth	0.321 m	0.250 m	0.250 m
Depth	0.219 m	0.188 m	0.188 m
Displacememt	46.060 kg	36.600 kg	36.850 kg
GM	0.0264 m	0.019 m	0.0175 m
Freeboard	0.103 m	0.033 m	0.032 m
Rolling Period	1.538 sec	1.378 sec	1.367 sec

Figs. 1.25, 1.26 and 1.27 illustrate the results of the experiment, indicating a fair consistency with the results in usual method. Until the deck edge immerges, N is kept constant or tends to decrease somewhat, while the resistance suddenly increases after the ship heels beyond the deck edge. The extinction curve is expressed by $\delta\theta = \lambda\theta_m^{1.7}$ before the deck edge immerges, and by $\delta\theta = \lambda\theta_m^{3.2}$ after the deck edge immerges, indicating the sudden increase of the resistance.

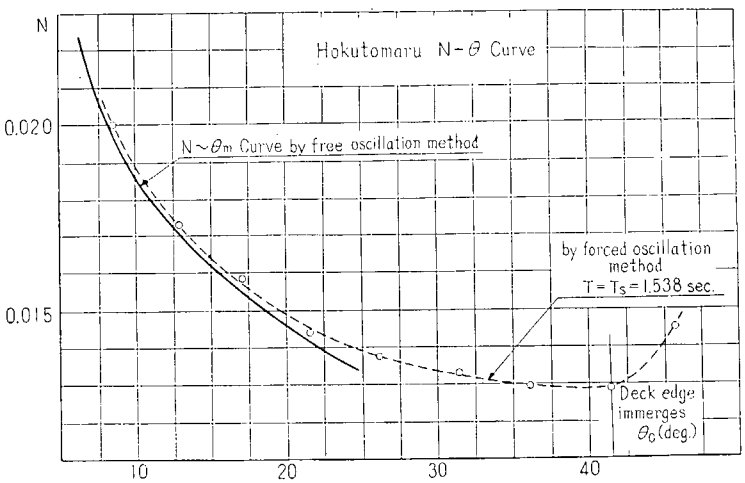

Fig. 1.25

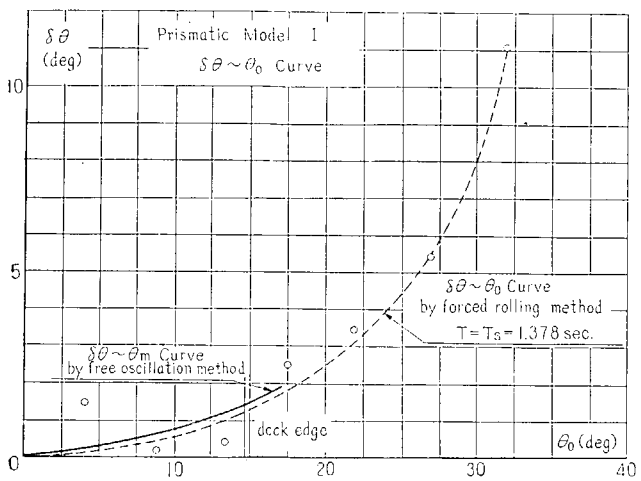

Fig. 1.26

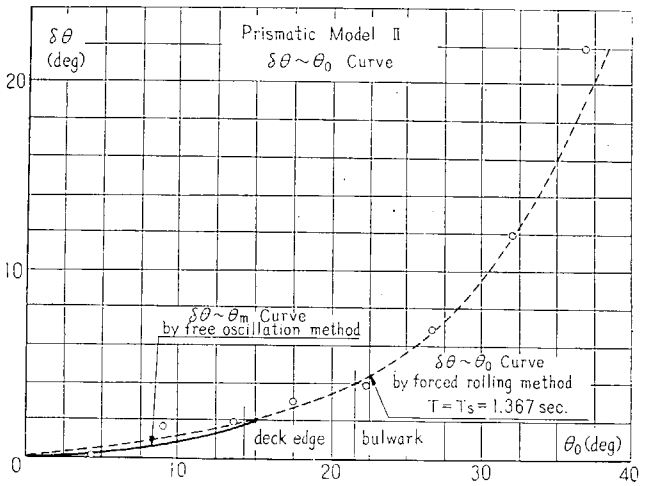
δθ
(deg)
Prismatic Model II
δθ~θ0 Curve
20
10
0
δθ~θm Curve
by free oscillation method
δθ~θ0 Curve
by forced rolling method
T=Ts=1.367 sec.
deck edge
bulwark
θ0(deg)
10
20
30
40

Fig. 1.27

PART II

The Heeling Moment due to the Wind Pressure

Chapter 1 Wind Pressure and Centre of it

In the discussion of the safty of a vessel at sea, the critically influential factor should be a heeling moment by the wind pressure as well as manoeuverability and dynamic stability of the vessel.

The series of wind tunnel experiments using models of three types of vessel, for the study on the effect by heeling angle of which was up to as large as 70°, were carried out, and results so obtained will be appeared hereinafter.

Types of vessels, used in the experiments, were three in all, one, of training ship "Hokuto Maru" who had often been selected as an actual ship for experimental study, in addition to two of small passenger vessel "Kogane Maru" and fishing boat "No. 5 Shinnihon Maru", for whom the experimental results of the effect of heeling angle up to only 30° in the previous experiment were already reported by Okada in 1952.

The study was made on two conditions of effect, with and without owning, for "Kogane Maru", and on two conditions of effect, with and without spanker to be occasionally used for the enhancement of manoeuverability for a fishing boat, and finally two conditions of effect with and without the on-the-deck fittings for training ship, namely on six conditions in total.

Following notations were used in analysis of the results obtained from the experiments.

V: Relative wind velocity (m/s)

ρ: Density of air ($kg \cdot s^2/m^4$)

ν: Coefficient of kinematic viscosity of air (m^2/s)

M: Heeling moment around the longitudinal centre of load water-plane ($m \cdot kg$)

R: Wind force (kg)

A: Longitudinal projected area of the above-waterpart of a model at the upright conditions (m^2)

θ: Heeling angle (plus mark means lee side heeling, minus mark means wind side heeling)

Wind force R and heeling moment M, as defined in the non-dimensional expression, can be obtained in coefficient by the following formulae ;

$$C_R = \frac{R}{\frac{1}{2}\rho A V^2}$$

$$C_M = \frac{M}{\frac{1}{2}\rho l V^2}$$

where l represents a height of the centre of the longitudinal projected area of the above water part, over the water level. Then C_R and C_M were plotted against the base of the heeling angle θ, using these we got empirical formula of R and M. (The curves of C_R and C_M were omitted for lack of space.)

C_R at the time of heeling angle equals to 0°, or coefficient of lateral resistance, is 1.0 to 1.2, and can be tabulated as Table 2.1, which gives the comparison of this experiment with that of previous ones, and shows a good coincidence with such results.

Table 2.1

Type of ship	Name of ship	(C)
Train-ferry (passenger)	Toya Maru	1.00
Train-ferry (trucks)	Kitami Maru	1.05
High speed cargo vessel	London Mariner	1.14
Oil tanker	San Gerardo	1.20
Atlantic liner	Mauretania	1.23
Cargo vessel	Nissei Maru	1.23
Tuna fishing boat	No. 5 Shinnihon Maru	1.33
Tuna fishing boat	No. 5 Shinnihon Maru	1.10
Small passenger vessel	Kogane Maru	1.19
Small passenger vessel	Kogane Maru	1.15
Tuna fishing boat	No. 5 Shinnihon Maru	1.14
Training ship	Hokuto Maru	1.17

In the term of C_M, it may be roughly unobjectionable to estimate that C_M is approximately 1.4 for any small passenger vessel with a seemingly rather large superstructure, being upright, and is 1.2 to 1.3 for any smaller fishing boat with rather small superstructure.

Plotting of D_W/h_0, the ratio of D_W, the height of the wind pressure over the water level experimentally measured, to h_0, the height of the centre of the broadside area when the vessel is upright condition, for every heeling angle, gives the curves in Fig. 2.1.

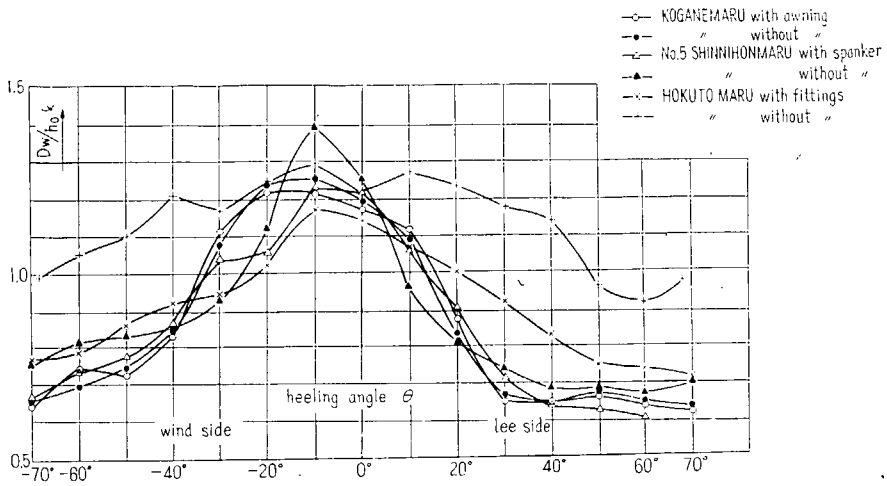

Fig. 2.1

Empirical formula, worked out from the results of the above, for the convenience of the calculation of R and M, other than D_W/h_0, which can be regarded as the most important factor, are as follows;

If heeling angle is given in degree, then for small passenger vessel and training ship,

$$R=\begin{cases}\rho V^2 A(0.553+0.00322\theta) & -70^\circ \leqq \theta \leqq 10^\circ \\ \rho V^2 A\{0.265+0.3\cos^2(15^\circ-1.5\theta)\} & 10^\circ \leqq \theta \leqq 70^\circ\end{cases}$$

$$M=\begin{cases}\rho V^2 Al\{0.2+0.465\cos^2(1.285\theta)\} & -70^\circ \leqq \theta \leqq 0^\circ \\ \rho V^2 Al\{0.2+0.465\cos^3(1.285\theta)\} & 0^\circ \leqq \theta \leqq 70^\circ\end{cases}$$

$$D_W/h_0=\begin{cases}1.27+0.545\sin\{1.285(\theta+5^\circ)\} & -70^\circ \leqq \theta \leqq -5^\circ \\ 0.647+0.623\cos(2\theta+10^\circ) & -5^\circ \leqq \theta \leqq 40^\circ \\ 0.647 & 40^\circ \leqq \theta \leqq 70^\circ\end{cases}$$

and, for fishing boat,

$$R=\begin{cases}\rho V^2 A)0.583+0.00322\theta) & -70^\circ \leqq \theta \leqq 10^\circ \\ \rho V^2 A(0.647-0.00322\theta) & 10^\circ \leqq \theta \leqq 70^\circ\end{cases}$$

$$M=\rho V^2 Al\{0.284+0.426\cos^3[1.285(\theta+5^\circ)]\} \qquad -70^\circ \leqq \theta \leqq 70^\circ$$

$$D_W/h_0=\begin{cases}1.27+0.545\sin[1.285(\theta+5^\circ)] & -70^\circ \leqq \theta \leqq -5^\circ \\ 1.222-0.0096\theta & -5^\circ \leqq \theta \leqq 50^\circ \\ 0.472 & 50^\circ \leqq \theta \leqq 70^\circ\end{cases}$$

Summary and result of the wind tunnel experiment using the ship models have been described precedingly in this paper, but, it should be noted that, needless to say, actual conditions on sea has varied factor which can never be

reproduced on the laboratory experiments, and that law of similarity between the model and the actual ship can not be strictly applicable, in regards to the details of structure, such as stanchion, funnel, rigging, mast and other deck installations and equipments.

In order to find out the effect of these installations and equipments, we tried out calculation for two types of vessels (one, small cargo and passenger boat, and another, large cargo boat) and we got the results that the amount of heeling moment due to wind pressure decreases on account of the roundness of their shapes.

Chapter 2 Investigation into the Centre of Water Pressure

In order to obtain the position of the centre of water pressure acting to the ship when drifting, the instrument as shown in Fig. 2.2 was used.

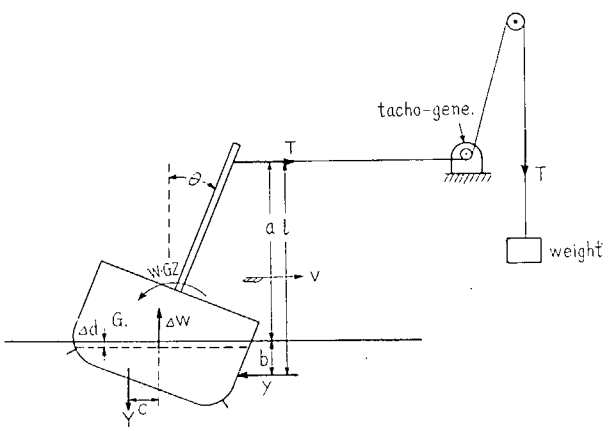

Fig. 2.2

It may be seen from this figure that a string was fixed at a proper position in the centre line of the ship, being pulled horizontally through a pulley and a weight was attached to the other end of the string. By changing the amount of the weight, the velocity of lateral drifting and the heeling angle of the ship can be varied.

On the other hand, as the lever of heeling moment can be estimated from the statical stability of the ship and the amount of weight, the distance from the position where the string is attached to the centre of water pressure can be obtained.

In Fig. 2.2, let X=horizontal force=T (tension of the string), Y=change of buoyancy due to the sinking or floating up of the ship, then we obtain as the balance of the moment:

$$W \cdot GZ(\theta - \theta_0) = Xl - Yc$$

as $l = a + b$, it follows:

$$X \cdot b - Y \cdot c = W \cdot GZ - Xa$$

If this moment is considered to be related to $X = T$ only, equivalent moment $T \cdot D_w'$ is assumed as:

$$D_w' = \frac{W \cdot GZ}{T} - a$$

Fig. 2.3 shows an example of D_w' obtained by the experiment. This is the case where bilge keels are fitted, and D_w' is plotted against heeling angles, C_b being taken as the parameter.

The results of this experiment indicate that the centre of water pressure rises apparently when the ship heels leeward and becomes even higher than the water line level when she heels to large angles. It may be seen from this fact that, though the ship heels as the wind pressure increases, the centre of water pressure rises remarkably when the ship heels beyond certain angle, causing the considerable decrease of the moment, and consequently the ship may not be easily capsized by the wind pressure only.

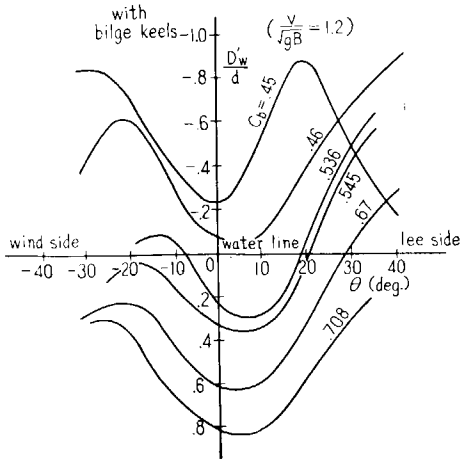

Fig. 2.3

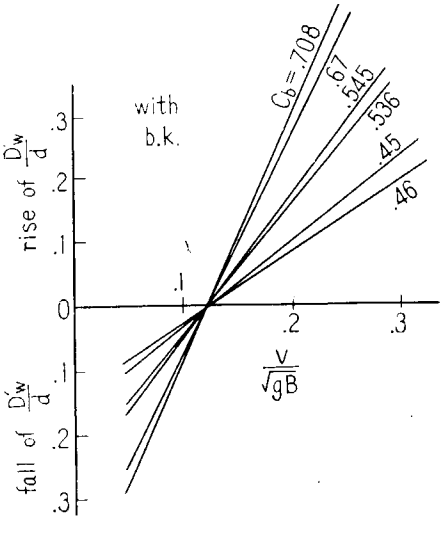

Fig. 2.4

On the other hand, the figure indicates that in ships with great C_b the centre of water pressure is low, and becomes higher as C_b decreases.

Nextly, let us consider the effect upon the velocity of lateral drifting. It may be seen from Fig. 2.4 that the centre of water pressure rises as the drifting velocity increases. It can be presumed from this fact that the increase in the wind pressure does not always result in the appreciable increase in the wind pressure moment.

Chapter 3 Summary of Observations regarding the Wind Pressure Moment

As a result of investigations mentioned in Chapters 1 and 2, an approach was made to the clarification of the wind pressure, and the position of its centre, and the centre of water pressure, which may be summarized as follows :

(1) The coefficient of resistance by lateral wind pressure C_b reaches the maximum value in the vicinity of $\theta=10°$ (windward heeling being taken positive) and decreases before and beyond that angle, but it can be regarded as constant within the range of $\theta=0°\sim25°$. In upright position C_b is $1.0\sim1.2$.

(2) The position of the centre of wind pressure is, on the contrary, the highest in the vicinity of $\theta=-10°$, and becomes lower before and beyond that angle. The position of the centre in upright condition is $15\sim25\%$ higher than that of the centre of gravity of the projected lateral area above water line.

(3) The position of the centre of water pressure is the lowest in the vicinity of $\theta=5°\sim10°$, and suddenly rises before and beyond that angle. It varies considerably according to the form of hull, but in general becomes lower as C_b increases. When bilge keels are fitted, the position of the centre slightly rises.

As the drifting velocity increases, the position of the centre rises almost linearly. The rate of rising increases as C_b increases, and is greater when bilge keels are fitted.

The comparison between the wind pressure moment obtained by summarizing the results mentioned in Chapter 1 and 2, and that estimated by usual method, that is, by (wind pressure) × (vertical distance between the centre of gravity of the projected lateral area below water line and that of the projected lateral area of wind pressure) is as shown in Fig. 2.5, where dotted and solid lines indicate the values estimated by usual method and those obtained by this

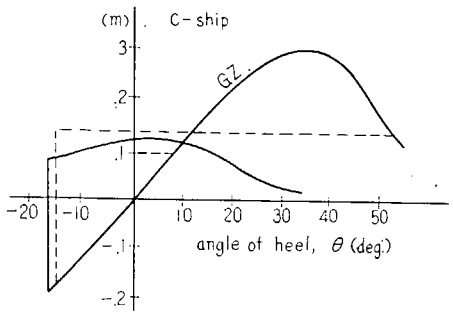

Fig. 2.5

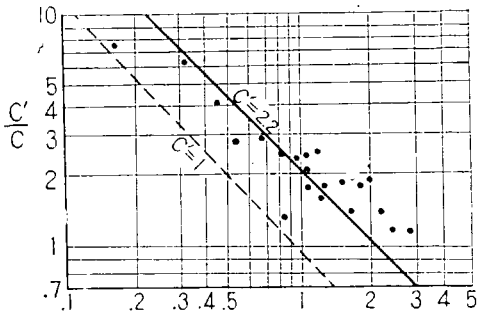

Fig. 2.6

experiment respectively. It may be seen from this figure that the wind pressure moment appreciably decreases when the ship heels to large angles.

Nextly, let us consider how the foregoing results affect the safety coefficient C (See Chapter 2, Part VI). In consequence with the decrease of wind pressure moment in large angles as compared with the results by usual method, the ship can stand against the wind velocity greater than usually considered; in other words, the degree of safety for the same wind velocity is greater.

The results of calculation as to several passenger ships are shown in Fig. 2.6, where C is the safety coefficient according to the standard of stability laid down by the Ministry of Transportation and C' is the C value estimated from the wind pressure moment obtained by this experiment. $C=1$ correspond to C' of about 2.2. It may, however, be needless to say that one can not come to a conclusion merely from this fact that the former standard was too severe.

On the other hand, when $C=1$ is taken as the criterion, it is very important whether or not ships of $C>1$, that is, ships conforming to the standard, and those of $C\leqq 1$, that is, ships not conforming to the standard, are divided into the same group as may be divided when $C'=2.2$ is taken as the criterion as equivalent to $C=1$. Fig. 2.6 indicates that ships of $C>1$ also lie within the range of $C'>2.2$. It can therefore be concluded that, if the new result based upon the wind pressure moment is adopted, the relative degree of safety for each ship remains same though the absolute value of the degree of safety changes.

PART III

Data on Ocean Waves and Wind in the North Pacific from a Marine Meteorological View Point and Their Analysis

1. Introduction.

This volume refers to the investigations on the characteristics of ocean wind and waves observed with a view to applying them to the standard of stability, and the analysis of the daily record registered for 36 years from 1920 to 1956 at 120 meteorological stations. In particular, the places which were considered important from the meteorological view point were visited by the author, and the pure characteristics of ocean wind were deduced by him, having regard to the geographical feature in the neighbourhood, long years' record of the self recordgraphs of Robinson and Dines anemometer and wind vane, barometer, thermometer, hygrometer, and of weather chart, weather book, etc. The locations of the observation stations are as shown in Fig. 3.1.

Based upon these data together with the records of coastal weather and by ships, a simple formula to enable to estimate the scale of ocean waves has been developed. In addition, a reference is made to the rolling of ship.

2. Characteristics of Ocean Wind and Wave in the North Pacific.

In the coastal sea of Japan, the growth or passage of typhoon is frequented and the wind forces are subject to increase and decrease repeatedly. After such a typhoon as shown in Fig. 3.2 passes through, prevailing wind to cold fronts often continues to blow for one day or thereabout. In the typhoon centre, therefore, violent and comfused "seas" are swirling, changing their force and direction constantly. The prominent ones among such "seas" grow to regular "swells" as they move radially from the typhoon centre to the outside of the typhoon area. And they become calm on a fine day before the next typhoon comes, and thus completely disappear.

3. Maximum Wind Velocity and Minimum Atmospheric Pressure.

The relation between the minimum pressure and the maximum velocity by Robinson anemometer at the typhoon centre is as given in Fig. 3.3. The

velocity of swirling air current in motion and the pressure distribution are expressed by :

$$u=u_m\frac{r}{a} \qquad P=P_m\exp\left[\frac{u_m^2}{2RT}\frac{r^2}{a^2}\right] \qquad 0\leqq r\leqq a$$

$$u=u_m\frac{a}{r} \qquad P=P_m\exp\left[\frac{u_m^2}{2RT}\left(2-\frac{a^2}{r^2}\right)\right] \qquad a\leqq r\leqq\infty$$

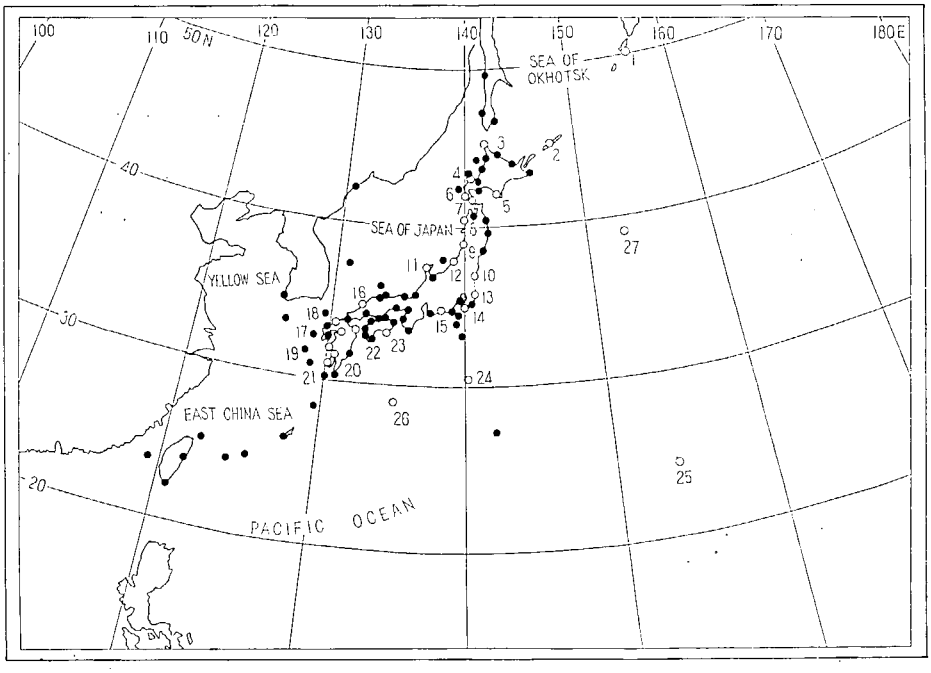

Fig. 3.1

No.	Station		No.	Station	
(1)	32—217	PARAMUSHIRU	(15)	655	OMAEZAKI
(2)	165	SYANA	(16)	755	HAMADA
(3)	47—401	WAKKANAI	(17)	806	SEBURIYAMA
(4)	421	SUTTSU	(18)	807	FUKUOKA
(5)	426	URAKAWA	(19)	823	AKUNE
(6)	428	ESASHI	(20)	827	KAGOSHIMA
(7)	430	HAKODATE	(21)	831	MAKURAZAKI
(8)	574	FUKAURA	(22)	815	ŌITA
(9)	587	SAKATA	(23)	899	MUROTOMISAKI
(10)	598	ONAHAMA	(24)	963	TORISHIMA
(11)	600	WAJIMA	(25)	91—131	MINAMITORISHIMA
(12)	604	NIIGATA	(26)		TANGO
(13)	648	CHŌSHI	(27)		X-RAY
(14)	673	TOMISAKI			

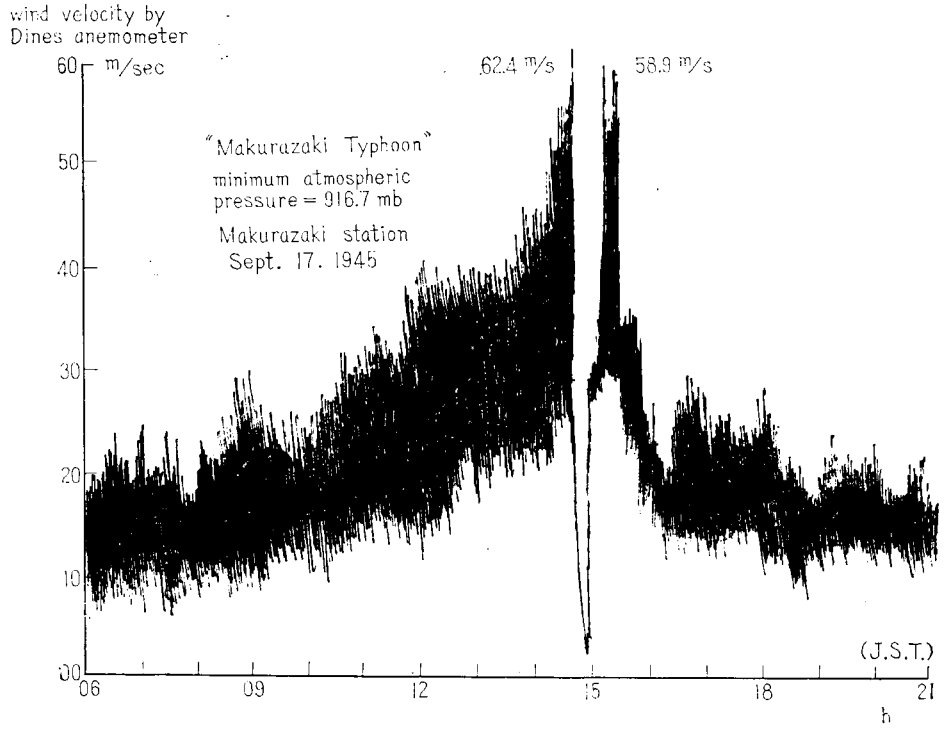
wind velocity by
Dines anemometer
m/sec
62.4 m/s
58.9 m/s
"Makurazaki Typhoon"
minimum atmospheric
pressure = 916.7 mb
Makurazaki station
Sept. 17. 1945
(J.S.T.)
h

Fig. 3.2

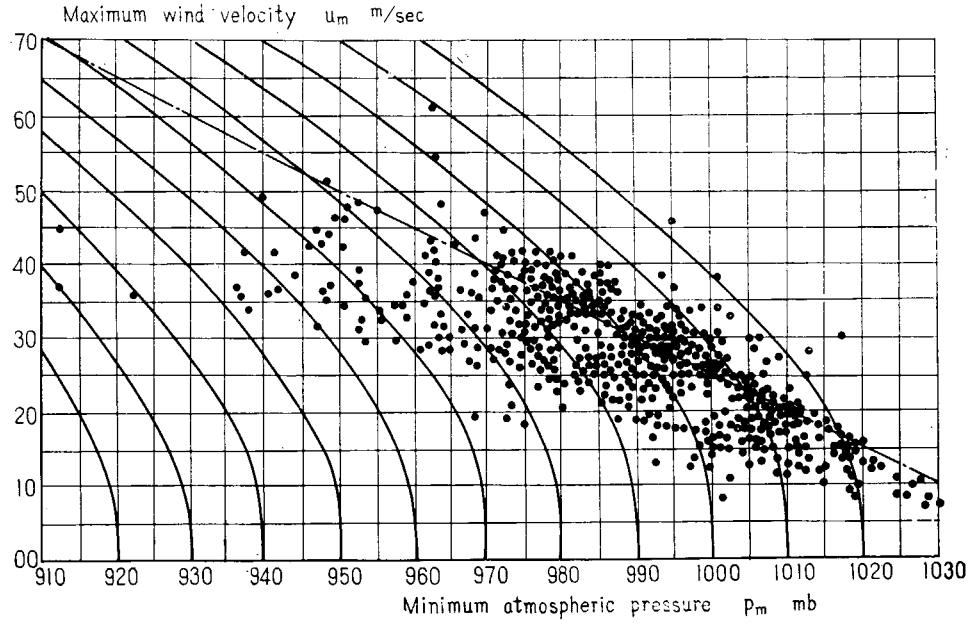
Maximum wind velocity u_m m/sec
Minimum atmospheric pressure p_m mb

Fig. 3.3

Where: r=Distance from typhoon centre
$2a$=Diameter of typhoon eye
$u(r)$=Wind velocity
u_m=Maximum wind velocity
$P(r)$=Atmospheric pressure
P_m=Minimum atmospheric pressure
R=Gas constant
T=Absolute temperature

Accordingly, taking the reading of surrounding high as P_0, it becomes:

$$P_0=P_m \exp\left(u_m^2/RT\right)$$

Since in many cases there exists a certain relation between the pressure on circular isobar with maximum diameter P_0 and the reading at the centre P_m, following formula can be developed statistically.

$$u_m\,(\mathrm{m/sec})=\frac{1050\,(\mathrm{mb})-P_0\,(\mathrm{mb})}{2} \qquad (1)$$

3. Gustiness of Ocean Wind.

Instantaneous fluctuation of the velocity of ocean wind or gustiness is the cumulation of enormous number of oscillations. When the energy of oscillation originated at the front surface between two superposed warm and cold air mass is considered to have been converted from the difference of kinetic energy of upper and lower air currents, we obtain:

$$a=\sqrt{\frac{\lambda}{g}\cdot\frac{T'\overline{u^2}-T\overline{u'^2}}{T+T'}}$$

$$c=\left[(T'u+Tu')+\sqrt{\frac{g\lambda}{2\pi}(T'^2-T^2)-(u-u')^2TT'}\right]\div(T+T')$$

Where: a=Amplitude of oscillation
λ=Wave length
c=Velocity of wave motion
T', T=Absolute temperature of upper and lower air current
u', u=Wind velocity of upper and lower air current

Accordingly, $c\fallingdotseq u$, or u'. Let gustiness $\sigma-1=2\pi a\,c/\lambda\div(u+u')/2$, it follows then:

$$\frac{\sigma-1}{\sigma_m-1}\fallingdotseq\left(\frac{\lambda}{\lambda_m}\right)^{-1/2},\quad \sigma_m\fallingdotseq 2\sqrt{\pi\frac{\Delta T/T}{\Delta u/u}\left(1+\frac{1}{2}\frac{\Delta T}{T}\Big/\frac{\Delta u}{u}\right)},\quad \lambda_m\fallingdotseq\frac{\pi}{g}\frac{(\Delta u)^2}{\Delta T/T}.$$

Fig. 3.5 illustrates the above relation. The components of these wave motions are statistically cumulative, and the mean gustiness is expressed by the following formula and indicated in Fig. 3.4.

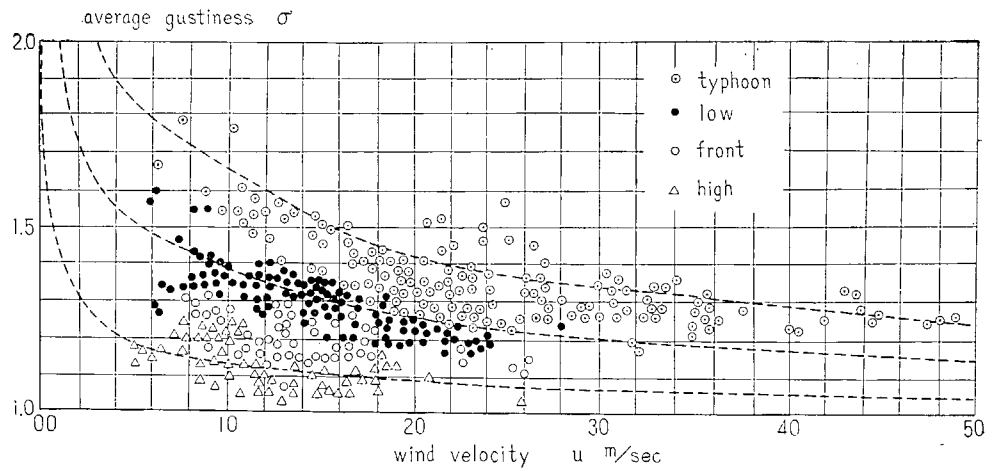

Fig. 3.4

$$\sigma-1\fallingdotseq\sqrt{\frac{20(\mathrm{m/sec})}{u(\mathrm{m/sec})}}\times\begin{cases}\sqrt{2.0}-1=0.414 & \text{Typhoon}\\ \sqrt{1.6}-1=0.265 & \text{Low and front}\\ \sqrt{1.2}-1=0.096 & \text{High}\end{cases}\qquad(2)$$

The statistical distribution of fluctuated amplitudes is expressed by the following formula:

$$\varphi(x)=\exp(-x^n)$$

Where: $\varphi(x)$=Probability to exceed x

$x=a/\bar{a}$

$\bar{a}$=n-ple root of mean value of n-th power of each amplitude $n<2$ indicates the vicinity of the centre and $n>2$ outside area.

Let $\bar{a}\bar{x}(q)$=the mean value of amplitudes taken in sequence from the greatest out of $1/q$ of the total number, then the following formula is obtained as shown in Fig. 3.6.

$$\bar{x}(q)=\sqrt[n]{\log q}\left[1-q\sum_{s=0}^{\infty}(-1)^s\frac{(\log q)^s}{s!\,(sn+1)}\right]+q\Gamma\left(1+\frac{1}{n}\right)$$

Similar tendency is seen in the statistical distribution of these amplitudes in case of ocean waves and the amplitude of ship's rolling, as mentioned in the next paragraph.

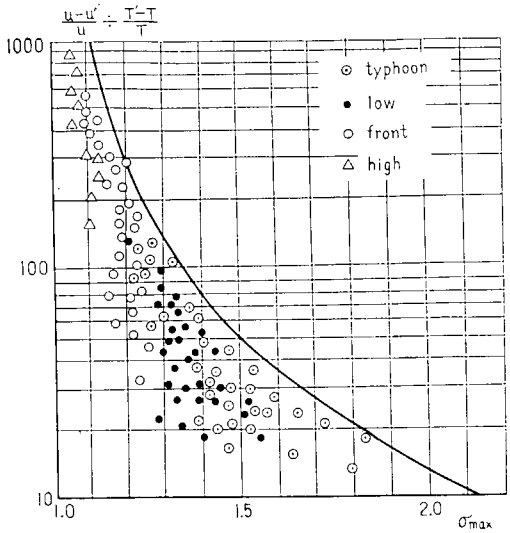

Fig. 3.5

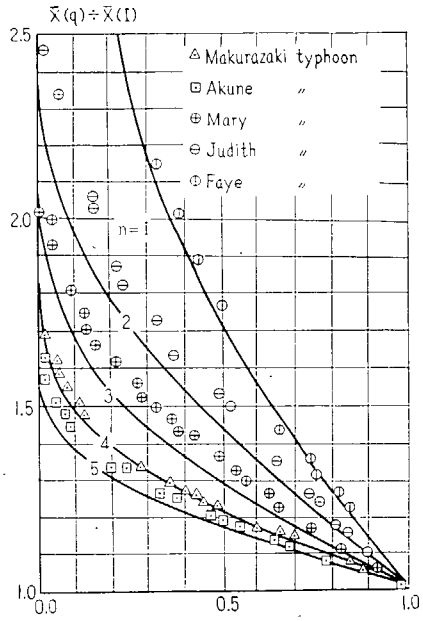

Fig. 3.6

4. Age and Steepness of Ocean Waves and Wind Factor of Drift Current.

The relation between wave steepness δ and wave age β observed at Tango, 29°N, 135°E and X-ray, 39°N, 153°E is illustrated in Fig. 3.8, where, let c=wave velocity, λ=wave length, H=wave height and u=wind velocity, then $\delta=H/\lambda$ and $\beta=c/u$.

These observed values exhibit the band distribution. If the energy of ocean wind is supplied to the energy of waves and drift current, we obtain:

$$\beta^2\delta^2=\frac{2}{\pi}\frac{\rho'}{\rho}\left[1-\frac{\rho}{\rho'}\varepsilon^2\right]$$

Where: ρ'=Air density of surface wind
ρ=Water density of surface current
$\varepsilon=v/u$=Wind factor
v=Current velocity

The relation between ε and β is as given in Fig. 3.7, which indicates that the greater the wind factor, the smaller the wave steepness, while high waves are more likely to be produced when the sea is still. If the steepness is converted to significant steepness, the following value may be available for practical use.

$$\left.\begin{aligned} \delta &= 0.10 && 0.0 \leqq \beta \leqq 0.4 \\ \delta &= 0.04/\beta && 0.4 \leqq \beta \leqq \infty \end{aligned}\right\} \qquad (3)$$

Fig. 3.7

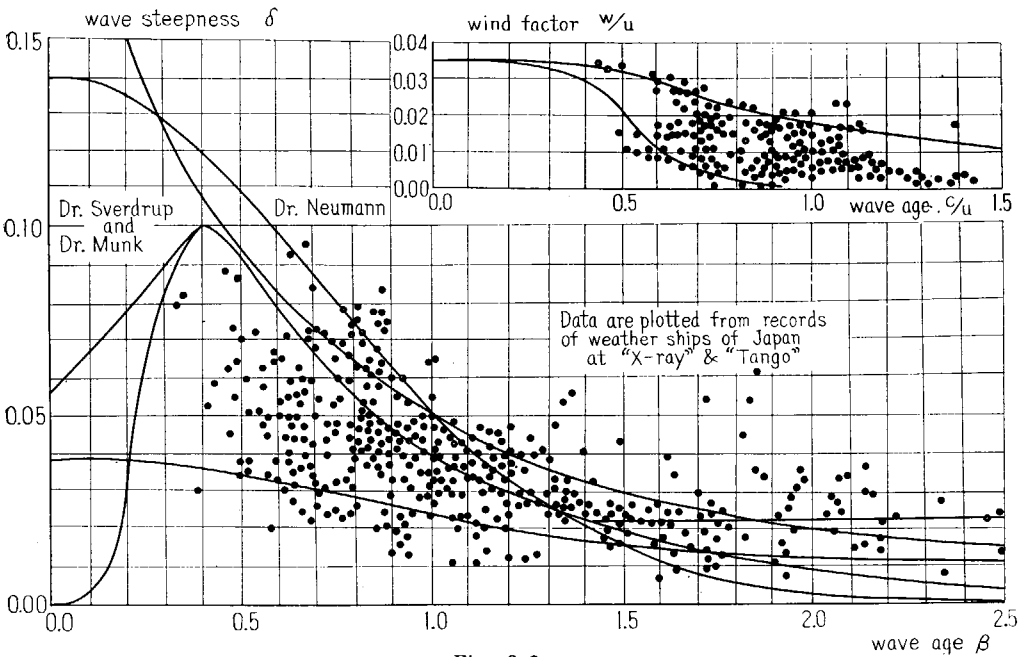

Fig. 3.8

5. Maximum Wave Height and Most Prevailing Period of Ocean Waves.

Ocean waves originated by ocean winds have such characteristics that in the moving typhoon area the inertia of wave $d(EC)/Cdt$, where E is the energy of wave, and wave-generating force of wind R_W, are balanced each other, and the wave age β_m is expressed by the following formula at the crest of the fluctuation of wind velocity or the maximum wind velocity.

$$\left|\frac{du}{dt}\right|_{u=u_m} = \frac{CR_W}{d(E/C)du} = 0.0448\frac{1+2.5(1-\beta_m)^2}{\beta_m{}^3}$$

In this case the existing "swells" join the newly orginated "seas". Within the range of wind velocity gradient $du/dt = 1 \sim 5$ m/sec·hour, it reaches the state of maximum steepness, as referred to by Drs. Sverdrup-Munk, that is:

$$\beta_m \fallingdotseq 0.4 \qquad \therefore \quad \delta_m \fallingdotseq 0.1$$

Accordingly, period and wave height become:

$$\left.\begin{aligned} H_m(\mathrm{m}) &= \frac{2\pi}{g}(\beta_m u_m)^2 \delta_m \fallingdotseq \left[\frac{1}{10} u_m(\mathrm{m/sec})\right]^2 \\ T_m(\mathrm{sec}) &= \frac{2\pi}{g}(\beta_m u_m) \fallingdotseq \frac{1}{4} u_m(\mathrm{m/sec}) \end{aligned}\right\} \tag{4a}$$

This prominent wave maintains the relation $EC \fallingdotseq E_m C_m$, after the drop of the wind force, without being affected by the wave-generating force.

Accordingly, as shown in Figs. 3.9 and 3.10, we obtain:

$$\frac{H}{H_m} \fallingdotseq \frac{u}{u_m}, \qquad \frac{T}{T_m} \fallingdotseq 1 \tag{4b}$$

Fig. 3.9

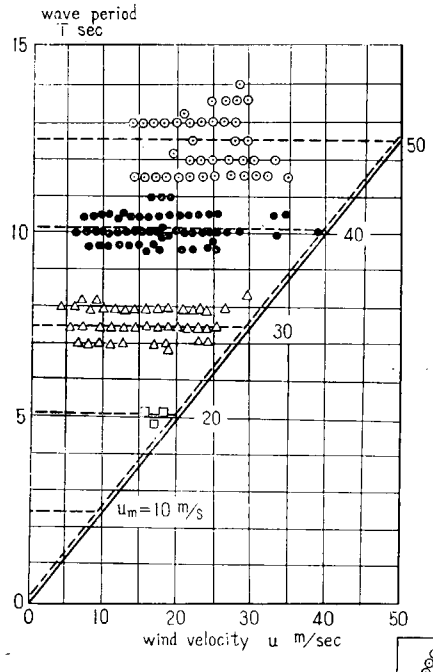

Fig. 3.10

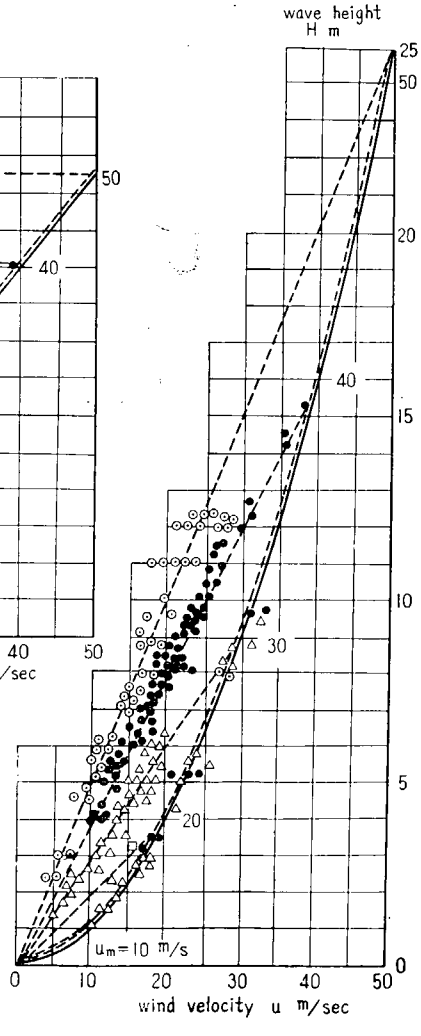

Using this relation, the scale of typhoon in remote place or in the past can be presumed.

6. Rolling of Ship.

The rolling of ships in rough sea is the composition of the amplitudes forced and synchronous rollings caused by every kind of component wave existing in that area. As each rolling has different phase, the total amplitude is in general smaller than the algebraic sum of the absolute value of each amplitude, and can be obtained from the statistical distribution of amplitudes. In the formula mentioned in paragraph 3, $n<2$ is likely to correspond to the generating "seas" abundant in the typhoon centre, $n=2$ to the surface of rough sea in the vicinity of the border of the typhoon eye, that is, the mingled state of "seas" and "swells", and $n>2$ to calm "swells" of outer region.

Let $\bar{\theta}(q)=1/g$ mean angle of rolling and θ_0=angle of synchronism, then:

$$\bar{\theta}(q)=\bar{x}(q)\times\sqrt[n]{\int_0^{g\,T_m/2\pi u}\{\pi\delta(\beta)\cdot R_s(T/T_s)\}^n d\beta}\,.$$

Where $R_s(T/T_s)$ indicates the curve of synchronism.

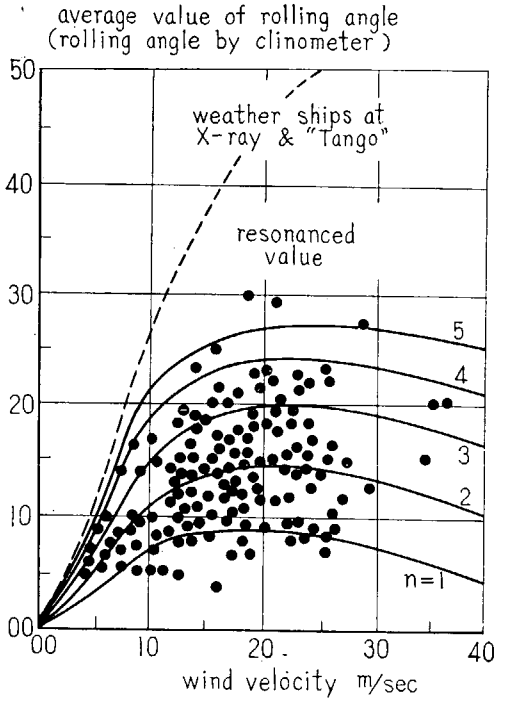

Fig. 3.11

Let T_s=natural period of rolling of ship, N_s=damping coefficient, γ_s= effective coefficient, then :

$$\theta_0=\sqrt{\frac{\pi\gamma_s}{2N_s}\cdot\pi\delta(\beta_s)}\,, \qquad \beta_s=\frac{gT_s}{2\pi}/u\,.$$

T_m is indicated in the preceding paragraph. Accordingly, rolling angle is determined from wind velocity of the sea area and the wave of maximum period.

As the spectrum of ocean waves has many absorption bands, wave steepness curve can also be used as the spectral steepness curve. Since, as shown in Fig. 3.11,

$$\frac{\overline{\theta}(3)}{\theta_0}=\frac{1}{3}\sim\frac{3}{4} \qquad (5)$$

the possibility that complete synchronism occurs decreases as the wind velocity increases.

7. Safetiness of Ship's Rolling.

Let GZ=righting arm, Sd=dynamical stability, $m=GM$, W=displacement, A=lateral projected area of ship subjected to wind pressure, a=distance from the centre of wind pressure to that of water pressure, c_a=coefficient of wind pressure resistance, σ=gustiness, then in general :

$$C_1=\frac{Sd}{\frac{1}{2}m\theta_0^2+c_a\frac{Aa}{W}u^2\{\theta_r+(\sigma^2-1)(\theta_r+\theta_0)\}}$$

As mentioned in the foregoing, however, $\theta_r\gg\theta_0\fallingdotseq 0$ at the typhoon centre, then C_1 is likely to become :

$$C_2=\frac{Sd}{c_a\frac{Aa}{W}u^2\sigma^2\theta_r}$$

Since $Sd=\int_0^{\theta_r}\overline{GZ}d\theta\fallingdotseq\frac{4}{\pi}GZ_{\max}\cdot\theta_r$, and $u\sigma=u_m$ the above value may determine whether or not the ship rights herself against the gust. In general, as shown in Fig. 3.7, when there is a sea current, following 3 kinds of the periods of synchronous wave are in co-existence.

$$T_3=\frac{T_s}{2}\left[1+\sqrt{1-\frac{w}{c_s}}\right]$$

$$T_4=\frac{T_s}{2}\left[1-\sqrt{1-\frac{w}{c_s}}\right]$$

$$T_7=\frac{T_s}{2}\left[-1+\sqrt{1+\frac{w}{c_s}}\right]$$

Where $c_s=gT_s/2\pi$ and w is drifting speed of ship.

Their index numbers become $C_1<C_7<C_4<C_3<C_2$, which indicates that C_1 and C_2 are the minimum and the maximum of all values. Where the wind velocity is extraordinarily great, c_s becomes smaller than w, as shown in Fig. 3.12. In such case synchronism occurs no more, but merely inclination due to wind pressure exists.

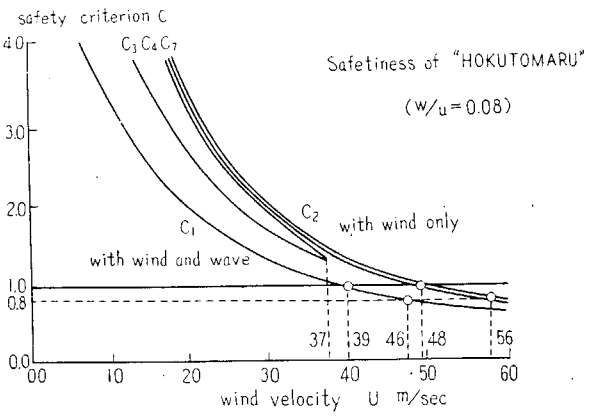

Fig. 3.12

PART IV
Actual Ship Observations
Chapter 1 Experiments on Ship Motion of M. S. "Hokuto Maru" in Ocean

1.1 Objectives.

The objectives of the experiments are firstly to study the meteorological and oceanographical characters of the sea near Japan and ship motion in it, and secondary by this study to obtain rolling angle and the critical heeling angle of the ship in irregular seas for the purpose of promotion of seagoing safety and ship performance.

Attaining this objectives, observation of sea waves and measurements of ship's rolling were mainly investigated, besides other possible items were planned to be measured simultaneously.

Experiments were performed during two voyages, that is, one was a northern voyage around the X-ray and the other was a southern voyage around the Tango.

1.2 Principal Dimensions and Main Performance of the Ship, etc.

The "Hokuto Maru" is a training ship which belongs to the Institute for Sea-Training of the Ministry of Transportation. Her picture is shown in

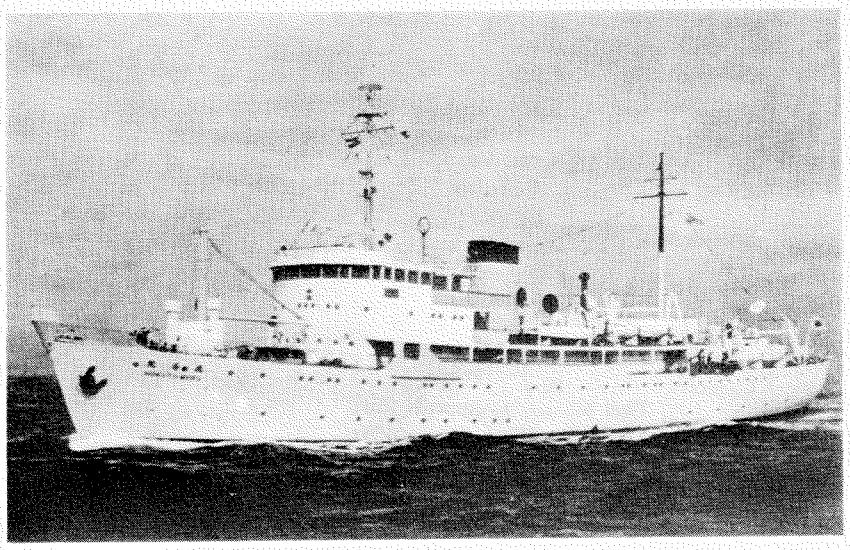

Fig. 4.1

Fig. 4.1, and her principal dimensions are tabulated in Table 4.1. She is a single-screw ship with Semi-Meiyer Form stem and cruiser stern, and has the bilge keels of 360 mm depth along 1/4 l length.

Table 4.2 shows her stability characteristics.

1.3 Voyage Routes and Condition of the Ship.

Two voyages, northern and southern, were scheduled. The northern one was an about 1300 nautical voyage... leaving Tokyo Harbour on Jan. 1,

Table 4.1 Principal particulars of "HOKUTO MARU"

Kind		Steam vessel		
Purpose of employment		Training ship		
Owner		The Institute for Sea-Training, Ministry of Transportation		
Plying limit		Ocean-Going		
Class, Type		The first class, Flush decker.		
Length (O. A.)		75.500m		
Length (P. P.)		68.500m		
Breadth (Mld.)		11.000m		
Depth (Mld.) to shelter deck		7.500m		
〃 to upper deck		5.400m		
Designed load draft (Mld.)		4.000m		
Initial trim		0.800m		
Designed load displacement		1.840 t		
Coefficients		C_b 0.597, C_p 0.633, $C_{\textcircled{x}}$ 0.943, C_w 0.790		
Tonnage	Gross	1631.27 tons		
	Net	449.99 tons		
Speed	Trial	14.207 kt		
	Service	12.5 kt		
Propeller		Number of blade	4	
	Diameter	3.000m	B. W. R.	0.238
	Boss ratio	0.200	B. T. R.	.0450
	Pitch ratio	0.950	Angle of rake	10°～1
	Expanded area ratio	0.414	Dir. of turning	righthanded
Rudder		1×All movable contra rudder		
Main engine		1×Ishikawajima steam turbine (with double reduction gears)		
		Full load 1.400 SHP (168 R.P.M.)		
		Service 1.200 SHP (160 R.P.M.)		
Main boiler		2×W. T. boiler (oil burning)		
Fuel consumption		13.5 t/day		
Rad. of action		4,920 miles		
Complement	Officers	21	Total 143	
	Crew	42		
	Cadets	80		
Bunker, Tank & Hold	Fuel oil	approx. 216 t		
	Feed water	〃 130 t		
	Fresh water	〃 136 t		
	Cargo hold	Cap. 160 m³ Weight 560 t		
Builder		Fujinagata Shipbuilding Co. Ltd., Osaka		
Completed		25th Dec., 1952		

Table 4.2 Stability Characteristics.

Given by Nagasaki Shipyard

Item \ Condition		Light	Full load	Normal (1/3 consumed)	3/4 consumed without W.B.	3/4 consumed with W.B.
Displacement	(t)	1324.49	1919.30	1731.69	1508.45	1689.18
Draft Fore	(m)	2.63	3.39	3.05	2.48	2.99
Draft Aft	(m)	3.60	4.84	4.58	4.40	4.49
Draft Mean	(m)	3.12	4.12	3.82	3.44	3.74
Trim by the stern (including initial trim 0.800)	(m)	0.97	1.45	1.53	1.92	1.50
KM	(m)	5.00	4.91	4.89	4.92	4.89
KG	(m)	4.84	4.00	4.19	4.61	4.18
GM	(m)	0.16	0.91	0.70	0.31	0.71
OG	(m)	1.73	−0.11	0.38	1.18	0.45
Freeboard	(m)	4.47	3.47	3.77	4.15	3.85
GZ_{max}	(m)	0.491	1.060	0.945	0.665	0.945
Angle of GZ_{max}	(deg)	54.5	51.5	53.0	52.5	53.0
Range of stability	(〃)	82.7	115.0	105.0	90.6	106.6
Max. dynamical stability	(m-t)	477.38	2319.70	1689.73	815.10	1678.90
A	(m^2)	542.0	473.5	495.0	520.5	500.0
A/A'		2.67	1.74	1.98	2.32	2.02
h	(m)	5.848	5.875	5.863	5.854	5.862
Rolling period	(Sec)	17.98	8.69	9.75	13.89	9.71

A……Projected lateral area of portion of vessel above water line.
A'……Projected lateral area of portion of vessel below water line.
h……Vertical distance between the C.G. of A and C.G. of A'

1955, she sailed northward along the coast of Honshu for the X-ray and then came back through the same course to Yokohama on Feb. 5, 1955.

The southern one was also an about 1300 nautical miles voyage . . . leaving Nagasaki on March 2, 1955, she sailed southward for the Tango and turning to the north-east, the arrived at Shimizu on March 9, 1955. Fig. 4.2 indicates the routes of these voyages as well as the weather charts and ship position at specified time.

It may be reasonably said that the ship condition was very close to the normal condition (i.e. 1/3 consumed condition) in accordance with the measured draft records throughout the voyages.

1.4 Measuring Devices and Apparatus used.

Items measured and apparatus used in this experiments are shown in Table 4.3.

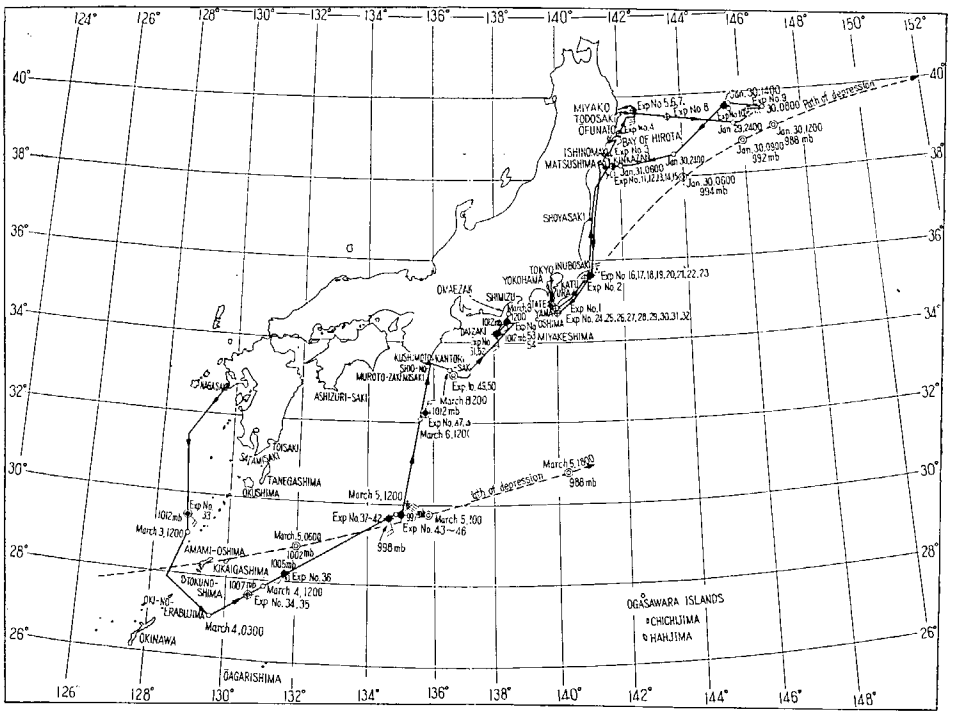

Fig. 4.2 Track Chart of "HOKUTO MARU"
From Jan. 21, 1955 to Feb. 5, 1955. From March 2, 1955 to March 9, 1955

1.4.1 Ship's Rolling Measurements.

Every effort was made for rolling measurements which were most important for the objectives of the experiments. To record absolute angles of rolling, pitching and yawing, an oscillation-recorder which consists of a so-called artificial level of pneumatic-gyro type and a free-gyro, was used as a displacement meter. Angular velocity of rolling was measured by an angular velocity meter made of a restrained gyroscope, and angular accelaration of rolling was also measured by an inertia type angular accelerograph. For the purpose of comparison and correction, absolute angles of rolling and pitching were recorded by a Sperry rolling-recorder.

On the other hand, a pendulum type rolling recorder was adopted to measure relative rolling angles to the effective wave slope.

1.4.2 Wave Measurements.

Waves being the most important item to measure in the experiments, great emphasis was placed on wave observation. Encounter marks were recorded whenever the stem of ship crossed the crest line of sea or swell. The direction and the pattern of the crest lines of sea or swell were sketched.

Table 4.3

Items		Measuring Devices
Condition of the ship	Position	
	Ship speed	SAL-log
	R.P.M. of propeller	Electric tachometer
	Tank conditions	
Wind	Direction	Light vane type anemometer Robinson cup.
	Velocity	
Oscillations	Absolute	
	Rolling	Sperry recorder (Absolute angle)
	Pitching	Pneumatic-Gyro oscillation recorder
	Yawing	Short pendulum (Relative angle)
	Relative	
	Rolling ang. vel.	Angular vel. rec.
	Rolling ang. acc.	Angular acc. rec.
Wave	Length	16 mm cine camera
	Height	35 mm camera
	Profile	Wave profile rec.
	Period	Wave pole and launcher
	Encountering angle	Observation
Directions Encounter mark Signal mark		Interphone

Average wave length and significant wave height were also recorded by observations. As regards wave period, the average of the values observed by all the staff was adopted. To assure the accuracy of observation, on the southern voyage buoys were floated on waves as the measure for comparison.

To obtain the wave profile along the side shell, wave profile recorders (a number of electric contact points) were installed on the ship's hull.

Besides the items mentioned above, as the general information for oceanographical condition, the waves were photographed with a 16 mm cine camera.

1.4.3 Meteorological Observation (wind direction, wind velocity, etc.).

Weather charts were drawn on the basis of weather forecast (J. M. C.) received, and weather, atmospheric temperature, water temperature and barometric pressure were recorded at every measuring time. Wind direction and wind velocity were continuously self-recorded by a Light Vane Type anemometer.

At the same time, the general ship condition was recorded by instruments equipped on the ship.

The simultaneity of many kinds of recordings was secured by regulating the time marks in all recordings.

1.5 Kinds of Experiments and Results obtained.

1.5.1 Kinds of Experiments.

Totally 54 Tests were carried out on both the northern and southern voyage at specified times as a rule. In these measurements, the above mentioned items were measured under ordinary voyage condition without changing in speed and course of the ship. Besides these, as a special case the following conditions were made, that is:

(1) When circumstances allow, in the same area of sea, tests were carried out successively changing the course direction of the ship so as to vary the wave encounter angle of the ship from dead ahead to dead follow.

(2) When prominent swell existed with seas, the cases above mentioned were measured with respect to the swell direction.

(3) In some of the aforementioned cases, engine speed was varied from stop to over-load-speed including service speed and dead slow.

(4) In order to study the rolling characteristics of the ship and to observe the then ocean waves correctly, observation was carried out while she sailed parallel to the "Kaio Maru".

(5) Rolling of the ship was recorded during a complete turning with rudder angle of 10 degrees.

1.5.2 Results obtained.

The sketch of weather chart and oceanographical condition were made for each test, and Table 4.4 shows an example.

All the recordings obtained by various instruments were replotted on the same time axis for the comparative purpose. (An example is shown in Fig. 4.3.)

1.6 Analysis and Discussion on Results obtained.

1.6.1 Wind and Ocean Waves.

This article is a summary of the meteorological records obtained on the "Hokuto Maru". Some typical studies on the records are now explained below.

Tabel 4.4

Experiment No. 45		
Date	March 5, 1955	
Time	13·15~13·20 J.S.T.	
Weather		0
Atm. Press.		997.0 mb
Atm. Temp.		16.0℃
Sea Water Temp.		19.0℃
Position		29°48′ N 134°58′ E
Ship's Head		145°
Ship Speed		10.3 kt
Revolution		122.0 R.P.M.
Wind	Average Vel.	10.5 m/sec
	Average Dir.	°
	Beauf. Scale	
Sea	Wave L. (λ)	m
	Wave H. (h)	m
	Period of Encounter (T_e)	10 sec
	Rel. Dir. (α)	S 135°
Swell (I)	λ	m
	h	m
	T_e	sec
	α	°
Swell (II)	λ	m
	h	m
	T_e	sec
	α	°
Sea Condition		
Remarks		

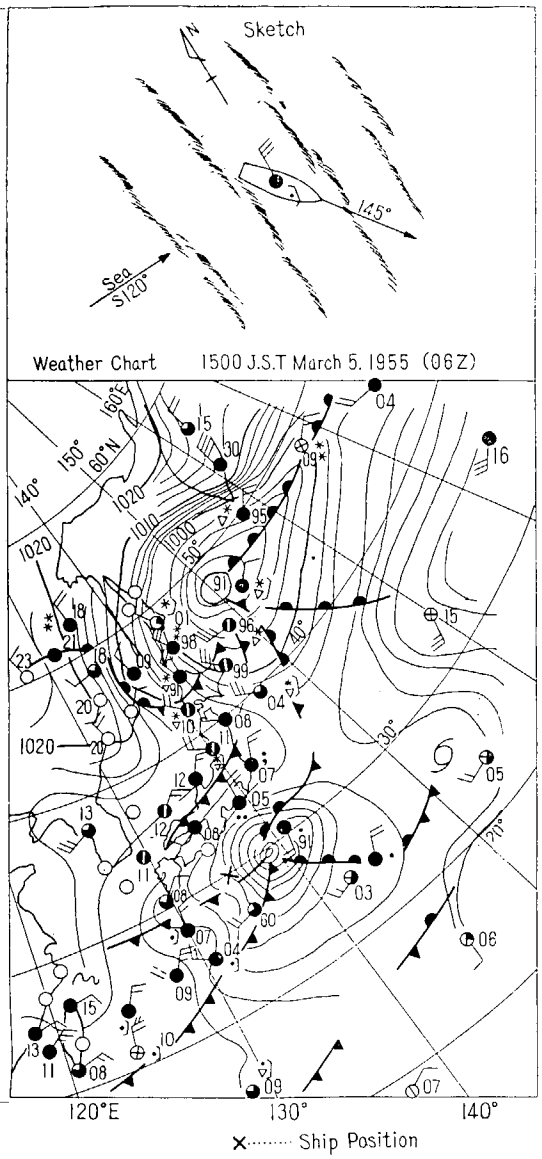

Fig. 4.4 and Fig. 4.5 indicate wind, waves, atmospheric pressure, atmospheric temperature and wave direction at the Tango, and at X-ray respectively while the ship was nearest to the centre of depression. At the Tango, as the warm front approached, weather became rough. Just after the centre of depression passed, the wind blow reached at its maximum. While the centre of depression went away from the point, the wind continued to

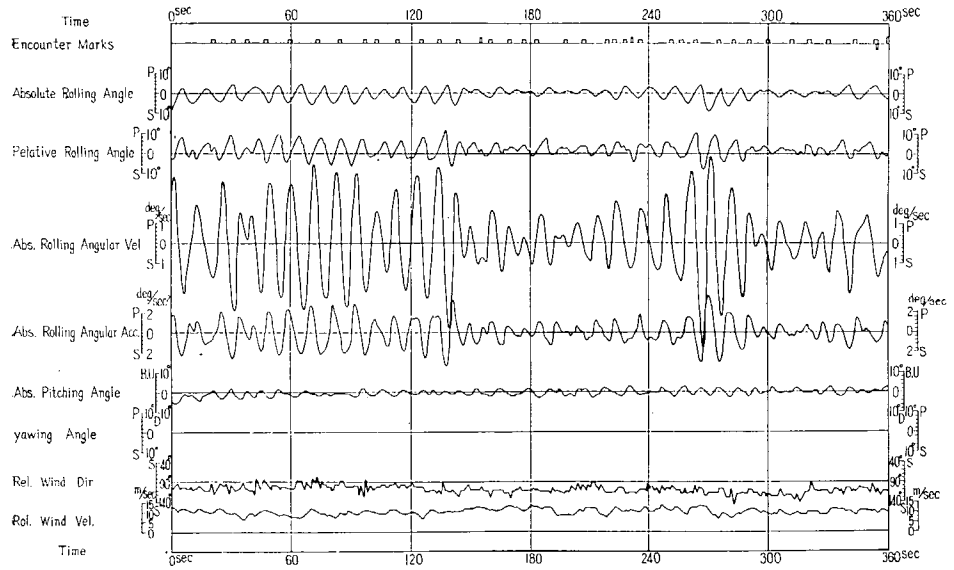
Time
Encounter Marks
Absolute Rolling Angle
Relative Rolling Angle
Abs. Rolling Angular Vel
Abs. Rolling Angular Acc.
Abs. Pitching Angle
yawing Angle
Rel. Wind Dir
Rel. Wind Vel.
Time
0sec
60
120
180
240
300
360sec

Fig. 4. 3

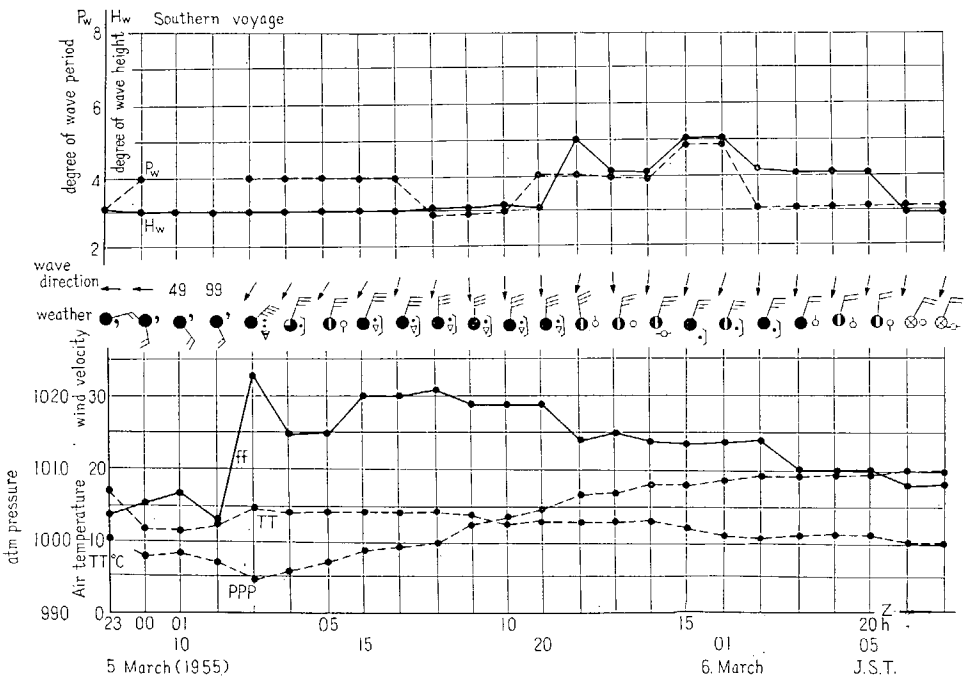
Southern voyage
degree of wave period
degree of wave height
Pw
Hw
wave direction
weather
wind velocity
ff
TT
TT°C
PPP
dim pressure
Air temperature
5 March (1955)
6. March
J.S.T.

Fig. 4. 4

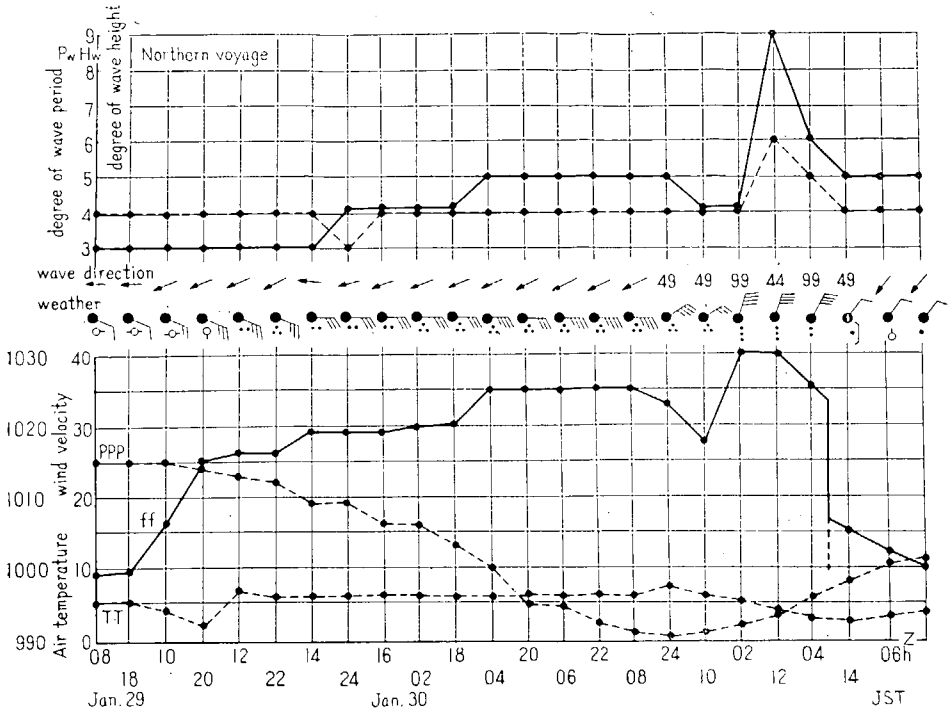

Fig. 4.5

blow into the stagnant front for about 20 hours.

In the case of X-ray, the situation was quite similar to that at the Tango.

The gradient of the atmospheric pressure, however, being very steep, the strong wind blew constantly beforehand and then stopped as the center of depression went by. The analysis of the ocean waves under this weather condition at the X-ray is shown in Fig. 4.6.

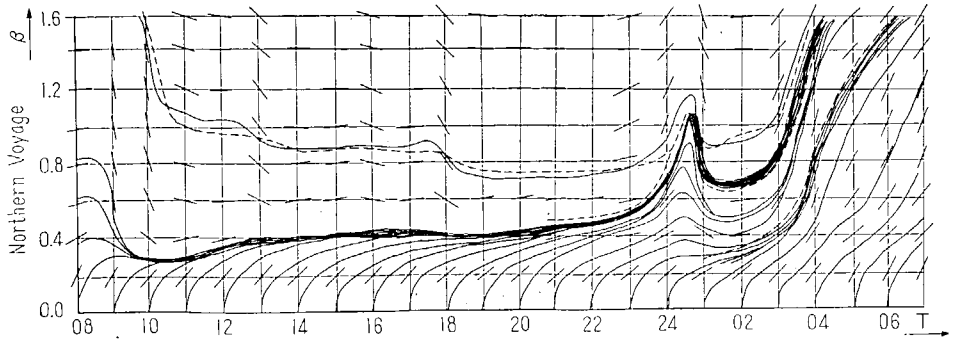

Fig. 4.6

The Fig. was made by the graphical integration over every hour, using Sverdrup-Munk's ocean wave theory. The solid line shows the changing pattern of waves hourly, and the dotted line is the results observed.

From these lines it is concluded that the ocean waves do not seem to be a single group of waves but consists of several group of waves, and an observer is apt to look at one of the groups which he selects. However, in general the waves corresponding to the spot where curves crowded (see Fig. 4.6) being mainly observed, they may be supposed to be the representation of the oceanographical condition.

1.6.2 Statistical Analysis of Rolling and Pitching of the Ship.

1.6.2.1 Correlogram and Spectrum of Rolling and Pitching of the Ship.

The rolling characteristics of the "Hokuto Maru" was analyzed by making correlogram and spectrum of absolute rolling angles and absolute pitching angles. These analytical calculations were carried out by a relay-type electrical computer.

Provided that time series obtained from the rolling records are $X_1, X_2, \ldots X_N$, auto-correlation coefficient is described by the following equation,

$$\gamma_\tau = \frac{1}{N-\tau} \sum_{t=1}^{N-\tau} (X_t - \bar{X}_{1\tau})(X_{t+\tau} - \bar{X}_{2\tau}) / S_{1\tau} S_{2\tau} ,$$

where $\bar{X}_{1\tau}$ and $S_{1\tau}^2$ are sampling mean and sampling variance of $X_1, X_2, \ldots X_{N-\tau}$, and $\bar{X}_{2\tau}$ and $S_{2\tau}^2$ are also sampling mean and sampling variance of $X_{\tau+1}, X_{\tau+2}, \ldots X_N$ respectively. Using correlogram thus obtained, the spectral density is determined by Fourier-cosine transformation as follows,

$$F'(\lambda) = \frac{1}{2\pi} \left[1 + 2 \sum_{t=1}^{\tau} \gamma_\tau \cos \tau\lambda \right].$$

An example of correlogram and spectrum thus obtained are shown in Fig. 4.7 and 4.8 respectively.

The statistical analysis based on these spectra resulted the following findings: It is seemed that the spectrum of pitching was similar to that of waves which offered external forces. Therefore, the encounter period may be obtained from the peaks of the pitching spectrum and consequently the shape of distribution of wave spectrum may be known. On the other hand, every spectrum of rolling has a prominent peak at the period which corresponds to the natural rolling period of the ship. It is reasonably said that in the case of rolling, the ship selects only the waves, period of which equals to her natural

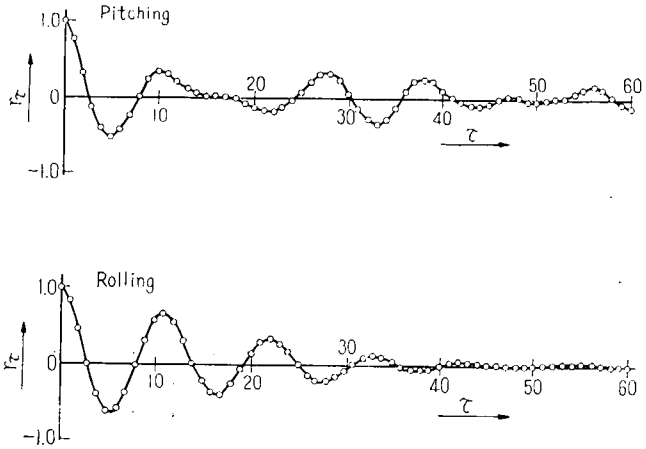

Fig. 4.7 HOKUTO MARU No. 45 Correlgram.

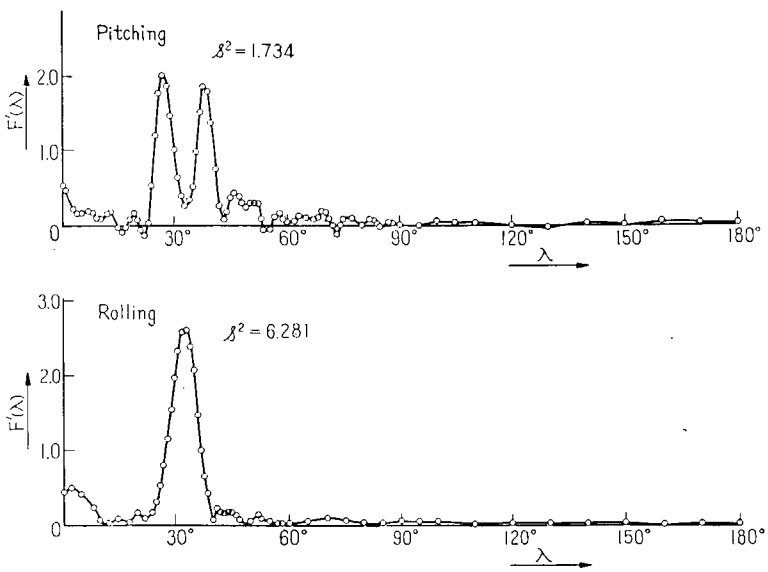

Fig. 4.8 HOKUTO MARU No. 45 Spectrum.

rolling period, out of irregular waves.

1.6.2.2 Relation of Cumulative Energy Density to the Amplitude Distribution and Mean Value of Rolling and Pitching.

An example of the diagrams in which half-amplitudes taken from the records of rolling and pitching are arranged according to size is shown in Fig. 4.9. The shape of amplitude distribution follows well the theoretical curve of Longuet-Higgins. The mean amplitude obtained from the records agrees well

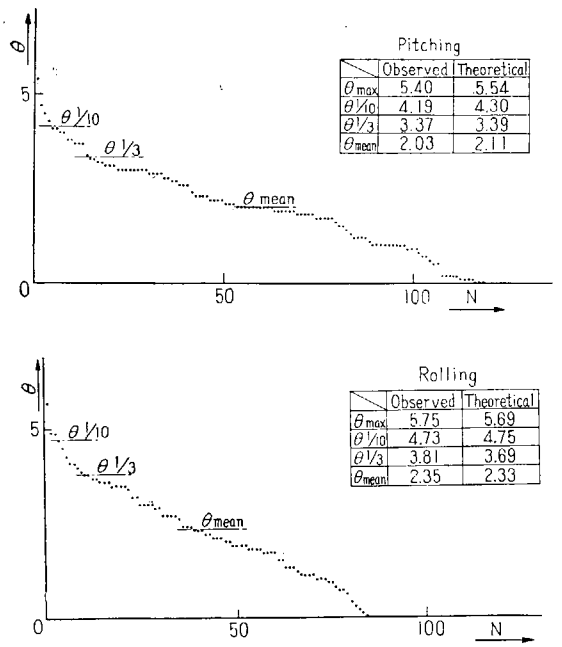

Fig. 4.9 (Exp No. 44)

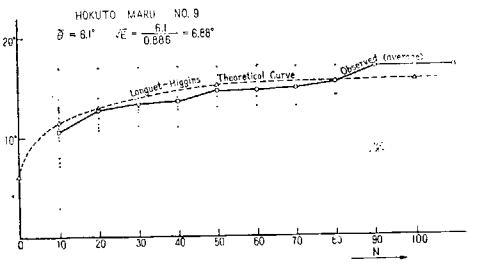

Fig. 4.10

with that computed by the theory. (These are show in Fig. 4.9). It is then found that the amplitude distribution of rolling and pitching fairly coincide with Longuet-Higgins' narrow-band-theory, in spite of its energy-spectral distribution is not narrow.

1.6.2.3 Relation between the Maximum Amplitude and the Number of Rolls.

According to the Longuet-Higgins' theory, the relation between the number of rolls and the expectation of the max. amplitude can be defined by cumulative energy. This relation computed from the actual data is shown in Fig. 4.10. This Fig. is drawn by the following process: Firstly, 100 rolls of rolling are chosen from the rolling records and are divided into 10 sections each of which contains 10 rolls. Then the max. amplitude in each section is read and the average of 10 max. amplitude is computed. These max. amplitudes and their average value are plotted above scale 10 of the roll number axis. In the same way, the max. amplitudes and the average value obtained by dividing the wave records into successive 20 rolls, are plotted on scale 20, and so on.

On the one hand, the equation, the mean angle$=0.886\sqrt{\overline{E}}$, gives the value $\sqrt{\overline{E}}$ by which Longuet-Higgins' theoretical curve was obtained. It is in

consequence known that the measured values are scattered over wide range, but the mean values are very close to the theoretical value of Longuet-Higgins. Therefore, the storm wind being supposed to blow constantly, the possible max. amplitude of the ship struggling in the storm within certain hours may be presumed by measuring certain number of rolls, which provides the value of E, in the early stage of storm. However, the above mentioned possible max amplitude is the expectation $E(a\,\max)$ and the actual max. value can be greater than this $E(a\,\max)$ with the possibility $P[a\,\max \geqq E(a\,\max)]$. $E(a\,\max)$ is therefore, not sufficient to estimate the max. amplitude for the case like ship's rolling in which the critical limit exists, but the distribution of the value $E(a\,\max)$ should also be considered. Suppose N rolls are expected for a ship to sail through a storm area. Then the probability with which actual max. amplitude becomes greater than the expectation of the max. amplitude, $\alpha\sqrt{E}$, is given by Longuet-Higgins as follows,

$$P[a\,\max \leqq \alpha\sqrt{E}] = (1-e^{-\alpha^2})^N.$$

This expression is computed for various N values and plotted in Fig. 4.11.

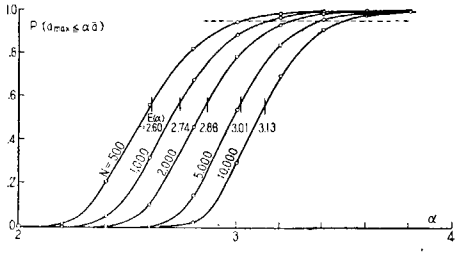

Fig. 4.11 Cumulative Distribution Function of a max.

For example, the probability with which the max. value exceeds the expectation of the max., is 0.45 whatever N may be. That is to say, it must be kept in mind that one out of two actual amplitudes exceeds the expectation of the max. amplitude. Therefore, in the case like ship's rolling having a critical limit, this significant level should be reduced far more. Now suppose the significant level is 0.05, i.e. one out of 20 rolls may be greater than the expectation of the max. amplitude. It is naturally seen that the critical value becomes $3.03\sqrt{E}$, provided the number of rolls is 500, and is greater than the then expectation $2.60\sqrt{E}$.

1.6.2.4 Correlogram and Spectrum of Encounter Period.

It is obvious that the sea condition is very important to analyse the

ship's oscillation. In the experiments the encounter marks being recorded, an analysis of wave period was carried out by using these data. The records of encounter marks are replaced by a series of rectangular waves which have unit amplitude and each half-wave-length of which corresponds to a interval between two successive encounter marks. This series of irregular waves gives a simple time series, and its auto-correlation coefficient and then spectrum are easily obtained. An example of the spectrum described above is shown in Fig. 4.12. The shape of spectral distribution in Fig. 4.2 is quite similar to that of pitching obtained in 1.6.2.1. It is then noticed that the main frequency component of wave spectrum can be deduced from the spectrum obtained by encounter marks, considering, as stated before, the spectrum of pitching is similar to that of waves.

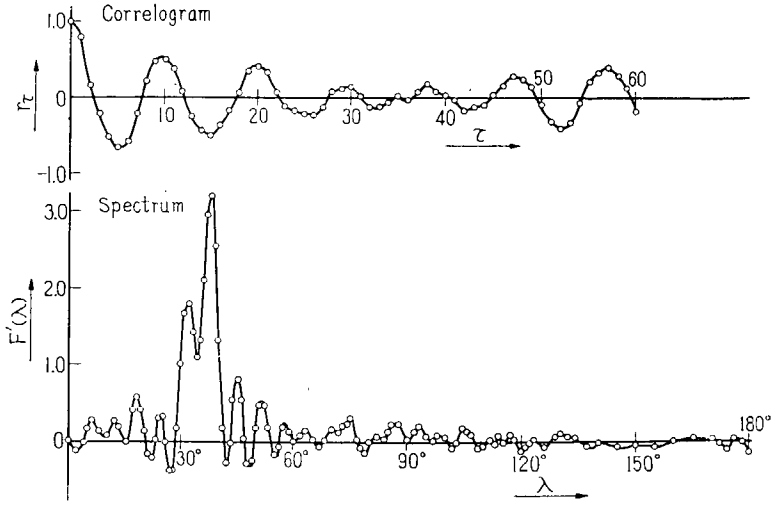

Fig. 4.12 HOKUTO MARU No. 45 Period of Encounter.

1.6.3 Influence of Wind Velocity on Rolling Angle and the Critical Heeling Angle.

Ship's rolling due to waves and heel due to a gust of wind are two big factors in the stability of ship. Many methods to estimate the critical heeling angle caused by this two external forces, have been proposed. In this report, the method used in the stability standard of the Ministry of Transportation, and a statistical method are adopted to compare the theoretical values with the measured ones.

Fig. 4.13 and 4.14 show the aforementiond comparison performed for test No. 44 and 9 respectively. In these Figs., "θ ex Observed" is measured

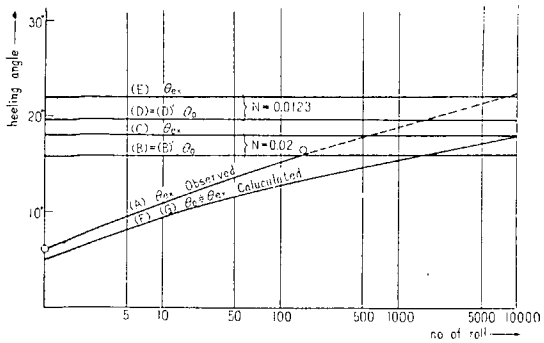

Fig. 4. 13

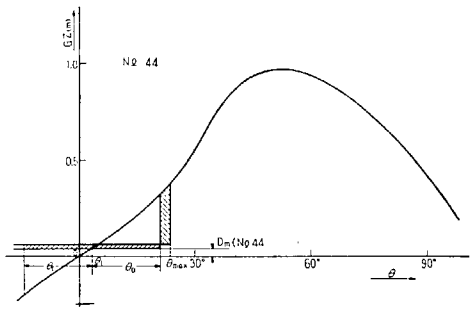

Fig. 4. 14

critical heeling angle and "θ_0 Calculated" is calculated by the cumulative energy density which is obtained in the following way. That is, the wave spectrum which is assumed by Neumann's Method under 17 m/sec wind condition, and the response function of ship give a rolling spectrum from which cumulative energy density can be computed.

Furthermore, the effect of a gust of wind is added to "θ_0 Calculated" and this is shown as "θ ex Calculated".

On the other hand, the equation used in the stability standard of the Ministry of Transportation,

$$\theta_0 = 0.7\theta \text{ resonance} = 0.7\sqrt{\frac{\pi\gamma\Theta_w}{N}},$$

where $N=0.02$, is numerically treated and then the additional term due to a gust of wind is also considered according to the standard.

As a result of the comparing these values, the following facts are made clear:

(1) In the No. 44 test, the method described in the stability standard of the Ministry of Transportation over-estimates rolling angle of the ship. This is due to the lack of the waves with steepness given by Sverdrup-Munk's theory and with long period corresponding to the natural rolling period of the ship. Because, in the test No. 44 there were only the young waves with steep slope but short-period which appear in the first stage of duration.

It is, therefore, quite possible that after long duration the waves grow faster and rolling angle may approach to the angle prescribed in the stability standard of the Ministry of Transportation. In the case of No. 9 test in which prominent swell existed, rolling angle coincides with the critical heeling angle shown in the standard after 500 rolls. In other words, ship's rolling being

rather under-estimated, it is advisable to use the observed value of $N=0.0123$ instead of $N=0.02$ for the safety purpose.

(2) The theoretical values calculated by Neumann's imperfectly-arisen spectrum, show a good agreement with the actual measured values.

(3) The critical heeling angles were computed by using the fluctuation of wind velocity obtained from spectral analysis of the records. Consequently, rolling angle due to the fluctuation of wind velocity was found to be much smaller than that due to a gust of wind.

1.6.4 Reduction of the Amplitude, Velocity and Acceleration of Rolling due to the Irregularity of Waves.

In rough seas, the waves would not be regular but should be a superposition of random waves. Rolling of ships in such rough water may be treated as follows: The resultant of rolling angles corresponding to their component waves ... so-called cumulative value ... being expressed as $F(\beta_s)\theta_0$, the mean rolling angle which will appear most frequently, is given by

$$\bar{\theta}=\theta_0 F(\beta_s)\frac{\sqrt{\pi}}{2},$$

provided the distribution of wave height obeys Longuet-Higgin's theory. That is to say, 0.886 $F(\beta_s)$ is the reduction of resonance rolling angle due to the irregularity of waves. $F(\beta_s)$ can be easily obtained if wind and oceanographical condition are known, so $\bar{\theta}$ becomes calculable using $F(\beta_s)$.

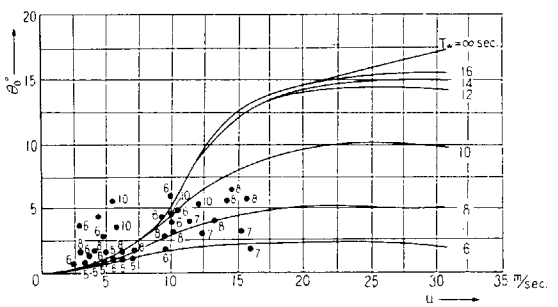

Fig. 4. 15

Fig 4.15 shows a comparison between the theoretical values thus obtained and the values observed. Statistically it may be said that a satisfactory agreement is attained. It is also found that ordinary rolling angles of ship reach up to only about 70% of the extreme case where $T_w=\infty$. $T_w=\infty$ means fully arisen sea.

1.6.5 Effective Wave Slope.

In the experiments, absolute rolling angle (θ), relative rolling angle (θ_a), absolute rolling angular velocity ($\dot{\theta}$) and absolute rolling angular acceleration ($\ddot{\theta}$) were measured.

Knowing $\theta-\theta_a=\gamma\theta_w$,

where γ is the effective wave slope coefficient, the effective wave slope coefficient of actual irregular wave can be computed by using the records obtained (shown in Fig. 4.16 by a solid line).

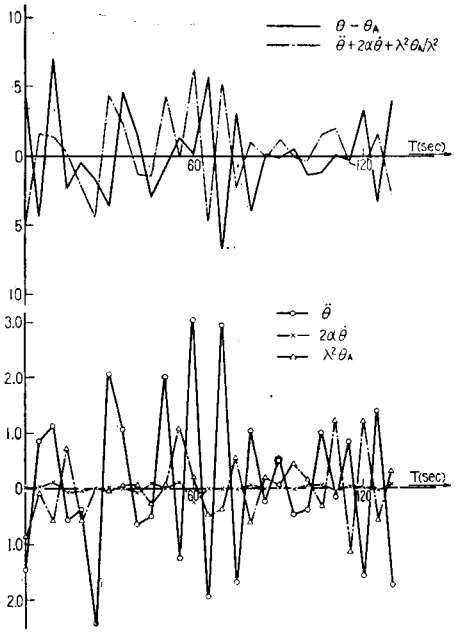

Fig. 4.16

On the other hand, the effective wave slope may be determined by a equation,

$$\frac{I}{g}\ddot{\theta}+k\dot{\theta}+W\cdot GM(\theta-\gamma\theta_w)=0\,,$$

providing that all the factors but γ in the equation were actually measured. The results of this calculation are shown in Fig. 4.16 by a dotted line. Both the solid and the dotted line show a satisfactory agreement with slight phase lag. Consequently, it may be concluded that the effective wave slope thus obtained is fairly dependable.

Chapter 2 Experiment by Observation Ship "Ojika"

Need for the direct measurement of ocean waves had been fully recognized in the light of the experiences mentioned in Chapter 1, so that the experiments mentioned in Chapter 2 to 4 were conducted. In the experiments referred to in Chapters 2 and 3, observation ships "Ojika" and "Atsumi" were offered, which are sister ships, built as a coast-defense ship, converted to patrol ship later and now used for the observation of typhoon. Their principal particulars are as given in Table 4.5.

Table 4.5 Principal Particulars of "OJIKA" [and "ATSUMI"]

Length (O. A.)		78.77 m
Length (P. P.)		71.50 〃
Breadth (W. L.)		9.10 〃
Depth (Mld.) (from top of keel)		5.34 〃
Load draft extreme		2.92 〃 (2.76 m)
Load displacement		951.78 t (877.34 t)
Coefts. at load draft		C_b 0.487 (0.484), C_p 0.610 (0.605)
		$C_{\boxtimes}$ 0.798 (0.784), C_w 0.718 (0.705)
Tonnage	Gross	877.97 tons
	Net	307.29 〃
Speed (Trial)		15.834 kt (2,243 IHP, 300.5 R.P.M.)
Propeller	Dia. × Pitch	1.800 m × 2.023 m (Starboard) 1.800 m × 2.067 m (Port)
	No. of blade	4
	No. of prop.	2
Main engine, Diesel		1,600 BHP × 2 (380 R.P.M.)
Complement		74
Bunker, Tank & Hold	Fuel oil	125.23 t
	Fresh water	58.40 〃
	Ballast water	77.94 〃

Note: Figures in the bracket are those of normal condition.

The observations were made from 4th to 24th October, 1955 within the range of area, 50 miles in radius, centered at Tango, 29°N, 135°E. Three observers participated in the experiment. In the observation, oscillation of ship (pitching and rolling of ship) and waves (length, height, period, velocity, slope and direction) were made as the main object of the measurement. Regarding the meterological observation, records taken in the weather observation room of the ship were supplied. General arrangement of the instruments for the measurement is shown in Fig. 4.17. Manila ropes with buoy were used for the measurement of the length and velocity of waves, and a nylon boat of

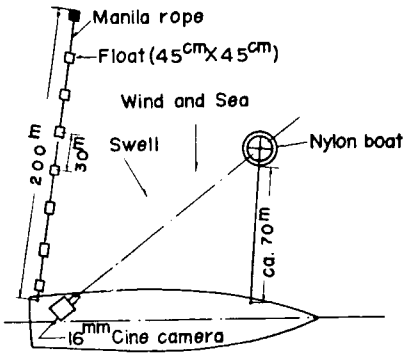

Fig. 4.17 Arrangement of the Devices for Wave Observation.

3 metres in outside diameters was fitted with an alminium mast of 2 metres in height, in order to measure the component of wave slope by recording to the cine-film the inclination of the mast to horizontal line. In addition, a wave height meter of Froude's type of 15 metres in over all length was prepared, but as it sank by accident, a bamboo wave height meter of 7.4 metres in over all length was made as a substitute and used for the measurement after 17th. Ship's rolling was measured by 2 sets of pendulum type rolling recorder and 1 set of Sperry's rolling recorder. During the period of measurement, displacement, mean draught, height of the centre of gravity, GM and GM_L of "Ojika" varied approximately linearly. These values on 4th an 24th October are shown in Table 4.6.

Table 4.6 Condition of Ship

	Displacement	Mean Draught	KG	GM	GM_L
4th Oct.	1002 t	3.01 m	3.04 m	1.07 m	142.7 m
24th Oct.	881	2.76	3.13	0.94	149.2

The results of the measurement are given in Tables 4.7 and 4.8, where the wave height h referred to in Table 4.7 indicates the data by visual observation. The analysis of these results, together with the record by observation ship at Tango in September and October from 1952 to 1954, has disclosed the facts mentioned in the following.

2.1 Wave.

The relation between wave length λ and wave period $\tilde{T}$ obtained by the observation is expressed by the following formula as shown in Fig. 4.18.

Table 4.7 Results of the Measurements

Exp. No.			1	2	3	4	5	6	7	8	9	10
Date			6	7	7	8	8	9	9	10	10	13
Time			14·10–14·22	10·10–10·25	15·00–15·20	10·00–10·10	14·00–14·30	8·00–8·30	15·00–15·20	9·00–9·20	15·00–15·20	10·00–10·20
Ship speed (kt)			0	0	0	0	0	7	7	0	0	0
Course			113	120	90	120	135	328	0	135	110	113
Abs. wind (Ave.)	B. scale		3	3	3	4	5	6	7	8	8	1
	Vel. (m/sec)		—	—	—	—	—	18.8	17.8	—	—	—
	Dir.		—	—	—	—	—	7	40	—	—	—
Rel. wind (Ave.)	Vel. (m/sec)		6.3	8.1	6.8	7.9	12.4	21.7	20.2	19.8	18.0	2.6
	Dir.		P100	P90	P110	P90	P100	S32	S34	P110	P110	P130
Wave	Sea	Dir.	P110	P100	P90	P90	P100	S35	S40	P90	P90	P130
		λ (m)	90	40~50	40~60	40	50~60	100	100~120	120~150	120~130	50
		h (m)	1.5	1.5	1.5~2.0	1~1.5	2	6~7	6~7	7	7~8	1
		T (sec)	7	6~7	7~8	5	6	8.5	—	10~17	10	6
		T_e (sec)	—	—	—	—	—	7.5~8.5	7~8	—	—	—
	Swell	Dir.	—	—	—	P140	P130	—	—	—	—	P70
		λ (m)	—	—	—	60	70~80	—	—	—	—	90~120
		h (m)	—	—	—	2	2	—	—	—	—	1~1.5
		T (sec)	—	—	—	6~7	8~9	—	—	—	—	9
	Wave height (m)	Max. H_{max}	—	—	—	—	—	—	—	—	—	—
		Ave. $\bar{H}$	—	—	—	—	—	—	—	—	—	—
	Wave slope (deg.)	Max. S_{max}	—	—	—	—	—	—	—	—	—	—
		Ave. $\bar{S}$	—	—	—	—	—	—	—	—	—	—
Rolling	Rel. angle (deg.)	Max.	11.0	9.5	8.5	9.5	12.5	18.5	18.5	18.0	19.0	10.5
	Abs. angle (deg.)	Max.	13.5	8.5	13.5	11.0	11.5	—	18.5	24.0	20.5	9.0
		Ave.	4.8	4.2	4.9	4.1	5.2	—	6.2	8.2	7.5	3.7
	Ave. period (sec.)		7.15	—	7.51	7.05	6.94	—	7.97	7.99	7.76	7.06
Pitching	Max. angle (deg.)		1.0	1.0	1.0	1.0	2.0	3.5	4.0	1.5	1.5	0
	Ave. period (sec.)		—	—	—	—	5.3	5.5	7.2	5.5	—	—

A swell of 4 sec. period was observed in the direction of P 155 at Exp. No. 12

on board the "Ojika", 1955

11	12	13	14	15	16	17	18	19	20	21	22	23
14	14	15	15	18	18	19	19	20	21	21	22	22
10·15–10·30	15·00–15·20	8·20–8·40	14·00–14·20	9·00–9·30	13·45–14·05	10·00–10·15	12·45–13.15	12·45–13·15	8·50–9·20	14·00–14·20	9·00–9·20	15·00–15·20
0	0	0	0	0	0	0	0	0	0	0	0	0
115	145	180	200	275	280	270	260	20	90	90	110	125
2	1	3	4	4	3	4	5	4	5	4	3	3
—	—	—	—	—	—	—	—	—	—	—	—	—
—	—	—	—	—	—	—	—	—	—	—	—	—
3.4	3.3	3.7	8.8	10.0	5.6	10.0	10.0	6.7	9.5	7.0	9.5	7.3
180	S100	S120	S105	P110	P100	P100	P90	P110	P90	P90	P110	P100
—	—	S120	S105	P110	P100	P100	P90	P110	P100	P90	P110	P100
—	—	5～10	15～20	15～20	25	35	35	120～140	30～40	30～60	20～30	25～30
—	—	0.5～0.8	1	1	0.5～1.0	0.5～1.0	1	2.5～3	1～1.5	1～1.5	1	0.5～1.0
—	—	2.5	3～3.5	3～4	4.5	4.5	4.5～5.5	10	5～6	6	4～5	4.5
—	—	—	—	—	—	—	—	—	—	—	—	—
P55	P80	P100	Existed but weak	Existed but weak	Existed but weak	Existed but weak	P110	Existed but weak	P150	P140	P130	P125
160	140	160					90		80～100	70～100	60～80	70
1	1.5	0～1.5					1		2～2.5	2.5～3	1.5～2.0	1～1.5
10～12	10	10					9		8	8	8	7～8
—	—	—	—	1.8	1.8	1.2	2.2	3.2	—	3.4	2.4	1.9
—	—	—	—	0.61	0.65	0.52	0.73	1.59	—	1.16	0.92	0.86
—	—	—	—	—	10	—	14	2.8	—	2.5	9	2.8
—	—	—	—	—	3.3	—	4.3	0.9	—	1.1	4.3	1.1
10.0	11.0	6.5	5.5	6.0	5.0	8.5	8.0	14.5	13.5	12.5	10.0	8.0
9.5	11.5	8.5	6.5	5.0	5.0	7.5	6.5	15.0	11.0	12.5	12.0	8.5
4.0	5.0	3.4	3.2	1.5	1.7	2.5	2.9	5.5	5.1	6.1	4.2	3.5
7.16	7.65	7.59	7.36	6.11	6.17	6.73	6.78	7.68	7.35	7.83	7.20	7.08
0	0	0	0	0	0	0	0.5	1.0	1.0	1.0	0.5	1.0
—	—	—	—	—	—	—	—	—	—	—	—	—

Table 4.8 Meteorological and

Date	Time	Abs. wind Vel. (m/sec)	Abs. wind Dir.	Atm. press. (mb)	Atm. temp. (℃)	Sea Scale	Swell Scale	Swell Dir.	Date	Time	Abs. wind Vel. (m/sec.)	Abs. wind Dir.	Atm. press. (mb)
	03	13.8	S S E							03	4.8	WNW	
	06	9.7	S E		27.0	6	6	S E		06	2.3	WNW	09.9
	09	10.5	S S E							09	3.5	WNW	
4	12	9.5	S	10.5	27.8	2	4	S E	5	12	3.3	N	09.4
	15	6.3	S E							15	3.3	NNW	
	18	4.5	S S E	10.7	27.1	2	1	S E		18	2.3	N	08.1
	21	4.0	S S E							21	1.7	NNE	
	24	3.3	S S E	10.7	27.0	1	1	S E		24	3.5	NNW	08.1
	03	9.0	N							03	6.7	NW	
	06	8.8	NNW	04.9	26.3	4	2	N		06	6.7	N	04.6
	09	8.8	N							09	7.3	N	
7	12	7.0	N	06.2	28.2	3	1	N	8	12	9.3	NNE	05.1
	15	6.8	N	03.5	29.0	3	2	NNE		15	13.0	NNE	04.6
	18	5.2	N	04.3	26.2	2	2	NNE		18	15.7	NNE	05.5
	21	7.0	N							21	16.5	NNE	
	24	9.2	N	04.2	25.0	3	1	N		24	17.8	NNE	06.3
	03	14.0	NW							03	14.0	NW	
	06	19.0	NNE	99.7	25.3	7	6	NE		06	10.5	NNW	06.9
	09	19.8	N	00.5	24.8	7	6	NNE		09	8.7	NW	
10	12	19.8	NNE	87.0	25.9	7	8	NE	11	12	5.8	NNW	09.9
	15	18.0	NNW	98.3	25.0	7	8	NE		15	10.3	NWW	
	18	18.0	N	00.8	23.4	7	8	N		18	12.4	NNW	07.9
	21	17.2	N							21	10.5	WNW	
	24	14.2	NNW		23.0	7	8	NNE		24	6.7	N	11.0
	03	5.7	NE							03	4.2	WSW	
	06	4.0	NE	14.6	23.3	2	3	NNE		06	2.3	WSW	10.8
	09	3.2	NNE	15.5	24.1	2	1	NE		09	4.0	WNW	11.0
13	12	1.0	WNW	15.0	26.9	1	2	NE	14	12	2.8	WNW	11.5
	15	1.9	N							15	3.3	WSW	09.1
	18	4.3	S	12.0	25.0	1	2	NE		18	3.0	SW	09.7
	21	2.7	S S W							21	6.7	W	
	24	5.7	S S W	12.7	25.4	1	1	NE		24	7.7	W	10.5

Wave Observation Records.

Atm. temp. (℃)	Sea Scale	Swell		Date	Time	Abs. wind		Atm. press. (mb)	Atm. temp. (℃)	Sea Scale	Swell	
		Scale	Dir.			Vel. (m/sec.)	Dir.				Scale	Dir.
					03	5.3	NNW					
26.2		2			06	0.0	—	06.9	25.7	1	1	NE
					09	3.5	N					
27.0	1	1	SSW	6	12	5.8	N	07.8	26.4	1	1	N
					15	6.5	NNE	05.5		3	2	N
26.6	1	1	SSW		18	9.2	N	05.7	26.0	3	3	N
					21	8.2	N					
26.4	1	1	SSW		24	8.3	NNW		26.0	2	2	N
					03	16.8	NE					
25.4	2	1	N		06	16.8	NE	05.5	21.7	6	7	NNE
					09	16.5	NNE	07.1	21.7	6	6	NNE
27.1	3	2	N	9	12	16.7	NNE	06.1	23.5	6	6	NNE
26.0	4	3	N		15	13.3	NE	04.0	24.0	6	6	NNE
25.0	4	3	N		18	14.1	NE	04.6	23.0	6	6	NE
					21	15.0	NNE					
24.0	6	7	N		24	16.2	NNE	03.2	24.3	6	6	NE
					03	6.8	NNE					
24.1	6	7	NNE		06	8.3	NE	13.5	23.6	3	2	N
					09	11.2	NNE					
23.8		5	N	12	12	10.8	N	15.5	23.1	4	2	N
					15	10.2	NNE					
23.8	4	5	N		18	8.5	NE	13.4	24.0	4	3	NNE
					21	6.3	E					
23.9	4	3	N		24	7.2	ENE	15.5	23.2	3	3	NNE
					03	6.2	W					
25.2	2	2	NE		06	5.8	W	09.5	24.8	2	2	NE
26.2	1	2	ENE		09	2.8	W	11.3	26.5	2	2	E
27.0	1	2	ENE	15	12	6.8	W	11.3	28.0	2	2	E
26.8	1	2	N		15	9.7	NW	11.2	25.5	2	1	NW
26.0		2	NE		18	7.5	NW	12.4	24.7	3	1	WNW
					21	6.8	NW					
24.8	2	2	NE		24	5.8	NW	13.5	24.0	3	1	WNW

Table 4.8 Meteorological and Wave

Date	Time	Abs. wind		Atm. press. (mb)	Atm. temp. (℃)	Sea Scale	Swell		Date	Time	Abs. wind		Atm. press. (mb)
		Vel. (m/sec)	Dir.				Scale	Dir.			Vel. (m/sec)	Dir.	
	03	5.3	NNW							03	5.7	E	
	06	5.5	N	14.7	23.2	2	1	NW		06	6.3	ESE	15.4
	09	5.2	NNE							09	7.0	ESE	
16	12	4.8	ENE	15.7	26.3	1	1	N	17	12	7.3	ESE	15.7
	15	4.8	NE							15	7.7	ESE	
	18	4.8	NE	15.2	24.5	1	1	NNW		18	7.7	SSE	14.8
	21	6.7	ENE							21	7.8	ESE	
	24	5.5	E	16.6	24.8	1	1	NNW		24	9.3	ESE	14.5
	03	4.7	S							03	13.5	S	
	06	7.3	SSE	10.7	26.2	2	1	SSE		06	8.3	SSW	08.7
	09	7.0	SSE							09	8.2	WSW	
19	12	10.5	SSE	10.7	26.8	2	1	SSE	20	12	7.2	WNW	
	15	11.2	SSE							15	11.0	WNW	09.0
	18	10.7	SSE	09.4	27.0	3	1	S		18	10.4	WNW	09.8
	21	13.0	SSE							21	11.8	WNW	
	24	12.8	SSE	09.2	26.7	3	2	S		24	6.0	NNW	10.7
	03	8.8	N							03	6.8	NE	
	06	10.7	N	15.0	21.4	3	3	NNW		06	6.3	NE	16.7
	09	9.5	N	17.0	23.0	3	3	NNW		09	6.1	NE	
22	12	8.3	NNW	17.0	25.5	3	3	NNW	23	12	6.3	NE	17.0
	15	7.3	NNE	15.2	22.5	3	3	NNW		15	5.5	NNE	
	18	7.5	NE	15.7	22.6	3	3	N		18	6.2	NNE	16.7
	21	8.0	NNE							21	5.8	NNE	
	24	6.8	NE	17.5	22.2	3	3	N		24	6.0	NE	17.2

Observation Record (Continued)

Atm. temp. (℃)	Sea Scale	Swell		Date	Time	Abs. wind		Atm. press. (mb)	Atm. temp. (℃)	Sea Scale	Swell	
		Scale	Dir.			Vel. (m/sec)	Dir.				Scale	Dir.
					03	8.8	S E					
22.5	1	1	E N E		06	8.3	S S E	13.0	25.9	3	1	S E
					09	10.0	S S E	13.4	26.3	3	1	S E
26.0	2	1	E	18	12	7.0	S	12.6	26.8	3	1	S E
					15	5.0	S	12.6	26.6	3	1	S E
26.6	2	1	E N E		18	5.0	S	11.0	27.0	1	1	S S E
					21	5.0	S S W					
25.5	2	1	E N E		24	7.7	S S E	11.5	26.3	1	1	S S E
					03	7.7	N					
26.1	4	4	S		06	8.5	N	12.0	23.0	3	3	NW
					09	9.5	N	13.5	23.9	3	3	NW
27.0	2	2	W	21	12	7.5	N N W	12.3	26.0	3	3	NW
26.9	4	2	NW		15	6.8	N N W	12.6	26.0	4	3	NW
24.7	3	3	NW		18	7.0	N N W	14.7	22.6	3	3	NW
					21	6.7	N					
24.0	1	2	NW		24	8.7	N	16.1	21.5	3	3	N N W
					03	8.8	N E					
22.0	3	3	N		06	9.8	N N E					
					09	8.2	N E					
23.0	2	1	N E	24	12	7.5	N E					
					15	8.3	N E					
22.2	2	1	N E		18	5.8	N E					
					21	7.1	E N E					
22.1	2	1	N E		24	9.5	N E					

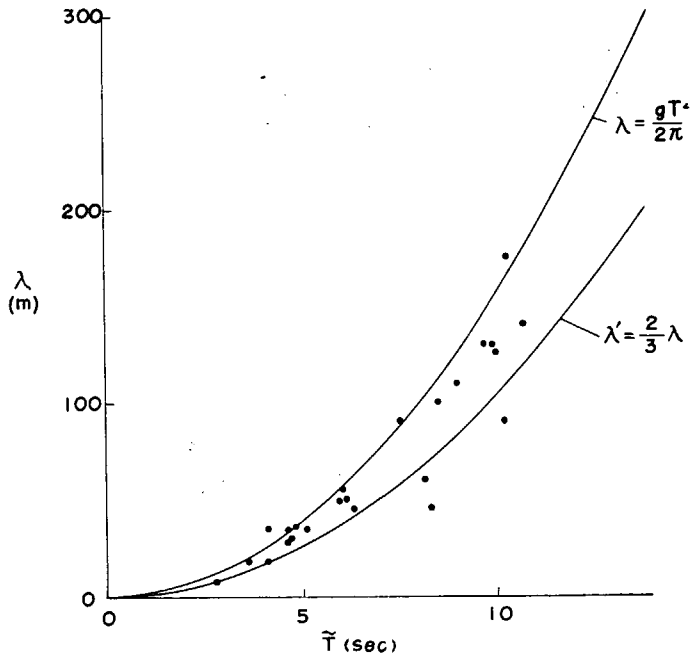

Fig. 4.18 Average Length of Waves *vs.* Average Period of Waves.

$$\lambda = k \cdot \frac{g\tilde{T}^2}{2\pi} \qquad k = 1 \sim \frac{2}{3}$$

Regarding the wave period $\tilde{T}$, following formula developed on the basis of Neumann's spectrum coincides very well with the measured value, when the mean wind velocity U for 6 hours before the measurement is used. (See Fig. 4.19)

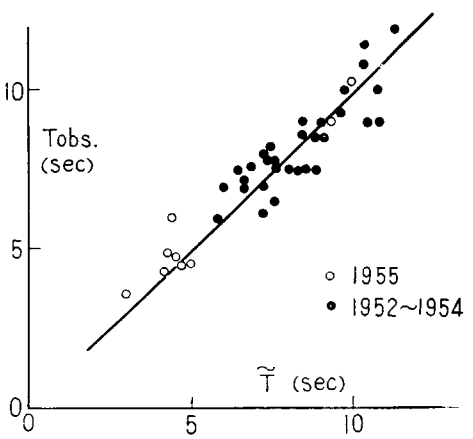

Fig. 4.19 Wave Periods from Neumann Spectrum.

$$\tilde{T}=0.568U \qquad \tilde{T} \text{ in sec.; } U \text{ in m/sec}$$

Regarding the wave height, satisfactory results were obtained by using the method of Sverdrup-Munk-Bredtschneider.

2.2 Oscillation of the Ship.

As the ship was made it a rule to drift during the observation at Tango and consequently was subjected to wind and wave approximately from athwartship direction, pitching of the ship was very small. In this Chapter, therefore, reference is made only to the rolling.

Since the ship is in general subject to at least 2 series of seas and swells in ocean, magnification factor μ was obtained in the following form when several wave series existed:

$$\mu=\frac{\text{Average angle of rolling}}{\text{Average effective slope of waves}}$$

$$=0.30\frac{\bar{\theta}}{H_e^{0.2}}=f_n(\Lambda) \qquad H_e \text{ in m; } \bar{\theta} \text{ in deg.}$$

$$\Lambda=\frac{T_s}{T_e}=0.24\frac{T_s}{H_e^{0.4}} \qquad T_s \text{ in sec.; } H_e \text{ in m}$$

where, $\bar{\theta}$ is the mean amplitude of rolling, T_s is the natural period of rolling, H_e and T_e are the values to be regarded as significant wave height and wave period respectively. Let H_i=height of each wave series in m and α_i=angle from the longitudinal direction of the ship to the crest line of waves, then H_e and T_e are assumed as:

$$H_e^2=\sum_i H_i^2\cos^2\alpha_i$$
$$E=H_e^2/2.83^2$$
$$T_e=6.24E^{0.2}$$

Fig. 4.20 indicates the relation between μ and Λ. Owing to the irregularity of external force, μ is smaller than that for regular waves applied to the ship from athwartship direction.

Nextly, let $[\theta(\omega)]^2$=energy spectrum of rolling angle and $[r(\omega)]^2$=energy spectrum of wave height, then the vertual response amplitude operator $A_a(\omega)$ is obtained by the following formula and indicated in Fig. 4.21.

$$[A_a(\omega)]^2=[\theta(\omega)]^2/[r(\omega)]^2$$

$A_a(\omega)$ can vary according to the divergence of the directions of component

wave series, but their forms fairly resemble each other. $A(\omega)$ is the response amplitude operator for waves applied to the ship from athwartship direction obtained by the calculation.

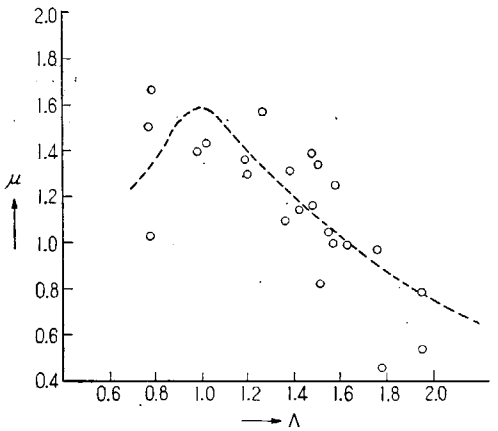

Fig. 4.20 Magnification Factor in Confused Sea.

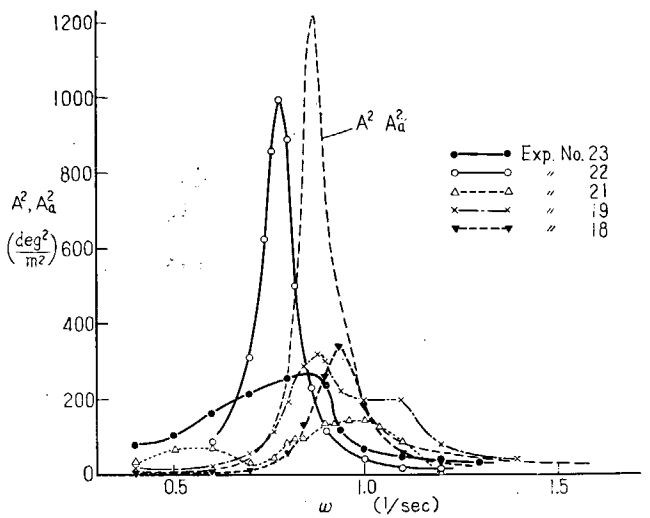

Fig. 4.21 Apparent Response Amplitude Operator.

Chapter 3 Experiment by Observation Ship "Atsumi"

The experiment by observation ship "Atsumi" was carried out from 2nd to 17th October, 1956. Though the time of this experiment was later than that by "Miyajima Maru" described in the next Chapter, the results of this

experiment is mentioned succeedingly, as it was conducted by the ship of the same form and at the same place as that mentioned in the preceding Chapter.

The measuring instruments were nearly the same as those in the previous year, except that a few improvements were made in small parts. The wave height meter was, however, fitted with a ring buoy, movable to vertical direction along the pole, containing a recording cylinder in the inside to enable to record automatically the relative movement between the pole and buoy. The outline is illustrated in Figs. 4.22 and 4.23. This apparatus was proved effective in the experiment, though there was a difficulty in its use when the sea condition was violent. The wave slope was not measured in this experiment. Three observers participated in the experiment similar to that in the previous year.

The results of the observation are given in Table 4.9. As the sea was calm during the period of observation, number of measurements were considerably fewer than anticipated at the beginning. It is much regretted, however, that the analysis of the results made later disclosed that even the data for small wave height was available to a great extent.

It was recognized that the assembly of the readings of wave height, rolling angle, etc. at equal intervals exhibited normal distribution. The results of the statistical analysis will be summarized in Chapter 4.

Fig. 4.24 shows an example of the record of ship's rolling expressed, through analysis, in energy spectrum (Exp. No. 4). In this example, continuous recording of wave height could be made simultaneously, so that energy spectrum of wave height is also shown in the above figure. It may be noted from this figure that the sensibility to frequency in rolling motion is remarkable.

Fig. 4.25 indicates the results of vertual response amplitude operator obtained according to the definition mentioned in Chapter 2. In Exp. No. 16, it is expressed in term of $[r(\omega)]^2$ by using Neumann's spectrum, where wind velocity was assumed to be 14 m/sec and duration of wind blowing to be 12 hours. The value in Exp. No. 4 coincides very well with $A(\omega)$ mentioned in the preceding Chapter, while that in Exp. No. 16 is appreciably small. This difference may be due to the deviation of $[r(\omega)]^2$ from actual value.

Table 4.9 Results of the Measurements

Exp No.			1	2	3	4	5	6	7
Date			4	4	4	5	6	9	9
Time			9·00	12·00	15·00	14·00	9·00	9·00	12·20
Position			135°06′E 28°47′N	136°05′E 28°50′N	135°02′E 28°50′N	134°52′E 28°53′N	134°56°E 28°57′N	134°57′E 28′56′N	134°59′E 28°56′N
Ship speed			0	0	0	0	0	0	0
Beauf. Scale			2	2	3	1	2	3	4
Abs. Wind	Vel. (m/sec)	Max.							
		Var.							
		Average	2.8	4.8	7.5	1.2	4.2	8.3	10.5
	Direction		11 ESE	10 ESE	11 ESE	06 ENE	16 SSE	25 WSW	29 WNW
Wave	Sea	Wave L. λ	1.2~1.5	1.2~1.5	7.5~10	2~3		20	40
		Wave H. h	0.3	0.3	0.5~0.8	0.1~0.05		1	2
		Rel. Dir. α				S 60		P 130	P 130
		Period T	3	3	2.2~3.5			3.5~4.5	4.5~6.3
	Swell	Wave L. λ	120~190	90~130			30~50		
		Wave H. h	1	1.5	1.5	1	0.5~0.7		
		Direction α	S 80	S 90	S 80	S 70	P 70~40		
		Period T	8.6~13.1	6.5~11.2	6.5~8.5	5.4~7.8	6.6~8.0		
	Swell	Wave L. λ			25~30	20	70~90		
		Wave H. h	0.8	1	1~1.5	0.8~1	0.8~1		
		Direction α	S 130	S 150	S 140	S 140	P 130~160		
		Period T	9	5.0~5.5	4.7~5.1	3.6~5.2	8~9.2		
Rolling	Rel.	Max. Ang.	5.40	7.20	7.00	7.90	3.85	5.45	6.75
		Aver. Ang.	2.19	3.05	2.92	2.36	1.05	1.20	2.21
		Period	6.77	6.89	7.05	7.08	6.89	5.87	5.75
Course			7	2	5	351	271	343	21

Remark: λ and h in m. T in sec. Roll. angle in deg. Period in sec.

on board the "Atsumi", 1956

8	9	10	11	12	13	14	15	16
11	12	12	13	14	14	15	15	15
14·00	13·00	14·00	9·30	12·30	14·00	8·30	10·00	15·40
135°28′E 28°47′N	135°36′E 28°45′N	135°35′E 28°43′N	135°27′E 28°32′N	135°19′E 28′37°N	135°18′E 28°39′N	135°05′E 28°29′N	135°02′E 28°26′N	134°58′E 28°23′N
0	0	0	0	0	0	0	0	0
3	3	3	4	2	3	5	5	5
7.2	7.3	8.3	9.5	3.2	4.0	13.3	15.2	14.0
23 SW	03 NNE	03 NNE	34 NNW	10 E	7 ENE	05 NE	03 NE	03 NNE
			8～10			40～50	50	50～70
			0.3～0.5			1.5～2.0	2.0～2.5	2.5～3.0
			P90			P80～110	P90	P110
						5～7	5～7	5～8
			50～70					
			1.5～2.5					
			S110～120					
			7.2～8.5					
			30～40					
			1.5					
			P150～160					
			5.5～7.5					
2.40	4.05	9.45	11.80	7.50	8.75	18.20	15.90	20.00
0.88	1.44	2.98	4.23	2.84	3.78	6.74	5.98	6.30
7.03	7.35	7.32	6.69	6.92	7.29	6.95	7.08	7.38
127	278	277	184	175	157	145	140	127

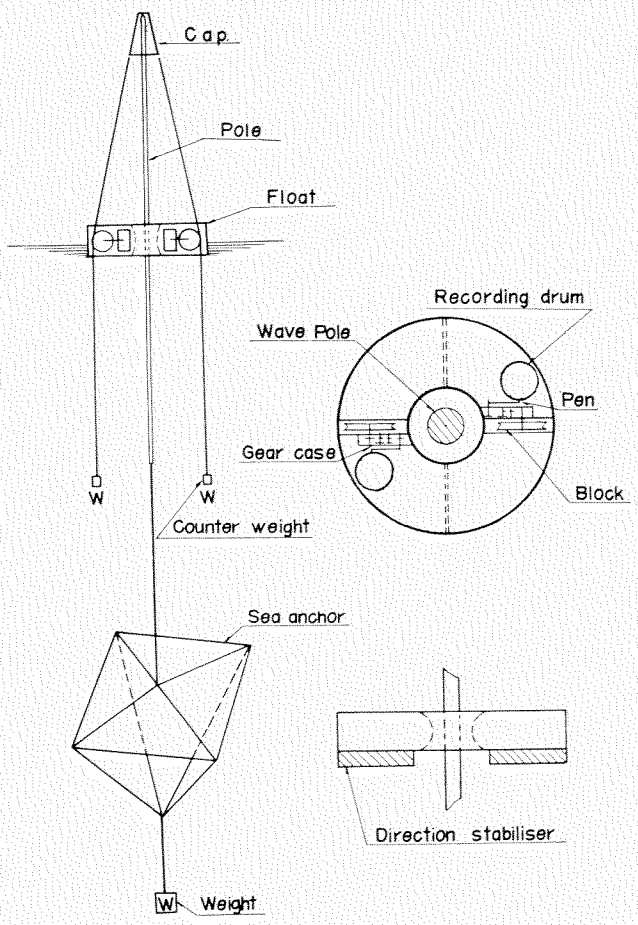

Fig. 4.22 Wave Recorder.

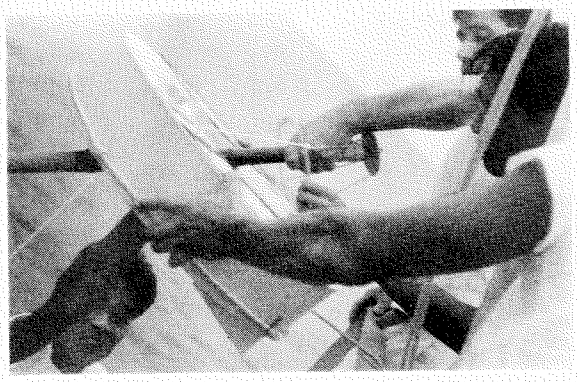

Fig. 4.23

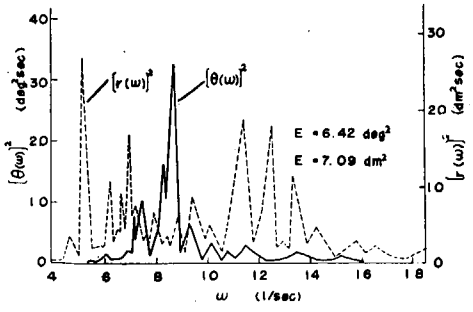

Fig. 4.24 Energy Spectrum of Exp. No. 4.

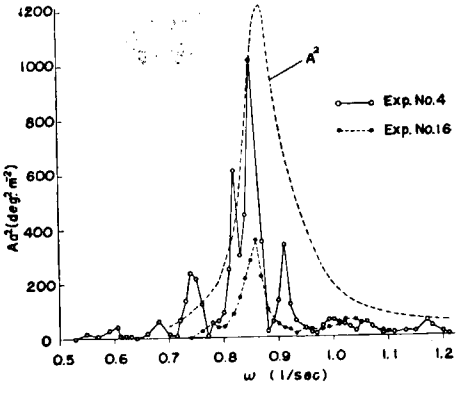

Fig. 4.25 Apparent Response Amplitude Operator.

Chapter 4 Experiment by Factory Ship "Miyajima Maru"

This experiment was conducted from 7th May to 15th June, 1956 in the sea area where salmon and trout fishing by a fleet of fishing boats was made. The locations of the ship at noon are as shown in Fig. 4.26. The observations were made in their vicinities. Number of observers participated in the experiment were limited to two.

Table 4.10 Principal Particulars of the "Miyajima-Maru"

Length (O.A.)	151.25 m	
Length (P.P.)	140.00 m	
Breadth (Mld.)	19.00 m	
Depth (Mld.)	10.50 m	
Load draft	8.321	
Coefficients at load draft	$C_b=0.700$ $C_p=0.709$ $C_w=0.821$	
Tonnage	Gross 9598.76 Net 5253.88	
Main engine	Type...Hitachi *B* & *W* 2 Cycle Single Acting Diesel Engine.	
Propeller	Service	5100 BHP×112 rpm
	No. of prop.	1
	No. of blade	4
	Dia × Pitch	5.200×4.110 m
Speed	Trial	17.28 kt
	Service	14.5 kt
Capacity	F.O.T.	2201.18 t
	F.W.T.	2589.19 t
	B.W.T.	1709.12 t
Refrigerating cargo hold	7575.51 m³	
Salted cargo hold	871.78 m³	
Salt space	560.98 m³	
Complement (in April, 1956)	351	

Principal particulars and the profile of "Miyajima Maru" are shown in Table 4.10 and Fig. 4.27 respectively. The ship has, being a factory ship, facilities of canning, refrigerating and salting. When salmons and trouts are carried on board by the fishing boats 70 *GT* in the mean in the day time, they are briefly disposed of on the working deck, then carried to the factories on upper deck and stored in the hold. For this purpose, wooden frame work is temporarily fitted on the working deck during the fishing season, which causes to increase in a small amount the projected lateral area of the ship subjected to wind pressure and to produce free water surface at various places. On the other hand, in order to expedite the work on the deck, the ship goes ahead slowly

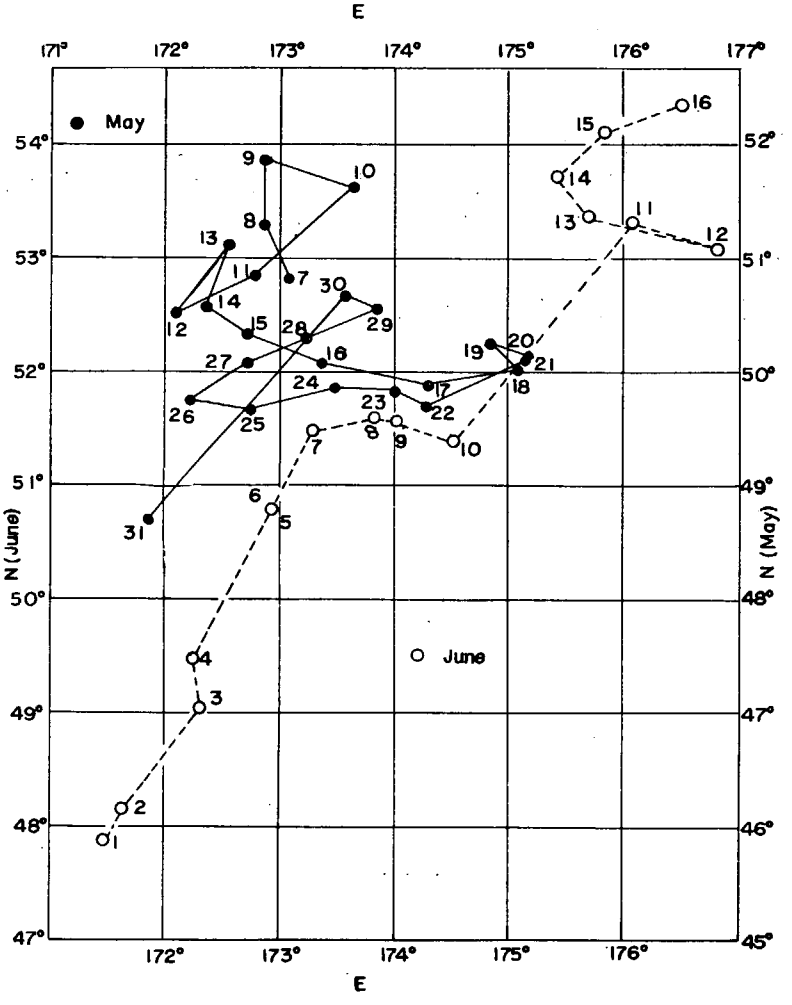

Fig. 4.26

facing waves and avoids the rolling as far as possible. Consequently, no record of rolling of large angle was registered, which is quite contrary to the results mentioned in preceding two paragraphs.

Mean draught, displacement and GM during the period of observation are shown in Fig. 4.28. Longitudinal GM_L were approximately constant and

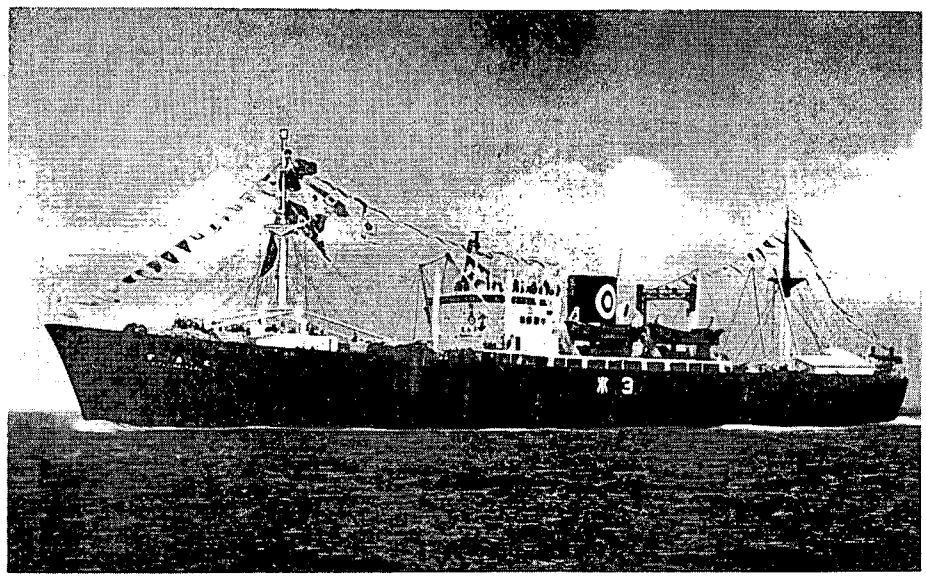

Fig. 4.27

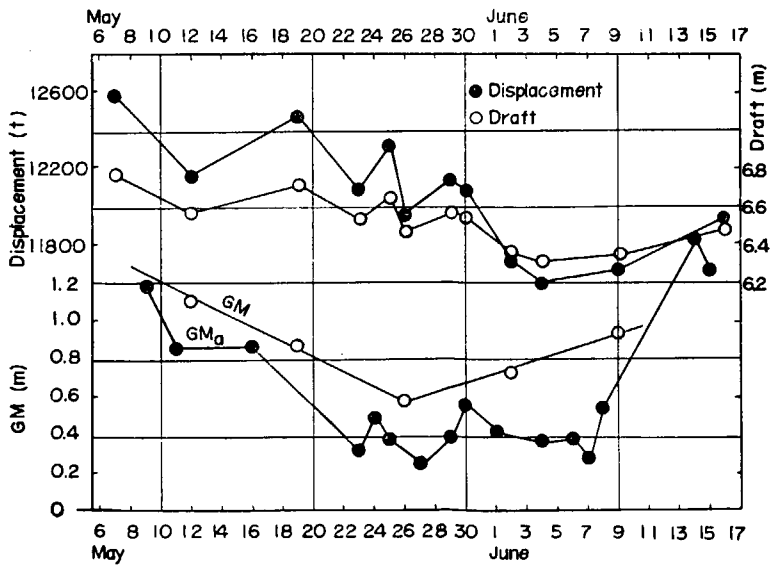

Fig. 4.28

Table 4.11 Records of the Observations

	Date	May 7	7	7	7	8	8	8
	Time[1]	8·00	12·00	14·00	16·00	8·00	12·00	16·00
	Position	50°33′N 173°03′E	50°49′N 173°04′E	50°48′N 173°07′E	50°47′N 173°09′E	51°11′N 172°55′E	51°17′N 172°51′E	51°28′N 172°46′E
	Course	100	115	95	68	265	255	255
	Dispt. (t)	12600	12600	12600	12600	12500	12500	12500
	Ship speed (kt)	0	0	0	0	0	0	0
Wind	Rel. ave. vel. (m/sec)	6.0	5.5	5.0	5.0	7.0	10.0	13.0
Wind	Relative direction	P130	P150	P125	P115	P100	P108	P100
Wind	Beauf. scale	5	5	5	5	6	7	9
Rolling	Max. θ_{max} [2]	1.0		0.5			0.5	1.8
Rolling	r.m.s. $\sqrt{\overline{\theta^2}}$ [3]							
Pitching	Max. ψ_{max} [2]	2.0		1.3			1.3	2.3
Pitching	r.m.s. $\sqrt{\overline{\psi^2}}$ [3]							
Sea	Length λ (m)			20				40
Sea	Height h (m)	0.8	0.5	0.5	0.5	0.8		1.0
Sea	Ave. period T (sec)	5.65	5.31	4.78	5.12	4.62	4.96	4.68
Sea	Range of period T_{max}/T_{min}	6.2/5.0	6.4/4.5	6.2/3.7	6.2/4.0	5.0/4.0	5.8/3.3	5.9/3.5
Swell (1)	Length λ (m)							
Swell (1)	Height h (m)	1.3	1.2	1.3	1.0	0.5	1.0	1.1
Swell (1)	Ave. period T (sec)	8.58	8.10	8.10	7.86	4.00	6.04	6.75
Swell (1)	Range of period T_{max}/T_{min}	10.5/7.6	9.6/7.0	10.5/6.3	10.0/6.9		6.6/4.7	8.5/5.3
Swell (1)	Angle of encounter	P75	P75	P45	P38	P60	P70	P67
Swell (2)	Length λ (m)							
Swell (2)	Height h (m)							
Swell (2)	Ave. period T (sec)							
Swell (2)	Range of period T_{max}/T_{min}							
Swell (2)	Angle of encounter							
Swell (3)	Length λ (m)							
Swell (3)	Height h (m)							
Swell (3)	Ave. period T (sec)							
Swell (3)	Range of period T_{max}/T_{min}							
Swell (3)	Angle of encounter							
	Rolling Period (sec)							
	Pitching Period (sec)	7.3		7.6			6.0	6.9

on board the "Miyajima Maru", 1956

9	9	9	10	10	10	11	11	11
8·00	12·00	16·00	8·00	12·00	17·00	8·00	12·00	16·00
51°49′N 172°48′E	51°51′N 172°51′E	51°55′N 172°58′E	51°21′N 172°31′E	51°37′N 173°37′E	51°35′N 172°37′E	50°50′N 172°36′E	50°50′N 172°46′E	50°49′N 172°51′E
0	345	0	305	98	160	80	82	70
12400	12400	12400	12300	12300	12300	12200	12200	12200
0	0	0	0	0	0	0	0	0
13.0 P90 9	12.0 P100 8	12.5 P100 9	0.3 P90 0	4.5 P60 4	4.7 P105 4	8.0 P110 6	8.5 P105 7	7.0 P105 6
2.3						1.3	1.8	0.5
2.0						2.0	1.0	1.3
1.5 5.96 6.5/5.5	2.0 7.70 9.4/6.9	1.0 5.65 6.4/4.8	1.0 7.87 8.2/7.6			1.4 5.95 7.6/4.1	1.3 6.13 8.0/4.6	0.8 5.86 7.2/4.7
		1.0 8.46 10.5/6.9 P160	1.3 9.66 12.5/7.7 P118	0.9 9.56 11.5/8.2 S55	0.9 9.80 11.9/7.8 S30	0.8 5.18 6.0/4.3 P30	1.0 5.17 5.7/4.4 P48	0.7 5.89 6.8/5.0 P40
					2.5 5.00 5.3/4.7 P38			
19.7 7.2	7.2					6.8	7.3	6.9

Table 4.11 Records of the Observations on

Date		May 12	12	12	12	13	13	13
Time		8·00	12·00	16·00	17·00	8·00	10·00	12·00
Position		50°27′N 172°14′E	50°30′N 172°05′E	50°28′N 172°10′E	50°25′N 172°11′E	51°10′N 172°44′E	51°08′N 172°38′E	51°07′N 172°33′E
Course		285	257	306	162	250	258	260
Dispt. (t)		12200	12200	12200	12200	12200	12200	12200
Ship speed (kt)		0	0	0	7	2.7	2.7	2.7
Wind	Rel. ave. vel. (m/sec)	8.0	14.0	10.0	12.5	18.0	15.0	20.0
	Relative direction	P105	P105	P95	S85	S10	P5	S10
	Beauf. scale	6	9	7	9	11	10	12
Rolling	Max. θ_{max}		0.8	1.0	1.0	3.5	6.0	4.0
	r.m.s. $\sqrt{\overline{\theta^2}}$					1.55		1.54
Pitching	Max. ψ_{max}		2.0	1.5	2.5	3.5	3.5	4.0
	r.m.s. $\sqrt{\overline{\psi^2}}$					1.43	1.63	1.90
Sea	Length λ (m)							
	Height h (m)	1.0	2.0		2.0	4.8	5.0	5.7
	Ave. period T (sec	4.94	6.40	5.13	6.63	10.93	11.51	11.83
	Range of period T_{max}/T_{min}	5.6/3.7	7.1/5.5	6.2/4.7		14.3/7.6	12.6/10.8	14.1/8.9
Swell (1)	Length λ (m)							60
	Height h (m)	0.7	1.0	1.8		2.0		2.0
	Ave. period T (sec)	7.46	7.20	8.53	4.63	6.24		
	Range of period T_{max}/T_{min}	7.8/6.3	7.9/6.6	9.5/7.6		7.6/5.6		
	Angle of encounter	P55	P30	S40	P8	P25		P45
Swell (2)	Length λ (m)							
	Height h (m)							
	Ave. period T (sec)							
	Range of period T_{max}/T_{min}							
	Angle of encounter							
Swell (3)	Length λ (m)							
	Height h (m)							
	Ave. period T (sec)							
	Range of period T_{max}/T_{min}							
	Angle of encounter							
Rolling Period (sec)			8.5			12.1	12.2	10.5
Pitching Period (sec)			7.9	8.0	6.7	8.9	8.3	9.2

board the " Miyajima Maru ", 1956 (continued)

13	13	14	14	14	15	15	15	16
14·00	16·00	8·00	12·00	16·00	8·00	12·00	16·00	8·00
51°06′N 172°28′E	51°06′N 172°26′E	50°36′N 172°18′E	50°33′N 172°21′E	50°32′N 172°25′E	50°13′N 172°33′E	50°19′N 172°42′E	50°24′N 172°52′E	50°14′N 173°28′E
265	260	208	210	215	7	0	356	135
12200	12200	12200	12200	12200	12300	12300	12300	12300
2.7	2.7	0	0	0	0	0	0	0
17.0	15.0	10.0	8.2	6.5	7.0	6.5	6.7	7.0
S 10	S 30	S 105	S 105	S 105	P 90	P 100	P 105	P 100
10	10	7	7	5	6	5	6	6
7.0	4.5	0.8			0.8	0.5		
1.42	1.57							
6.8	4.5	3.0			1.5	1.5		
1.64	1.33	0.87						
5.7	4.7	1.3	1.4	1.0	1.0	1.0	0.8	0.7
11.11	11.08	6.90	6.67	6.62	5.60	5.58	5.42	4.40
14.1/9.0	13.3/8.7	8.1/5.9	7.9/5.6	6.9/5.5	6.0/5.2	6.2/4.5	7.0/4.0	5.2/3.8
2.3	1.9	2.0	1.9	1.8	1.3	1.5	1.5	1.0
6.53	6.68	9.38	9.72	9.78	8.20	9.22	9.29	9.60
7.0/6.1	7.4/6.0	12.0/6.4	11.9/7.8	11.0/8.5	8.7/8.0	11.0/8.0	11.4/8.1	9.8/9.4
P 50	P 45	S 50	S 40	S 50	P 115	P 130	P 135	S 130
10.9	11.8	8.5				9.2		
8.1	9.3	7.5			6.3	7.0		

Table 4.11 Records of the Observations on

Date	May 16	16	17	17	17	18	18
Time	12·00	16·00	8·00	12·00	16·00	8·00	9·00
Position	50°04′N 173°21′E	50°00′N 173°24′E	49°50′N 174°10′E	49°53′N 174°17′E	49°53′N 174°12′E	49°55′N 175°07′E	49°56′N 175°07′E
Course	105	45	34	8	336	261	271
Dispt. (t)	12300	12300	12400	12400	12400	12400	12400
Ship speed (kt)	0	0	0	0	0	0	0
Wind: Rel. ave. vel. (m/sec)	6.5	5.0	5.5	5.0	3.5	10.0	14.0
Wind: Relative direction	P105	P90	P95	P90	P95	P00	P00
Wind: Beauf. scale	6	5	5	5	4	7	9
Rolling: Max. θ_{max}	0		1.3	1.0		0.3	
Rolling: r.m.s. $\sqrt{\theta^2}$							
Pitching: Max. ψ_{max}	1.0		2.0	1.5			
Pitching: r.m.s. $\sqrt{\overline{\psi^2}}$							
Sea: Length λ (m)				18	20		
Sea: Height h (m)	1.1	0.5	1.0	0.5	0.5	1.3	1.8
Sea: Ave. period T (sec)	4.48	3.89	5.15	4.04	4.03	4.71	5.73
Sea: Range of period T_{max}/T_{min}	5.7/3.1	4.5/3.1	5.7/4.4	5.2/2.6	4.4/3.6	5.5/4.4	6.1/5.4
Swell (1): Length λ (m)					75		
Swell (1): Height h (m)			0.8	1.8	1.8	1.0	
Swell (1): Ave. period T (sec)			5.42	8.54	8.70	6.30	
Swell (1): Range of period T_{max}/T_{min}			6.2/4.8	9.2/7.7	9.7/6.7	6.7/5.8	
Swell (1): Angle of encounter			P40	P150	P140	P40	
Swell (2): Length λ (m)							
Swell (2): Height h (m)					1.8		
Swell (2): Ave. period T (sec)					8.60		
Swell (2): Range of period T_{max}/T_{min}					9.5/7.2		
Swell (2): Angle of encounter					P130		
Swell (3): Length λ (m)							
Swell (3): Height h (m)							
Swell (3): Ave. period T (sec)							
Swell (3): Range of period T_{max}/T_{min}							
Swell (3): Angle of encounter							
Rolling Period (sec)							
Pitching Period (sec)			8.4	7.7			

board the "Miyajima-Maru", 1956 (continued)

18	18	18	18	19	19	19	19	19
10·00	12·00	14·00	16·00	3·00	6·20	8·00	10·00	12·00
49°57′N 175°06′E	50°01′N 175°05′E	50°04′N 175°05′E	50°06′N 175°05′E	50°28′N 175°05′E	50°27′N 174°59′E	50°25′N 174°56′E	50°22′N 174°50′E	50°15′N 174°50′E
269	288	300	300	340	230	235	152	160
12400	12400	12400	12400	12500	12500	12500	12500	12500
0	0	0	0	2	2	3	0	0
15.0	12.0	12.0	9.0	16.0	18.0	13.0	11.5	8.0
P95	P110	P100	P100	P110	S30	S40	S110	S100
10	9	8	7	10	11	9	8	6
1.3	2.0	2.5	3.5	9.8		3.0	6.8	10.5
				3.20			2.70	3.10
2.5	2.3	2.0	1.8	2.0		4.3	3.0	2.0
						1.79	0.93	
				80				
1.8	2.1	2.4	1.9	6.0	6.5	7.5	6.0	4.6
6.05	7.03	7.23	7.27	11.53	11.70	11.73	10.63	9.96
6.8/5.6	7.8/6.3	8.5/6.1	9.0/6.1	13.4/10.2	16.5/7.9	13.5/10.5	12.5/9.2	12.5/8.3
				40	45			
	0.9		1.0	2.0	2.0			1.8
	5.04			6.20				5.80
	5.8/3.8			7.6/5.1				6.8/5.1
	P35		P70	P135	P55			S140
		8.8	9.9	11.4		18.0	14.1	12.9
6.3	8.4	7.7		6.9		7.3	7.1	6.8

Table 4.11 Records of the Observations on

Date		19	20	20	20	21	21	21
Time		16·00	8·00	12·00	16·00	6·00	8·00	10·00
Position		50°09′N 174°59′E	50°03′N 175°05′E	50°08′N 175°10′E	50°11′N 175°11′E	50°31′N 174°57′E	50°31′N 174°57′E	50°17′N 175°00′E
Course		165	25	8	280	245	255	160
Dispt. (t)		12500	12400	12400	12400	12300	12300	12300
Ship speed (kt)		0	0	0	0	0	0	7.5
Wind	Rel. ave. vel. (m/sec)	7.0	4.0	3.5	10.0	14.0	9.5	10.0
	Relative direction	S95	P85	S120	P120	P100	P95	S35
	Beauf. scale	6	4	3	7	9	7	7
Rolling	Max. θ_{max}	6.0	1.0	1.0			3.3	1.0
	r.m.s. $\sqrt{\overline{\theta^2}}$	2.26						
Pitching	Max. Ψ_{max}	2.3	1.8	1.3			1.8	4.5
	r.m.s. $\sqrt{\overline{\Psi^2}}$							1.75
Sea	Length λ (m)				18			
	Height h (m)	4.6	0.5		0.7	4.3	4.3	4.3
	Ave. period T (sec)	12.05			3.64	9.14	9.47	9.56
	Range of period T_{max}/T_{min}	16.4/8.9			4.2/3.0	11.4/7.9	10.7/7.3	11.5/8.2
Swell (1)	Length λ (m)							
	Height h (m)	1.8	2.3	1.8	1.8		1.5	
	Ave. period T (sec)	6.16	7.84	8.51	8.82		4.41	
	Range of period T_{max}/T_{min}	8.1/4.7	10.5/6.1	9.2/8.1	10.3/7.8		5.2/3.8	
	Angle of encounter	S45	P130	P140	P30		P45	
Swell (2)	Length λ (m)							
	Height h (m)							
	Ave. period T (sec)							
	Range of period T_{max}/T_{min}							
	Angle of encounter							
Swell (3)	Length λ (m)							
	Height h (m)							
	Ave. period T (sec)							
	Range of period T_{max}/T_{min}							
	Angle of encounter							
Rolling Period (sec)		10.7					9.0	
Pitching Period (sec)		6.9	7.3	8.5			8.3	6.5

board the "Miyajima Maru", 1956 (continued)

21	21	21	21	22	22	22	22	22
12·00	14·00	15·00	16·00	8·00	10·00	12·00	14·00	16·00
50°06′N 175°06′E	49°53′N 175°00′E	49°40′N 174°50′E	49°40′N 174°42′E	49°49′N 174°32′E	49°47′N 174°22′E	49°42′N 174°16′E	49°41′N 174°08′E	49°44′N 174°00′E
223	225	228	227	250	265	262	277	295
12300	12300	12300	12300	12200	12200	12200	12200	12200
7.5	8.5	8.5	8.5	2.4	2.4	3.3	3.3	3.3
11.0	20.0	22.0	20.0	18.0	18.8	19.0	17.0	15.0
0	S 60	S 50	S 55	S 20	S 10	S 15	S 24	S 30
8	12	12	12	11	11	11	11	10
3.3	3.3		2.8	5.5	9.0	5.3		5.0
				2.68	3.44	2.04		1.66
4.3	4.5		5.8	5.0	4.0	5.3		5.3
1.39	1.42		2.13	1.98	1.45	2.09		1.52
				200			180	
1.5	3.0	4.0	4.0	7.1	7.5	8.6	8.5	8.3
4.07	6.04	6.50	7.16	10.89	10.45	10.20	10.52	8.96
5.1/3.2	6.7/5.4	7.9/5.3	8.0/6.1	13.5/9.5	12.7/8.4	13.0/8.1	12.0/8.5	
				55			48	
4.7	1.8	2.8	3.0	1.8	3.5		3.0	3.0
8.65	7.30	8.35	8.93		6.89			
9.4/8.0	7.8/6.8	9.7/7.4	9.7/8.4		7.7/5.8			
P 45	P 20	P 15	P 20	P 45	P 45	S 40	P 40	P 40
				12.9	14.0	13.8		13.6
7.1	6.9		7.1	7.3	9.4	8.7		7.8

Table 4.11 Records of the Observations on

Date	May 23	23	23	24	24	24	24
Time	8·00	10·00	16·00	8·00	10·00	12·00	13·00
Position	49°54′N 173°56′E	49°50′N 174°00′E	49°54′N 173°56′E	49°40°N 173°25′E	49°54′N 173°27′E	49°51′N 173°28′E	49°54′N 173°28′E
Course	92	88	105	275	285	291	290
Dispt. (t)	12100	12100	12100	12200	12200	12200	12200
Ship speed (kt)	0	0	0	0	0	0	0
Wind: Rel. ave. vel. (m/sec)	7.0	6.0	4.0	8.3	9.0	10.0	10.5
Wind: Relative direction	P100	P110	P100	P95	P110	P100	P110
Wind: Beauf. scale	6	5	4	7	7	7	8
Rolling: Max. θ_{max}	2.3	1.5				1.8	
Rolling: r.m.s. $\sqrt{\theta^2}$							
Pitching: Max. Ψ_{max}	1.8	2.5				1.8	
Pitching: r.m.s. $\sqrt{\Psi^2}$							
Sea: Length λ (m)		30		30	35		
Sea: Height h (m)	0.9	1.0	0.5	1.3	1.5	1.8	2.3
Sea: Ave. period T (sec)	4.10	4.26		5.00	5.85	5.93	7.03
Sea: Range of period T_{max}/T_{min}	4.4/3.6	4.9/3.9		6.5/3.2	6.3/5.0	7.2/4.8	8.1/6.3
Swell (1): Length λ (m)					30	40	30
Swell (1): Height h (m)	2.5	1.8	1.7	1.0	1.0	0.8	1.0
Swell (1): Ave. period T (sec)	8.66	9.44	8.39	5.97	5.65		
Swell (1): Range of period T_{max}/T_{min}	9.8/7.7	11.6/7.4	10.6/6.4	7.0/5.0	6.4/4.7		
Swell (1): Angle of encounter	P60	P50	P55	P35	P40	P40	
Swell (2): Length λ (m)							
Swell (2): Height h (m)							
Swell (2): Ave. period T (sec)							
Swell (2): Range of period T_{max}/T_{min}							
Swell (2): Angle of encounter							
Swell (3): Length λ (m)							
Swell (3): Height (m)							
Swell (3): Ave. period T (sec)							
Swell (3): Range of period T_{max}/T_{min}							
Swell (3): Angle of encounter							
Rolling Period (sec)	8.3					8.3	
Pitching Period (sec)	8.0					9.1	

board the " Miyajima Maru ", 1956 (continued)

24	25	25	25	26	26	26	27	27
16·00	8·00	12·00	16·00	8·00	12·00	16·00	8·00	12·00
49°58′N 173°28′E	49°39′N 172°39′E	49°39′N 172°43′E	49°40′N 172°40′E	49°43′N 172°10′E	49°44′N 172°13′E	49°47′N 172°22′E	50°07′N 172°43′E	50°04′N 172°42′E
290	339	25	18	7	5	5	0	22
12200	12300	12300	12300	12000	12000	12000	12000	12000
0	0	0	0	0	0	0	0	0
12.5	4.0	6.5	9.0	13.0	8.5	12.0	5.5	3.5
P100	P30	P85	P90	P95	P95	P100	P100	P100
9	4	6	7	9	7	8	5	3
		0.3		4.0	3.3	3.0		0.5
		0.8		4.3	1.8	2.0		1.0
1.8	0.5	0.7	1.2	2.3	2.3	2.8		
7.04		3.67	5.98	7.30	7.05	7.42		
8.3/5.6		4.0/3.4	7.8/4.7	9:8/5.6	9.1/5.0	10.5/6.3		
1.0	1.5	1.0	1.0	1.3	1.0	1.0	1.3	1.2
4.72	7.45	7.20	7.41	5.84	6.17	4.83	7.96	7.98
6.0/3.4	8.3/6.4	7:7/6.4	8.2/6.7	7.6/4.5	7.4/5.1	5.8/3.5	10.2/5.9	8.7/7.3
P40	P140	P170	P150	P145	P40	P140	P90	P110
								25
	1.0						1.0	0.5
	5.12						6.08	
	5.9/3.7						6.6/5.7	
	180						P20	P30
				9.8	9.8	8.5		13.6
		9.6		8.5	8.0	7.8		9.7

Table 4.11 Records of the Observations on

Date	May 27	28	28	28	29	29	29
Time	16·00	08·00	12·00	16·00	08·00	12·00	16·00
Position	50°06′N 172°46′E	50°28′N 173°13′E	50°17′N 173°13′E	50°18′N 173°17′E	50°36′N 173°50′E	50°32′N 173°05′E	50°33′N 173°53′E
Course	40	55	60	65	318	317	312
Dispt. (t)	12000	12100	12100	12100	12200	12200	12200
Ship Speed (kt)	0	0	0	0	0	0	0
Wind: Rel. ave. vel. (m/sec)	3.5	10.0	6.5	5.0	4.0	4.5	4.0
Wind: Relative direction	P60	P95	P110	P100	P105	P105	P105
Wind: Beauf. scale	4	7	6	5	4	4	4
Rolling: Max. θ_{max}		0.5	1.3			1.5	
Rolling: r.m.s. $\sqrt{\overline{\theta^2}}$							
Pitching: Max. ψ_{max}		2.3	1.8			0.5	
Pitching: r.m.s. $\sqrt{\overline{\psi^2}}$							
Sea: Length λ (m)							
Sea: Height h (m)		1.8	1.5	1.3	0.7		0.5
Sea: Ave. period T (sec)		7.61	7.54	6.82	4.95		3.60
Sea: Range of period T_{max}/T_{min}		8.4/6.6	9.4/6.7	7.9/6.3	5.0/4.9		4.4/2.7
Swell (1): Lenhtg λ (m)						110	
Swell (1): Height h (m)	0.9	1.0	0.5	0.8	0.8	1.0	1.0
Swell (1): Ave. period T (sec)	7.92	6.98	5.06	4.00	8.04	9.50	8.20
Swell (1): Range of period T_{max}/T_{min}	10.3/6.2	8.0/6.1	6.0/4.0	5.3/3.0	8.4/7.4	10.3/8.5	9.2/7.1
Swell (1): Angle of encounter	P130	P150	P130	P140	P110	P160	S90
Swell (2): Length λ (m)	45					40	
Swell (2): Height h (m)	0.6					0.5	0.8
Swell (2): Ave. period T (sec)							8.90
Swell (2): Range of period T_{max}/T_{min}							9.7/7.8
Swell (2): Angle of encounter	P40					P45	P100
Swell (3): Length λ (m)						80	
Swell (3): Height h (m)						1.0	0.5
Swell (3): Ave. period T (sec)							5.04
Swell (3): Range of period T_{max}/T_{min}							5.6/4.3
Swell (3): Angle of encounter						S20	P30
Rolling period (sec)			7.6			7.8	
Pitching period (sec)		10.0				8.2	

board the "Miyajima Maru", 1956 (continued)

30	30	30	31	31	31	June 1	1	1
8·00	12·00	16·00	8·00	12·00	16·00	8·00	12·00	14·30
50°49′N 173°38′E	50°40′N 173°32′E	50°17′N 172°48′E	48°42′N 171°20′E	48°42′N 171°51′E	48°05′N 172°20′E	47°55′N 171°33′E	47°51′N 171°29′E	47°47′N 171°27′E
345	350	245	335	135	340	185	145	145
12100	12100	12100	12000	12000	12000	11800	11800	11800
0	0	9	0	12.8	0	0	0	0
2.5	3.5	6.7	6.7	8.0	4.7	7.0	8.7	13.0
S 100	S 75	S 25	P 105	S 70	P 105	P 100	P 100	P 105
3	3	6	6	6	4	6	7	9
	0	0		0.3		0	0	0.3
	0.8	1.8		1.0			0.5	1.3
					15			
			0.5	0.5	0.5	0.5	0.7	1.3
			4.00	3.54		3.58	3.38	5.26
			5.3/3.9	4.2/3.0		4.2/3.1	4.1/2.3	6.1/4.1
0.9	1.2	1.2	0.5	0.8	0.8	1.3	1.0	1.0
8.36	7.97	7.00	5.33	5.89	7.21	7.67	4.67	5.57
9.3/7.3	9.3/7.0	7.8/6.3	6.1/4.8	7.3/4.8	8.4/6.0	8.4/7.1	5.2/4.0	6.6/4.5
P 65	P 125	S 15	P 135	S 140	P 60	S 110	P 50	P 50
25		25						
0.5	0.9	0.7	0.7		0.8			
	7.24		7.68		5.41			
	8.9/5.6		8.6/6.7		6.0/4.9			
S 140	P 65	P 30	P 50		P 80			
1.0	1.0				0.8			
7.32	6.82				5.72			
7.6/7.0	7.4/6.0				6.7/5.2			
P 120	P 90				P 40			
	7.3	6.3		7.4			9.2	8.5

Table 4.11 Records of the Observations on

Date	June 1	2	2	2	2	2	3
Time	16·00	4·00	8·00	10·00	12·00	16·00	8·00
Position	47°43′N 171°25′E	47°21′N 171°29′E	48°10′N 171°30′E	50°09′N 171°34′E	48°08′N 171°38′E	50°04′N 171°49′E	48°48′N 172°03′E
Course	145	348	0	55	50	50	345
Dispt. (t)	11800	11700	11700	11700	11700	11700	11700
Ship speed (kt)	0	9	9	0	0	0	6.2
Wind: Rel. ave. vel. (m/sec)	13.1	17.0	17.1	13.0	13.4	15.0	14.8
Wind: Relative direction	P105	P40	P45	P110	P104	P100	P50
Wind: Beauf. scale	9	11	11	9	9	10	10
Rolling: Max. θ_{max}	0.3		1.0	2.0	4.0	4.3	1.5
Rolling: r.m.s. $\sqrt{\overline{\theta^2}}$				0.92	1.58	1.80	
Pitching: Max. Ψ_{max}	1.5		3.5	2.5	4.5	2.3	4.8
Pitching: r.m.s. $\sqrt{\overline{\Psi^2}}$			1.25	0.98			1.11
Sea: Lenthg λ (m)							
Sea: Height h (m)	1.8	2.8	2.0	2.8	2.8	3.0	2.3
Sea: Ave. period T (sec)	6.12	5.81	6.59	7.29	7.99	8.43	6.78
Sea: Range of period T_{max}/T_{min}	7.6/5.1	6.5/5.1	8.0/5.4	8.2/6.4	10.0/6.5	9.7/7.0	8.1/5.6
Swell (1): Length λ (m)							
Swell (1): Height h (m)	1.0	4.0	2.3	2.5	1.8	1.3	3.5
Swell (1): Ave. period T (sec)	6.01	7.85	8.66	8.08	7.73	5.20	9.02
Swell (1): Range of period T_{max}/T_{min}	6.7/5.2	8.4/7.2	9.3/8.0	8.7/7.2	8.8/6.7	5.5/5.0	10.1/7.6
Swell (1): Angle of encounter	P45	S40	S20	P10	P25	P35	S20
Swell (2): Length λ (m)							
Swell (2): Height h (m)	0.5					1.8	
Swell (2): Ave. period T (sec)	4.23					5.90	
Swell (2): Range of period T_{max}/T_{min}	4.5/3.8					7.4/5.0	
Swell (2): Angle of encounter	P130					P135	
Swell (3): Length λ (m)							
Swell (3): Height h (m)							
Swell (3): Ave. period T (sec)							
Swell (3): Range of period T_{max}/T_{min}							
Swell (3): Angle of encounter							
Rolling Period (sec)				10.9	10.8	10.4	14.5
Pitching Period (sec)	7.5		6.0	9.7	7.9	8.1	7.3

board the "Miyajima Maru", 1956 (continued)

3	3	4	4	4	5	5	7	7
12·00	16·00	8·00	12·00	16·00	8·00	12·00	8·00	12·00
49°01′N 172°19′E	51°02′N 172°31′E	49°30′N 172°10′E	49°27′N 172°15′E	49°25′N 172°17′E	50°02′N 172°03′E	50°46′N 172°55′E	51°24′N 173°14′E	51°28′N 173°17′E
40	30	70	76	75	19	250	180	177
11700	11700	11600	11600	11600	11600	11600	11600	11600
0	0	0	0	0	0	0	0	0
9.3 P110 7	6.0 P105 5	1.0 P110 1	3.0 P110 3	3.3 P120 3	5.0 P75 5	1.5 S155 2	7.3 P95 6	8.0 P95 6
2.5	1.0	1.3	1.3			0	0	1.0
2.5	1.5	1.0	1.3			0		1.3
2.7 6.83 8.5/5.1					15 0.5		1.5 4.68 5.3/4.0	1.7 5.15 5.18/4.4
2.3 8.41 9.6/7.4 P45	2.6 8.56 10.8/7.4 P30	2.5 9.90 11.4/8.4 P75	2.0 9.20 10.4/7.5 P70	1.0 5.18 5.5/4.6 P140	1.0 5.90 6.2/5.7 P60	1.0 5.28 5.7/4.8 S60	0.8 6.99 8.2/5.9 P35	0.9 5.91 7.0/4.5 P40
1.9 5.04 6.2/4.5 P135	1.5 6.14 7.1/4.9 P145	0.8 5.72 5.8/5.5 S150	1.0 5.03 6.3/4.1 S150	1.5 8.88 10.9/7.5 P45	1.3 7.55 8.7/7.0 P140		0.5 3.70 4.5/2.9 P150	1.0 3.85 4.4/3.2 P135
				0.8 6.10 7.3/4.9 S120				
10.4 7.7	8.4	10.0 7.8	7.0 7.0					7.1 6.1

Table 4.11 Records of the Observations on

Date	June 7	7	8	8	8	8	8
Time	14·30	16·00	8·00	10·00	12·00	14·00	16·00
Position	51°26′N 173°13′E	51°24′N 173°08′E	51°41′N 174°00′E	51°37′N 173°55′E	51°35′N 173°49′E	51°34′N 173°46′E	51°32′N 173°42′E
Course	180	182	183	180	182	176	178
Dispt. (t)	11600	11600	11700	11700	11700	11700	11700
Ship speed (kt)	0	0	0	0	0	0	0
Wind: Rel. ave. vel. (m/sec)	10.7	11.3	13.0	9.9	11.0	11.5	12.0
Wind: Relative direction	P100	P100	P100	P106	P105	P110	P95
Wind: Beauf. scale	8	8	9	7	8	8	8
Rolling: Max. θ_{max}	1.5	2.0	3.0	3.8	2.5		3.8
Rolling: r.m.s. $\sqrt{\overline{\theta^2}}$			1.47		1.15		1.19
Pitching: Max. Ψ_{max}	1.8	2.3	2.5	2.3	2.3		1.5
Pitching: r.m.s. $\sqrt{\overline{\Psi^2}}$							
Sea: Length λ (m)							
Sea: Height h (m)	1.8	2.5	2.8	2.8	3.5	3.3	3.0
Sea: Ave. period T (sec)	6.00	6.05	7.56	8.22	7.54	7.89	7.28
Sea: Range of period T_{max}/T_{min}	6.9/5.2	7.2/5.1	9.7/6.0	9.3/6.9	7.9/7.2	9.0/6.5	8.9/5.7
Swell (1): Length λ (m)							
Swell (1): Height h (m)	1.5	1.7	1.0	1.5	2.0	1.8	1.0
Swell (1): Ave. period T (sec)	6.75	7.04	6.29	4.61	5.43	5.31	4.89
Swell (1): Range of period T_{max}/T_{min}	7.1/5.3	9.3/5.5	8.3/4.7	5.3/3.8	5.8/4.6	7.2/4.4	6.0/2.9
Swell (1): Angle of encounter	P35	P30	P45	P140	P140	P140	P135
Swell (2): Length λ (m)							
Swell (2): Height h (m)	1.0	1.2	1.5				1.8
Swell (2): Ave. period T (sec)	4.51	4.27	5.18				7.51
Swell (2): Range of period T_{max}/T_{min}	5.5/4.1	4.5/3.9	5.5/4.9				8.7/6.3
Swell (2): Angle of encounter	P130	P130	P130				P50
Swell (3): Length λ (m)							
Swell (3): Height h (m)							
Swell (3): Ave. period T (sec)							
Swell (3): Range of period T_{max}/T_{min}							
Swell (3): Angle of encounter							
Rolling Period (sec)	8.0	7.5	8.4	8.0	10.1		9.7
Pitching Period (sec)	6.4	7.1	7.9	7.2	7.5		7.6

board the "Miyajima Maru", 1956 (continued)

9	9	9	9	10	10	10	10	10
8·00	10·00	16·00	16·00	8·00	10·00	12·00	14·00	16·00
51°32′N 174°04′E	51°34′N 174°03′E	51°33′N 174°01′E	51°34′N 173°50′E	51°22′N 174°34′E	51°22′N 174°33′E	51°22′N 174°31′E	51°23′N 174°27′E	51°24′N 174°24′E
340	262	265	320	240	230	240	247	10
11700	11700	11700	11700	11700	11700	11700	11700	11700
0	0	0	0	0	0	0	0	9.6
3.0	3.0	2.0	6.0	10.0	8.5	7.0	7.0	7.0
P145	P100	P180	S90	P110	P105	P110	P125	S55
3	3	2	5	6	5	4	4	4
		1.3		1.5		2.3		0.8
		1.8		1.3		1.8		1.3
			1.0 0.8	1.5 5.34 6.7/4.5	1.7 5.69 7.1/4.1	1.0 4.28 5.0/3.7		
2.0	1.8	2.0	1.5	1.8	2.0	2.0	2.0	1.3
7.91	7.50	8.41	6.62	7.01	8.15	7.05	6.65	7.83
8.9/7.1	7.9/7.0	11.7/6.4	8.4/5.0	10.4/7.3	9.8/7.2	8.7/5.7	7.9/6.1	9.3/6.7
S115	P90	P90	S140	P40	P45	P50	P60	S130
1.0	1.8	1.0	2.5	1.0	1.8	1.5	2.5	2.8
5.78	7.77	6.12	8.51	4.79	7.30	7.81	7.79	9.31
6.7/4.1	8.2/7.5	7.0/5.1	10.1/7.5	5.8/4.1	8.6/6.2	9.6/6.4	10.2/6.4	11.3/7.9
S40	180	P150	P130	P145	P110	P90	P100	S165
1.5 6.47 7.2/5.5 P170		1.8 6.73 7.0/6.7 S170						
		7.0		8.5 8.9		8.1 6.9		6.4

Table 4.11 Records of the Observations on

Date	June 11	11	11	12	12
Time	8·00	12·00	16·00	8·00	12·00
Position	53°13′N 176°01′E	53°19′N 176°05′E	53°20′N 176°16′E	53°16′N 176°41′E	53°05′N 176′49′E
Course	10	10	15	30	305
Dispt. (t)	11700	11700	11700	11800	11800
Ship speed (kt)	0	0	0	0	9.0
Wind: Rel. ave. vel. (m/sec)	9.5	11.5	11.5	12.0	15.8
Wind: Relative direction	P95	P95	P100	P100	P25
Wind: Beauf. scale	5	6	6	6	6
Rolling: Max. θ_{max}		1.8	0.8	1.5	2.0
Rolling: r.m.s. $\sqrt{\overline{\theta^2}}$					
Pitching: Max. Ψ_{max}		1.8	1.8	1.8	1.8
Pitching: r.m.s. $\sqrt{\overline{\Psi^2}}$					
Sea: Length λ (m)	10				
Sea: Height h (m)	0.8	1.0	1.3	1.2	1.5
Sea: Ave. period T (sec)		4.36	5.16	4.55	5.68
Sea: Range of period T_{max}/T_{min}		5.6/3.3	6.2/4.1	5.7/3.6	6.8/4.8
Swell (1): Length λ (m)					
Swell (1): Height h (m)	2.0	2.2	2.3	1.5	1.5
Swell (1): Ave. period T (sec)	9.46	12.33	12.33	10.18	9.14
Swell (1): Range of period T_{max}/T_{min}	13.8/8.0	16.1/9.4	16.1/9.4	14.2/7.1	10.8/8.0
Swell (1): Angle of encounter	S170	S170	P170	P170	P105
Swell (2): Length λ (m)					
Swell (2): Height h (m)	1.2	1.5	1.2	1.5	
Swell (2): Ave. period T (sec)	7.10	7.25	6.48	6.96	
Swell (2): Range of period T_{max}/T_{min}	9.7/5.2	8.5/6.4	7.0/5.6	7.9/5.6	
Swell (2): Angle of encounter	S120	S140	P140	P140	
Swell (3): Length λ (m)					
Swell (3): Height h (m)					
Swell (3): Ave. period T (sec)					
Swell (3): Range of period T_{max}/T_{min}					
Swell (3): Angle of encounter					
Rolling Period (sec)		9.5	10.2	8.9	9.1
Pitching Period (sec)		8.1	7.2	8.4	8.4

Note: 1) JST

2) $\theta_i(\phi_i)_{max.}$ in deg. See Fig. A

3) $\overline{\theta^2}=\frac{1}{\tau}\int_0^\tau \theta^2\,dt$, $\overline{\Psi^2}=\frac{1}{\tau}\int_0^\tau \Psi^2\,dt$, Fig. A

board the "Miyajima Maru", 1956 (continued)

12	13	14	14	15	15	15
16·00	8.00	12·00	16·00	8·00	12·00	16.00
53°21′N 176°11′E	53°25′N 175°36′E	53°42′N 175°25′E	53°40′N 175°28′E	54°08′N 175°50′E	54°06′N 175°50′E	54°02′N 175°50′E
170	107	125	110	129	135	130
11800	11800	11900	11900	11900	11900	11900
0	0	0	0	0	0	0
8.5	1.2	0	5.5	3.0	2.0	2.5
S 175	P 105	P 120	P 110	P 110	P 105	P 95
5	6	0	4	2	2	2
0.8		0.8			1.0	
1.8		1.3			1.3	
	15 0.5 3.47 3.8/3.5					
1.8	1.0	1.0	0.9	1.0	1.7	1.0
7.10	6.08	6.57	6.26	6.45	7.40	6.42
	6.4/5.5	7.8/5.2	7.6/4.6	7.5/5.7	9.6/5.7	7.5/5.4
S 105	P 65	P 55	P 40	P 80	P 85	P 85
1.3	1.3	0.8	0.9		0.8	0.8
7.40	7.40	7.30	5.68		5.20	4.61
9.2/6.0	7.8/7.1	8.2/5.9	6.7/5.1		5.5/4.9	5.2/4.4
S 30	P 170	P 139	P 155		P 140	P 140
2.3						
10.11						
11.7/7.5						
S 90						
		7.3			7.8	
7.6		8.0			5.7	

Fig. A

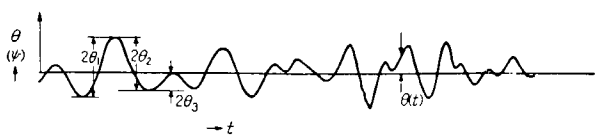

Table 4.12 Meteorological Observation Records

Data	7, May					8, May					9, May					10, May					11, May				
Time	①	②	③	④	⑤	①	②	③	④	⑤	①	②	③	④	⑤	①	②	③	④	⑤	①	②	③	④	⑤
0300		07.1	10.0	340	4		13.0	5.0	220	2		83.8	10.0	250	4		96.0	5.5	280	3		03.6	6.0	0	2
0600		09.3	4.0	200	2		12.1	6.5	190	2		84.6	15.0	260	6		98.1	6.0	250	2		—	5.0	0	3
0900	⊗	10.7	7.0	350	3	●	08.7	9.5	160	3	◎	86.3	15.0	260	6	◎	97.0	3.0	40	1	◐	08.1	9.5	340	3
1200	5.3	11.8	5.0	320	2	3.6	04.3	10.5	150	4	4.6	88.0	14.5	250	6	4.0	97.0	4.5	40	1	4.3	09.5	9.7	340	4
1500	3.5	12.8	5.5	320	2	4.3	98.6	13.5	150	5	4.0	89.6	14.0	260	6	4.0	92.0	5.5	40	2	3.8	11.8	9.5	330	4
1800		14.1	5.0	300	2		94.8	13.0	150	5		92.2	13.0	260	6		98.4	7.5	50	2		14.7	9.7	350	4
2100		14.4	4.5	250	2		90.1	7.0	160	3		93.4	12.5	260	6		99.7	9.5	30	3		16.3	6.0	320	3
2400		—	—	270	—		88.0	8.0	200	4		96.8	5.0	270	3		00.7	10.5	20	3		—	6.5	320	2

Date	12, May					13, May					14, May					15, May					16, May				
Time	①	②	③	④	⑤	①	②	③	④	⑤	①	②	③	④	⑤	①	②	③	④	⑤	①	②	③	④	⑤
0300		16.1	3.5	260	1		89.2	18.0	250	6		01.0	10.0	320	2		15.0	7.0	250	2		—	6.0	90	2
0600		14.8	4.0	200	1		88.0	19.0	250	7		05.8	11.5	300	3		16.0	10.5	290	3		99.7	8.5	40	2
0900	●	10.4	11.5	170	3	◎	86.9	21.5	270	7	◐	08.3	10.5	310	4	◎	16.0	7.5	260	3	⊖	00.5	8.5	20	3
1200	3.2	02.0	15.5	160	5	4.5	88.0	20.5	270	8	4.5	11.1	10.0	300	4	4.5	15.1	9.0	250	3	4.8	04.2	7.0	10	3
1500	4.0	92.6	12.0	190	4	4.0	89.8	19.0	290	8	3.8	13.2	8.5	330	4	4.2	13.2	6.5	250	3	4.8	09.5	6.5	300	3
1800		92.0	14.0	260	4		93.7	15.0	310	7		15.5	7.0	300	2		12.0	8.0	250	3		11.8	5.0	280	2
2100		91.8	15.5	240	6		97.0	11.0	300	5		16.3	6.0	310	2		09.2	5.0	260	3		12.8	10.5	250	3
2400		90.6	17.0	240	6		00.0	10.5	320	4		—	6.5	270	2		—	3.0	180	2		—	10.5	270	4

Date	17, May					18, May					19, May					20, May					21, May				
Time	①	②	③	④	⑤	①	②	③	④	⑤	①	②	③	④	⑤	①	②	③	④	⑤	①	②	③	④	⑤
0300		14.8	10.0	270	4		19.7	8.0	180	3		—	20.5	250	7		11.9	9.0	290	3		91.9	18.5	150	6
0600		17.6	8.0	290	3		15.3	13.0	210	4		95.8	20.5	270	7		13.6	5.5	300	3		84.9	17.5	140	7
0900	○	19.0	6.5	280	3	◎	11.5	16.5	160	5	◎	00.0	17.5	250	7	◎	14.6	4.0	290	2	⚌	81.5	10.5	190	6
1200	7.7	20.2	6.5	280	2	5.8	06.9	15.0	180	6	5.2	02.1	11.5	260	4	6.7	14.6	3.0	140	1	5.0	80.8	10.5	230	5
1500	4.5	21.0	3.5	270	1	4.2	04.6	13.0	200	6	4.0	03.2	9.5	260	4	5.3	13.3	7.5	140	2	4.5	85.9	22.0	290	7
1800		22.1	2.0	230	1		01.7	15.0	210	6		04.9	9.5	270	3		11.4	14.0	160	4		91.8	21.0	280	7
2100		21.3	4.5	220	1		97.5	17.5	220	6		06.1	10.0	270	3		06.0	14.5	140	4		93.2	22.0	280	7
2400		21.2	6.5	220	2		94.1	22.0	220	7		08.8	11.0	290	3		00.5	16.0	140	6		—	20.5	260	7

Date	22, May					23, May					24, May					25, May					26, May				
Time	①	②	③	④	⑤	①	②	③	④	⑤	①	②	③	④	⑤	①	②	③	④	⑤	①	②	③	④	⑤
0300		92.8	24.0	250	8		08.8	12.0	360	3		15.8	8.0	190	2		97.5	6.5	290	2		03.2	12.5	300	5
0600		91.2	23.5	260	8		11.0	8.0	360	3		13.0	10.0	180	3		96.0	5.0	330	2		05.4	15.5	279	5
0900	◎	89.6	24.5	270	8	◎	13.4	6.0	340	3	⊗	11.1	9.5	180	4	◎	94.6	3.5	320	1	◎	06.8	14.0	270	5
1200	4.5	88.3	26.0	280	8	5.1	14.9	7.0	340	3	5.2	07.3	12.5	190	4	4.0	92.9	8.0	300	3	5.1	07.3	10.0	270	4
1500	3.8	92.0	18.5	310	8	4.9	15.6	5.5	360	3	4.5	04.0	12.5	190	4	4.5	93.5	10.0	290	4	4.2	07.7	14.5	270	5
1800		98.5	12.5	320	6		17.1	4.5	340	2		01.7	12.5	200	4		95.7	12.0	280	4		08.2	14.0	270	5
2100		01.8	10.5	330	4		17.7	1.5	260	1		99.2	8.0	220	4		98.0	11.5	290	4		08.0	12.0	270	5
2400		06.2	15.0	10	4		16.8	2.5	330	1		98.7	12.5	220	4		99.2	13.5	300	5		07.0	9.5	270	3

Key

①	②	③	④	⑤
Weather Atm. temp. ℃ Temp. S. W. ℃	Atm. press. (mb)	Wind vel. (m/sec)	Wind dir.	Sea scale

Table 4.12 Meteorological Observation Records (Continued)

Date	27, May					28, May					29, May					30, May					31, May				
Time	①	②	③	④	⑤	①	②	③	④	⑤	①	②	③	④	⑤	①	②	③	④	⑤	①	②	③	④	⑤
0300		06.8	9.0	270	3		01.1	12.0	310	4		11.3	7.0	260	2		01.3	5.0	190	1		15.5	6.0	230	1
0600		05.5	8.0	260	2		02.0	16.0	320	4		10.4	4.0	290	1		02.7	3.0	270	1		16.0	10.5	230	2
0900	⊗	03.2	4.5	270	2	◎	04.7	12.5	320	5	◎	08.7	4.5	210	1	◎	04.8	4.0	90	1	⊖	16.8	7.0	230	2
1200	5.6	01.0	4.0	280	2	5.4	07.0	7.0	320	3	4.6	07.4	5.5	220	2	5.3	07.5	3.5	80	1	6.8	17.3	8.5	250	3
1500	4.5	98.2	5.0	280	1	4.8	08.8	7.5	320	3	4.0	05.5	4.0	170	1	4.7	10.4	4.0	320	1	4.8	17.8	6.0	230	2
1800		96.9	7.0	340	2		10.4	8.0	320	3		04.2	5.5	200	1		12.6	5.5	10	1		17.8	5.0	230	1
2100		97.0	7.0	350	2		11.2	6.5	330	2		03.0	7.0	180	2		15.5	6.0	310	1		16.9	4.5	220	1
2400		98.4	10.5	340	3		10.5	4.0	330	1		01.4	4.5	160	1		15.3	4.0	260	1		14.8	2.0	200	1

Date	1, June					2, June					3, June					4, June					5, June				
Time	①	②	③	④	⑤	①	②	③	④	⑤	①	②	③	④	⑤	①	②	③	④	⑤	①	②	③	④	⑤
0300		12.4	5.0	160	1		86.8	14.0	340	6		87.7	20.5	280	7		00.2	2.5	220	1		20.0	4.5	20	1
0600		08.8	8.5	12.0	2		86.0	19.0	320	6		89.5	13.0	280	7		01.3	3.0	270	1		23.8	4.5	290	1
0900	◍	04.8	7.0	70	2	◎	83.2	15.5	300	6	◎	91.0	13.5	300	7	◎	03.2	1.5	320	1		25.0	4.0	300	1
1200	4.9	99.7	10.5	40	3	4.8	83.0	17.5	310	7	5.9	93.0	11.5	300	6	6.5	05.9	2.5	320	1		25.4	2.5	280	1
1500	4.5	95.3	14.5	40	5	4.8	82.8	17.0	310	7	4.9	95.3	11.5	300	4	5.1	09.4	2.5	330	1		26.9	2.0	290	1
1800		92.0	17.5	30	6		83.5	18.5	310	7		97.6	8.0	290	4		13.2	4.5	320	1		28.3	1.5	350	1
2100		88.7	18.0	10	6		84.3	19.0	310	7		98.6	7.0	300	3		16.3	3.0	320	1		27.2	3.0	30	1
2400		87.5	17.0	10	6		86.5	17.5	290	7		99.0	2.0	260	1		18.4	2.0	340	1		26.7	1.5	90	1

Date	6, June					June, 7					June, 8					June, 9					June, 10				
Time	①	②	③	④	⑤	①	②	③	④	⑤	①	②	③	④	⑤	①	②	③	④	⑤	①	②	③	④	⑤
0300		26.6	5.0	60	1		18.7	13.5	80	3		06.0	17.5	60	7		98.7	10.5	340	4		84.7	10.5	70	3
0600		26.8	3.5	30	1		18.5	9.0	100	3		05.2	13.0	90	6		98.2	9.0	190	3		80.5	9.5	130	4
0900	◎	26.5	3.0	40	1	◎	18.3	11.0	90	4	◍	02.9	15.0	80	6	◎	98.0	4.5	170	2	☰	77.0	10.5	130	4
1200	8.3	25.5	2.0	50	1	4.8	16.8	11.5	80	4	4.5	01.5	16.0	80	6	7.4	96.8	3.0	80	2	6.0	73.4	9.5	120	3
1500	4.8	24.7	5.0	60	1	4.9	14.2	12.0	80	5	4.8	99.9	13.5	80	6	5.1	95.0	4.5	110	2	4.9	71.1	5.5	120	2
1800		24.8	6.5	70	2		12.2	15.0	80	5		99.0	14.0	80	6		94.0	7.0	70	3		70.8	5.0	90	2
2100		22.5	8.5	70	2		10.9	14.5	80	6		99.0	10.5	70	5		92.3	7.5	60	3		70.2	6.0	0	2
2400		20.8	7.5	70	3		08.3	13.5	70	6		98.8	10.0	60	5		89.7	6.5	10	3		70.0	4.5	330	2

Date	11, June					12, June					13, June					14, June					15, June				
Time	①	②	③	④	⑤	①	②	③	④	⑤	①	②	③	④	⑤	①	②	③	④	⑤	①	②	③	④	⑤
0300		69.6	9.5	310	2		79.0	9.0	290	3		90.5	14.5	20	4		02.0	6.5	50	1		06.3	2.5	0	1
0600		70.2	8.0	280	2		80.7	11.5	280	4		93.2	15.0	0	4		03.1	5.0	30	1		06.5	3.0	30	1
0900	◍	70.8	9.5	280	3	◎	82.1	11.0	280	4		95.4	11.0	0	4	◎	03.6	5.5	20	1	◎	07.0	3.0	30	1
1200	6.0	71.9	11.5	280	4	5.8	82.7	11.5	290	4		96.8	5.5	10	2	6.3	04.2	4.5	0	1	6.8	07.0	1.5	20	1
1500	4.6	72.9	11.5	270	4	4.7	83.6	8.0	290	3		98.3	5.0	30	2	5.7	04.7	5.5	0	1	5.1				
1800		74.5	12.0	270	4		85.7	10.0	360	3		99.7	3.0	30	2		05.3	5.5	340	1					
2100		76.0	11.0	270	4		87.2	10.5	360	4		00.5	3.5	0	1		05.7	5.5	0	1					
2400		77.7	9.5	270	4		89.5	9.0	350	3		01.2	4.0	20	1		06.0	3.0	10	1					

Key

①	②	③	④	⑤
Weather Atm. temp. ℃ Temp. S. W. ℃	Atm. press. (mb)	Wind vel. (m/sec)	Wind dir.	Sea scale

their mean value was 1.85 m. GM_a shown in the figure is the value of GM obtained by measuring the inclination of the ship when the work boat was being lowered or lifted. The true GM value was obtained by making the deduction of free water effect assumed by the data in engine department. A part of the results of observation are shown in Table 4.11. In May the sea condition was bad due to the passage of lows at the period of 3 to 4 days, but the sea became tranquil after 10th June. Wave velocity, etc. during this period and weather chart at 9 o'clock of 22nd May are given in Table 4.12 and Fig. 4.29 respectively.

By the reasons mentioned above, the rolling angle of the ship is small, and moreover the effect of free water is evident, though the amount of this effect is not certain for the present. On the other hand, since in case of pitching mean wave length is much smaller than the length of the ship, there are some uncertainties as to the accuracy of the absolute value of response amplitude operator. By these reasons, definite conclusion has not arrived at yet as to the analysis of irregular rolling of the ship by energy spectrum.

It has been reported, according to N. H. Jasper, that, when the displacement

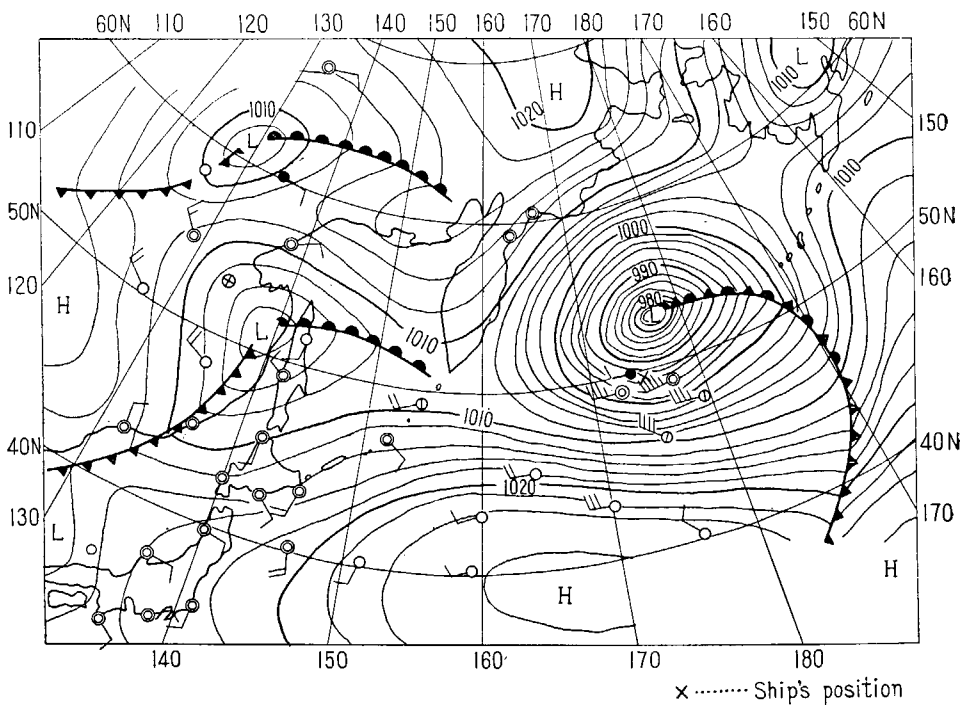

Fig. 4.29 Weather Chart at 0900 J.S.T. May 22, 1956.

from one maximum value to the next minimum is taken as the stochastic variable representing wave height and rolling angle, this variable x follows Rayleigh's distribution under approximately constant sea condition (1). Generalizing the above relation, T. Manabe suggested the following distribution pattern (2),

$$p_n(x)=\frac{nx^{n-1}}{\bar{x}^n}\cdot\exp\left[-\frac{x^n}{\bar{x}^n}\right] \tag{4.1}$$

$$P_n(x)=\int_0^x p_n(x)dx=1-\exp\left(-\frac{x^n}{\bar{x}^n}\right) \tag{4.2}$$

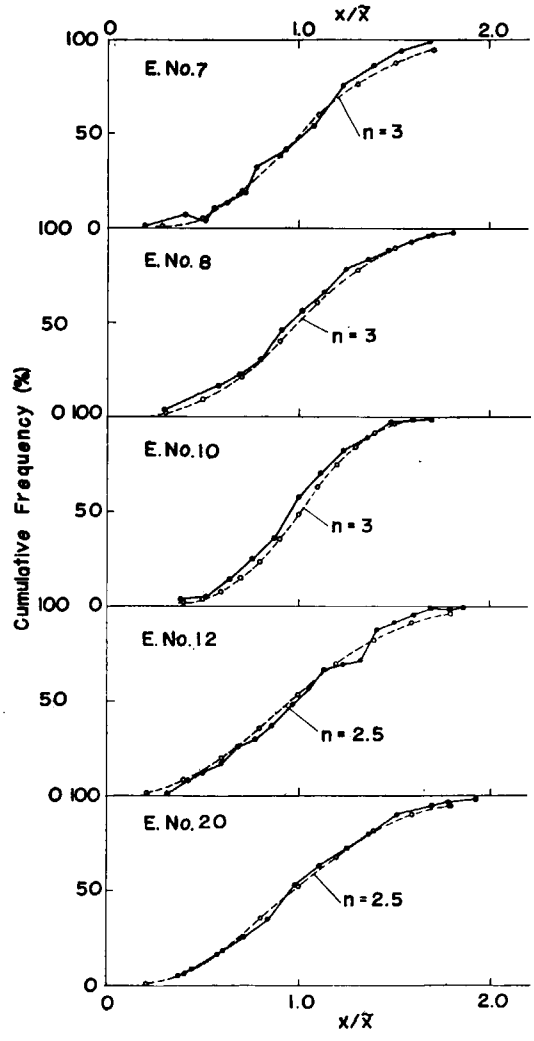

Fig. 4.30 Cumulative Distribution of Wave Height.

where, $\bar{x}^n$ is the mean value of x^n, having the following relation with the algebraic mean value $\tilde{x}$.

$$\tilde{x}=\bar{x}\cdot\Gamma\left(1+\frac{1}{n}\right) \tag{4.3}$$

$n=2$ represents Rayleigh's distribution. $p_n(x)$ tends to concentrate to the vicinity of $\tilde{x}$ according to the increase of n. It can be said that the smaller the value of n, the greater the dispersion or irregularity of x. The results of the observation indicate that x can be approximated by this distribution pattern when n is properly selected. Examples as to wave height and rolling angle

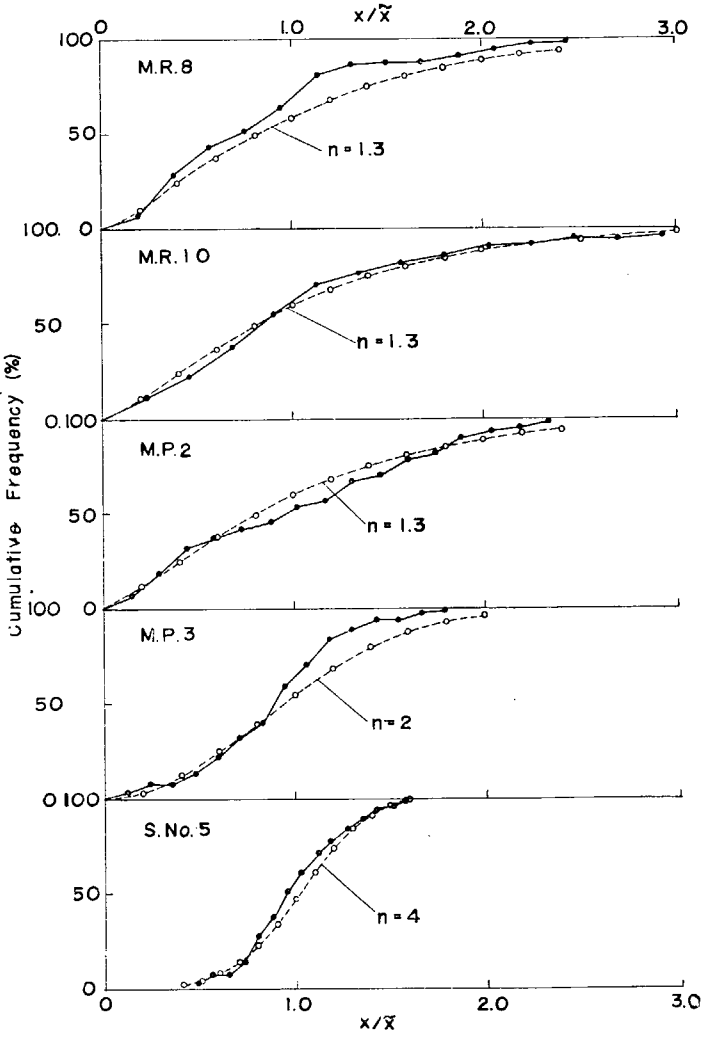

Fig. 4.31 Cumulative Distribution a sa Function of $x/\tilde{x}$ and n.

are shown in Fig. 4.30 and 4.31 respectively. As the rolling angle is considered as the output after the external force applied to the ship is filtered, the irregularity of x generally decreases and the majority of x follows Rayleigh's distribution. Fig. 4.31 shows, however, an example that the irregularity is rather appreciable even in case of generalized distribution. *MP* and *MR* indicate pitching and rolling of "Miyajima Maru" and S. No. 5 an example of the rolling of a fishing boat.

Mean rolling angle $\bar{\theta}$ was calculated from the observation data and the density of cumulative energy E was obtained from the relations of (4.1) to (4.3). On the other hand, E can be obtained directly from the mean value of the square of rolling angles. Fig. 4.32 shows the comparison of these values, the former being denoted as E_{th} and the latter as E_{ob}. In this figure also, considerable scatter of spots within the wide range of n can be observed. It is strange, in particular, that there is a case of $n<1$ in "Miyajima Maru". T. Manabe, applying this distribution to the sea condition, called n as the index number of sea condition. With regard to the ship's motion, n is considered to vary also according to the response characteristics of each ship.

Fig. 4.33 indicates that, in spite of the foregoing fact, the expectation value of maximum amplitude according to Longuet-Higgins gives close approximation to the results of observation, and moreover that there is a necessity of establishing the limits of, say, 90% confidence for the estimated maximum amplitude in order to avoid, the possible danger that the ship may be incurred.

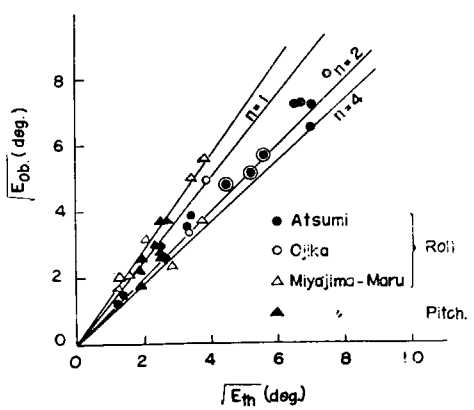

Fig. 4.32

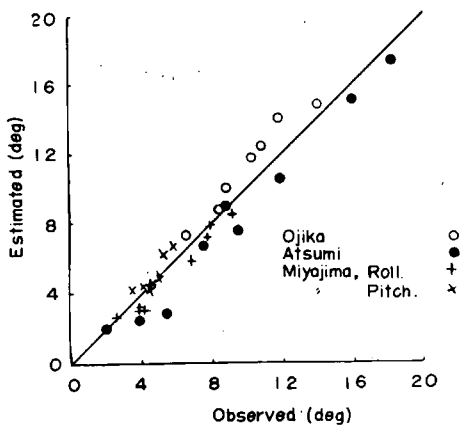

Fig. 4.33

PART V

Model Ship Experiments

Chapter 1 Ships Rolling in Irregular Seas

Attempts have recently been made, under the co-operative work of many naval architects and oceanographers, to the statistical analyses of irregular seas and to the investigation into ship's motion amongst them, and remarkable progress has been made in this field.

In order to examine the accuracy or adequacy of the results of these statistical analyses, an experiment was carried out as to a ship model. For this purpose, a platform was set up near the shore, where precise measurements were made of wave height, wind velocity and rolling of the ship in irregular seas caused by the wind. This chapter refers to the statistical analysis made of the results of the measurements.

For the purpose of statistical analyses, the method according to Peirson and St. Dennis was adopted, namely:

$$[\theta(\omega)]^2=[A(\omega)]^2[r(\omega)]^2$$

Where: $[\theta(\omega)]^2$=Energy spectrum of ship's rolling
$[r(\omega)]^2$=Energy spectrum of waves
$[A(\omega)]^2$=Response amplitude operator

1.1 Instruments for the Experiment.

A platform as shown in Fig. 5.1 was set up off shore at a place about 3 metre deep, where the rolling of the ship, wave height, wind velocity, etc.

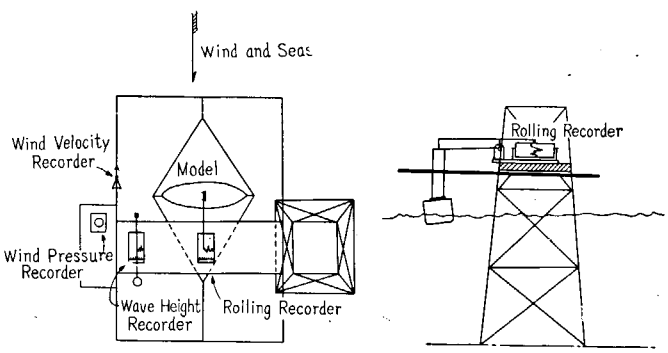

Fig. 5.1

were recorded. The ship was made free to pitching and heaving, and restrained to drifting by means of spring. The ship used with the experiment was the 1/34.25 model of "Hokuto Maru", a training ship.

1.2 Analysis of Results.

(1) Gaussian distribution.

Figs. 5.2 a), b) and c) illustrate the distributions of waves, rolling of the ship and wind pressure variation. It may be seen from this figure that these values are in fair consistency with the Gaussian distribution.

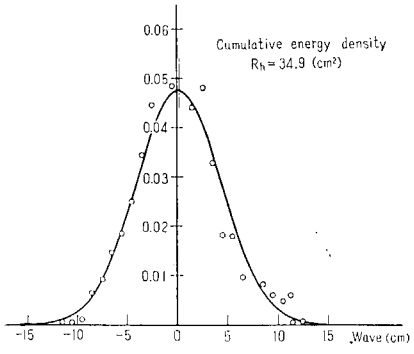

Fig. 5.2 a) Gaussian Distribution of Waves.

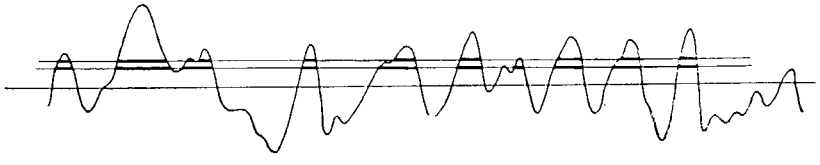

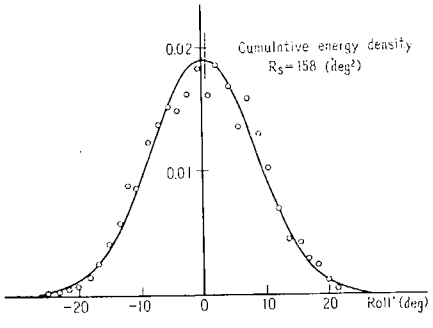

Fig. 5.2 b) Gaussian Distribution of Ship's Rolling Angle.

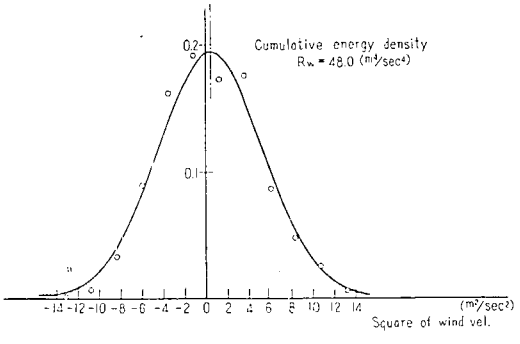

Fig. 5.2 c) Gaussian Distribution of Wind Pressure Variation.

(2) Distribution of amplitude.

Figs. 5.3 a), b) and c) indicate the distributions of amplitudes of waves, rolling of the ship and wind pressure variation respectively, which accord with the theoretical curve after Longuet-Higgins, especially, in case of rolling of the ship in which the consistency is remarkable.

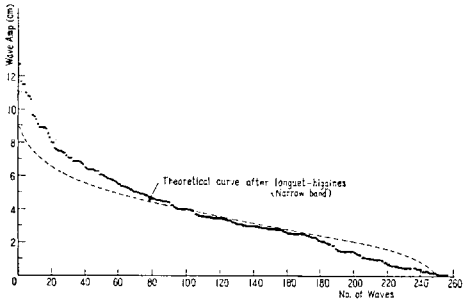

Fig. 5.3 a) Distribution of Wave Heights.

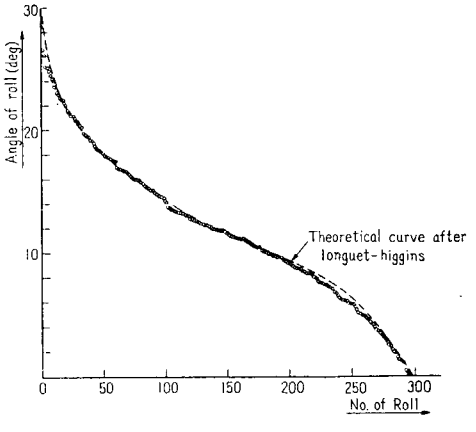

Fig. 5.3 b) Distribution of Amplitudes of Ship's Rolling.

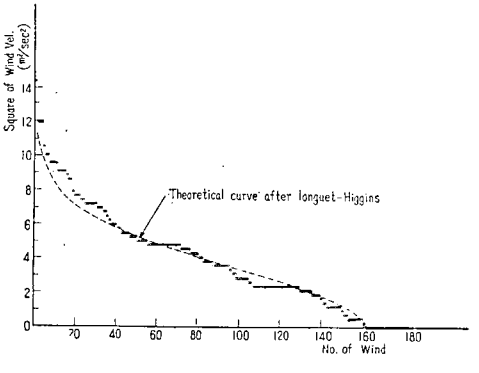

Fig. 5.3 c) Distribution of Amplitude of Wind Pressure Fluctuation.

(3) Correlation between wave spectrum and ship's rolling.

Figs. 5.4 a), b) and Fig. 5.5 indicate the energy spectrum of waves and response amplitude operators respectively. Figs. 5.6 a) and b) show the comparison between the spectrum calculated as the product of the above-mentioned energy spectrum of waves and response amplitude operators and that obtained from the results of the actual measurement of the rolling angle as to the ship model.

(4) Resonance curve in irregular seas.

Rolling angles obtained when the natural rolling periods of the ship were varied are as given in Fig. 5.7. It may be seen from this figure that the peak of resonance curve is lower at the synchronisum, while the rolling of the ship is greater at other periods, as compared with the rolling in regular seas.

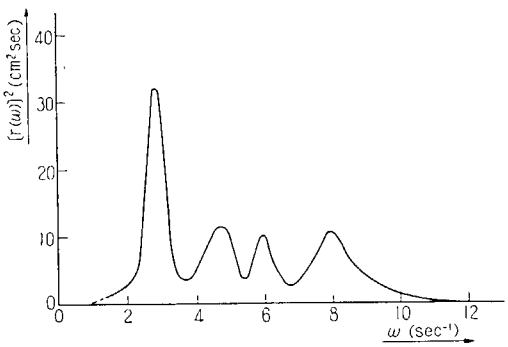

Fig. 5.4 a) Energy Spectrum of Waves.

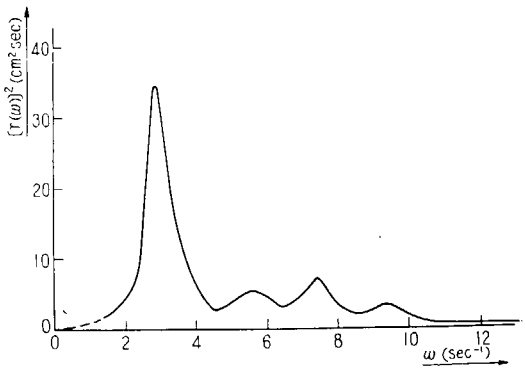

Fig. 5.4 b) Energy Spectrum of Waves.

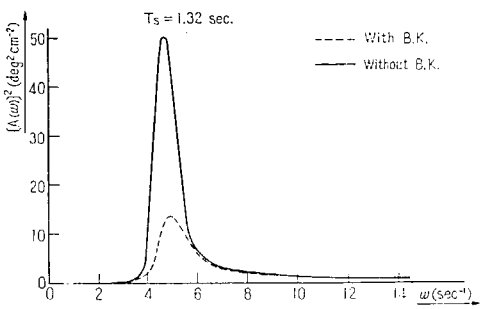

Fig. 5.5 Response Amplitude Operator of the Ship.

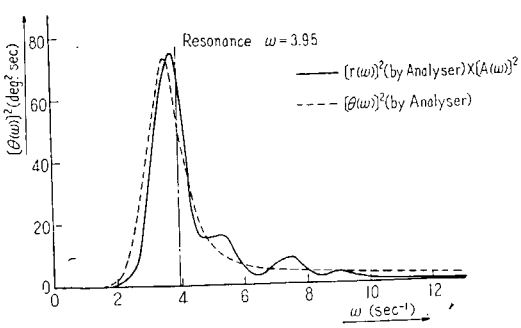

Fig. 5.6 a) Energy Spectrum of Ship's Rolling both observed and computed.

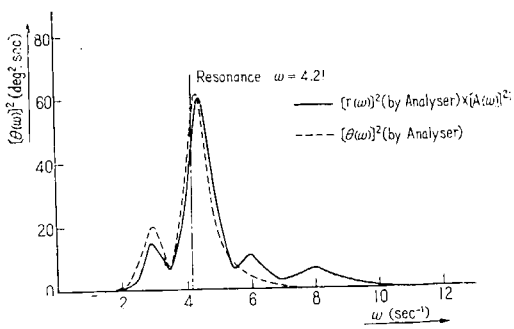

Fig. 5.6 b) Energy Spectrum of Ship's Rolling both observed and computed.

It has been clarified from the aforementioned experiment that, as far as rolling of a ship is concerned, the amplitudes obtained from the experiment agree with the theoretical value computed from the wave spectrum and response amplitude operator, and moreover that the correlation between the number of rolls and the maximum values is in agreement with the theoretical distribution.

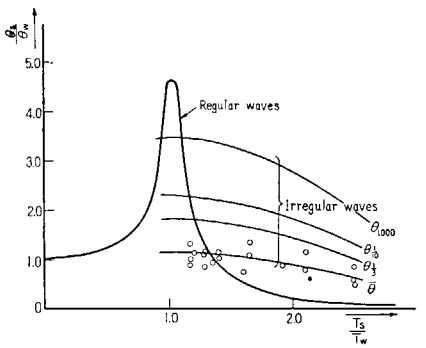

Fig. 5.7 Resonance Curve of Ship's Rolling in Regular and Irregular Waves (observed).

Chapter 2 Effect of Shipping of Sea Water upon the Stability of a Ship

2.1 Introduction.

Whether or not a ship has adequate stability is determined by GM and GZ_{max} that the ship has, and by the relation between the dynamical stability and external forces acting to the ship.

Though it is known that, of the external forces acting to the ship, the shipping of sea water has considerable adverse effect upon both statical and dynamical stability, the analysis of its effect is rather difficult, inasmuch as it relates to the problems of bulwark, freeing ports, etc. As a measure for this effect, therefore, there has so far been no established practice, but to give sufficient margin to the so-called safety criterion.

This chapter refers to the experiment carried out to study this problem.

2.2 Particulars of Ship model, Instruments and Method of Experiment, etc.

For the purpose of experiment, a 1/19.143 model of " Nichibei Maru, No. 8 ", a steel small trawler of 75 gross tons type, was used, the particulars being as given in Table 5.1.

As shown in Fig. 5.8, the instrument for the experiment consisted of

Table 5.1

	Actual ship	Ship model		Tokachi Maru (ship model)
		Over loaded Condition	Full Loaded Condition	
Length p. p.	26.80 m	1.400 m		2.000 m
Breadth, moulded	5.35 m	0.280 m		0.280 m
Displacement	245.37 t	34.980 kg	25.756 kg	28.35 kg
Draught, fore	2.480 m	12.96 cm	9.3 cm	
aft	3.080 m	16.09 cm	15.03 cm	
mean	2.780 m	14.52 cm	12.17 cm	8.719 m
Depth, moulded	2.65 m	0.138 m		0.120 m
KG	2.350 m	12.28 cm	11.35 cm	
GM	0.311 m	1.625 cm	1.66 cm	3.445 cm
T	5.47 sec	1.25 sec	1.35 sec	0.80 sec
Sheer, fore	1.20 m	6.3 cm		
aft	0.65 m	3.4 cm		
Camber	0.11 m	0.6 cm		

pulleys of various diameters fixed on the longitudinal axis through the centre of gravity of the ship. By hanging weights through pulley, the wind pressure moments corresponding to various wind velocities were applied to the ship. Then she was subjected to synchronous waves with various slopes, and the critical slopes of waves to cuase the capsize of the ship were measured.

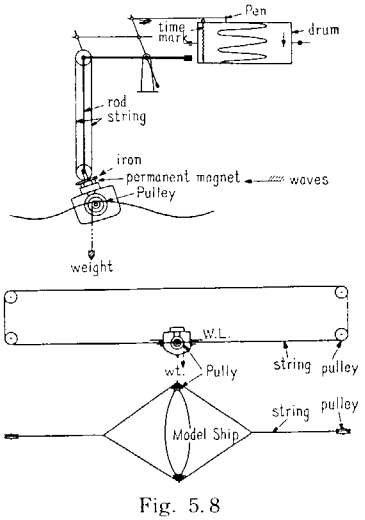

Fig. 5.8

2.3 Results of the Experiments.

An example of the results of the experiment is as shown in Fig. 5.9, in

which heeling angles of the ship are plotted against the wave slopes with the parameter of wind volocities.

The shipping of sea water occurs, as a matter of course, in small wave slopes where the wind velocity is big, and with the decrease of wind velocity, it begins after the wave slope becomes greater. Soon after the shipping of sea water has occurred, the ship capsizes.

The experiment with different heights of bulwark has indicated that there is a correlation between the bulwark height and the critical wave slope to cause the capsize of the ship, as shown in Fig. 5.10, which indicates bulwark heights on the basis of critical wave slopes.

It may be seen from this figure that the group of curves in the left side, which represent the over loaded condition of "Nichibei Maru, No. 8", have a trend that the greater the bulwark height, the greater the wave slope that the ship can withstand. This trend may by explained by the fact that, as this ship has very poor stability in over loaded condition, the shipping of sea water

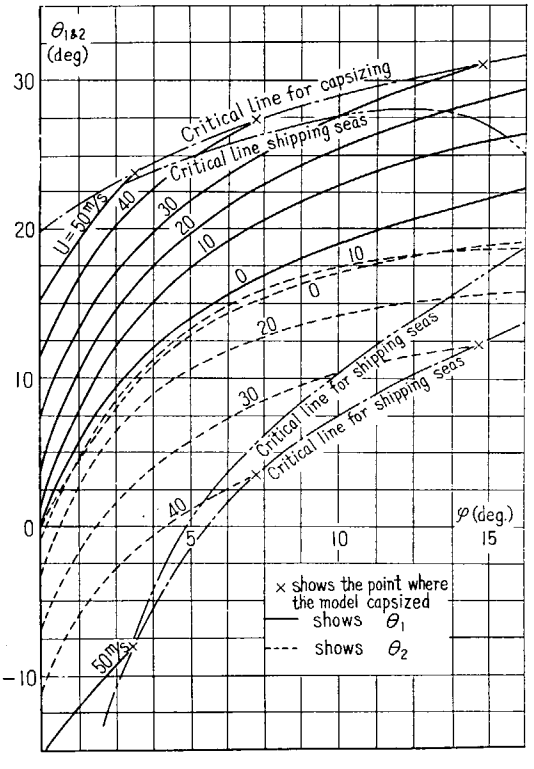

Fig. 5.9 No. 8 Nichibei-Maru Relation between the Wave Slope and the Heeling Angle. Loaded, Bulwark Height 0.8 m and Freeing Ports closed.

is prevented by the high bulwark. On the contrary, the straight line run from the right side below to the left side above, which represents "Tokachi Maru" (ferry boat), shows a tendency that the greater the bulwark height, the samller the critical wave height. As this ship has, different from "Nichibei Maru, No. 8", sufficient stability, the shipping of sea water will not cause a great free water effect where the bulwark is low, but where the bulwark is high, it brings a great free water effect and accordingly the critical wave slope decreases.

The straight line in the right side, which is almost vertical, indicates the full loaded condition of "Nichibei Maru, No. 8", which shows the trend midway between the above two cases.

It may be noted from the foregoing that ships having very poor stability will be affected favourably by the bulwark, while in ships with sufficient stability bulwarks have adverse effect upon the stability due to containing of free water.

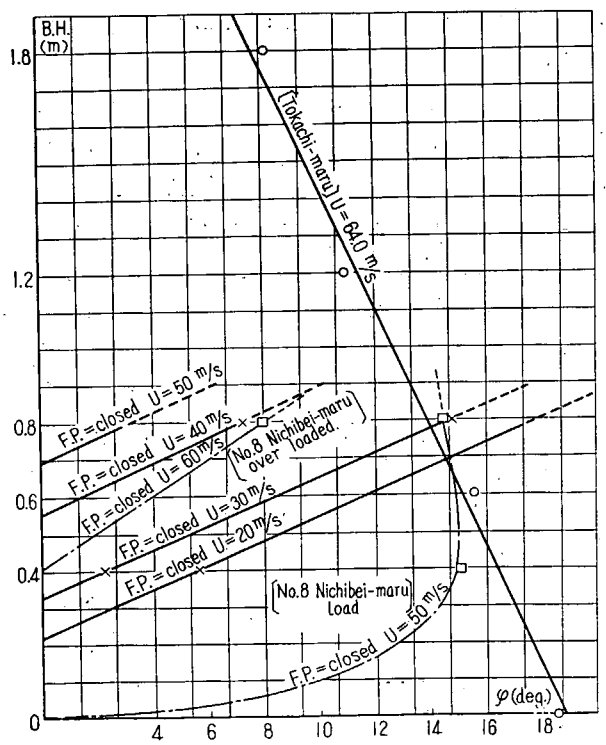

Fig. 5.10 Relation between the Critical for Capsizing and the Bulwark Height and the Wave Slope.

PART VI
Synthetic Observation on Stability of Ships

Chapter 1 Adequate Stability of Ships

1.1 Introduction.

It has been the practice to judge the stability of ships empirically on the basis of GM, OG, etc. According to the recent development of the theories in this field, however, there is an increasing tendency of judging the stability of ships on the basis of synthetic evaluation of respective elements affecting the stability expressed by righting arm curves (GZ-curves).

The elements composing GZ-curves comprise GM (tangent at 0°), maximum righting arm$=GZ_{\max}$, angle of heel corresponding to $GZ_{\max}$, range of stability$=\theta_R$, dynamical stability (area of GZ-curve), etc.

These elements govern respective responses of the ship. For instance, the safety of the ship against capsize and the comfortable feeling on board when the ship is rolling are often discussed. The former requests ample stability at large angle of heel, that is, sufficient maximum righting arm and range of stability, while the latter calls for small amount of GZ. These two requisites can not, in general, be satisfied at the same time. Primary importance should, of course, be attached to the first character, the safety of ships, and the second character, the comfortable feeling, should merely be considered as an incidental factor. In the design stage, accordingly, it is often requested to sacrifise the second character in order to ensure the first character. In certain cases, on the contrary, ships will be so designed as to avoid unnecessary increase of the safety of ships and to give much attention to the second character. In the design of ships, therefore, it is essential to make quantative evaluation of these conflicting factors and to give them reasonable balance according to the kind and intended purpose of the ship.

For this purpose, it is necessary, first of all, to establish a method to assess quantatively the effect of each element of stability upon the response of the ship. The important problem to be solved next is to determine their critical values. Thus the quantative analysis of the elements of stability will be feasible. This new method, that is, a method to evaluate critical values of stability elements corresponding to responses of the ship, has been established

by this Working Panel.

In the following, adequate stability of ships obtained by this method is described.

1.2 Criterion to the Capsize of Ships and External Forces.

As external forces affecting the stability of ships, the following factors may be considered.

(1) Wind
(2) Waves
(3) Steering
(4) Shift of persons on board
(5) Shipping of sea water
(6) Shift of weights aboard.
etc.

Of these factors, the wind and waves are considered predominent.

(1) Wind and waves.

A mechanism for capsizing a ship when she is rolling under fluctuating wind pressure has been developed by Watanabe, Kato, etc. According to this theory, the correlation between the critical wind pressure for capsizing the ship and the stability of ship is obtained based on the assumption that the ship, while rolling due to waves about an angle of heel caused by a steady wind pressure, is suddenly subjected to a gust when she is at the maximum angle of heel windward, and then she heels leeward due to this pressure and capsizes if the wind pressure is beyond the critical value.

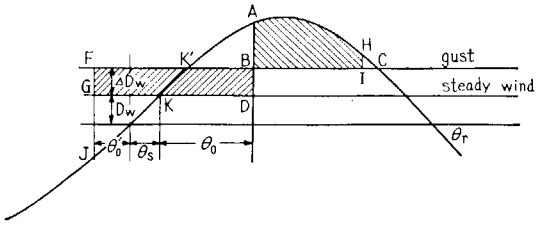

Fig. 6.1

The basic principal of this theory is explained in the following.

In Fig. 6.1 θ_s is the angle of heel due to steady wind, and θ_0 and θ_0' are rolling angles due to waves. Let us assume that, when the ship heels windward, the moment due to wind pressure changes from D_w (due to mean wind velocity)

to $D_w+\Delta D_w$ (due to gust). The ship then heels to the extent that the work done by the wind pressure $\Delta FGDB$ becomes equal to the work done by the righting moment $\Delta ABIH$. Accordingly, when $\Delta ABIH>\Delta FGDB$, it is considered that the ship can withstand this gust.

The above matter will also be expressed by $\Delta FJK'>\Delta ABC$, and this expression has been adopted by the Regulations for the Stability drawn up by the Ministry of Transportation mentioned later.

Watanabe, using the term of total dynamical stability Sd derived from the above relation, indicates that the ship would be safe, if:

$$C=\frac{Sd}{(D_w+\Delta D_w)(\theta_r+\theta_0')+D_w\theta_r+\frac{1}{2}\overline{GM}\theta_0}>1$$

(2) Steering

Outside heel of a ship due to centrifugal force caused by the turning will endanger the ship if GM is small. As a critical value of GM, the following formula was developed.

$$GM>\frac{K'Av^2(OG+d/2)}{V\tan\theta}$$

Where: θ=Certain critical value of heeling angle
K=Constant depending upon the ship's form
v=Progressive speed of the ship in turning
d=Drift
V=Volume of displacement
A=Rudder area

(3) Shipping of sea water and shift of weights aboard.

The safety of a ship against shipping of sea water, shift of weights aboard, etc. is dependent upon the capability of the ship to overcome these heeling moments and to turn to the upright position, and relates to $GZ_{\max}$.

On the other hand, the moment is considered to be proportional to the breadth of the ship, and therefore the following condition will be derived.

$$GZ_{\max}/B>k$$

(4) Shift of persons on board.

In ships where the weight of passenger has considerable portion as compared with the displacement, such as in sight-seeing boats, the movement of passengers on board will, in some cases, result in a large angle of heel enough to capsize the ship.

The effect of this movement is dependent upon the breadth of the ship B (the maximum athwartship distance of free passenger movement), the density of passengers (mean density before movement r and after movement r_0), etc. It is needless to mention that the greater the breadth of the ship and the density of passengers after movement to one side, the greater the effect.

In the foregoing, effects of four factors have been considered. The relation of these factors with the elements of ship's form will be summarized as follows, according to the aforementioned classification of each factor.

(1) Dynamical stability, projected lateral area of the ship above water line

(2) GM, OG

(3) GZ_{max}, bulwark height

(4) GM, freeboard

The Ministry of Transportation of the Japanese Government drew up the Regulations for Stability of Ships in 1957, taking account of the aforementioned factors, and have put them into effect. In these Regulations, GM, dynamical stability and GZ_{max} are specified by three regulations, A, B and C.

The outline of these regulations are described in the following.

1.3 Outline of the Regulations for Stability of Ships drawn up by the Ministry of Transportation.

The Regulations developed by the Ministry of Transportation consist of the following three regulations, namely:

(A) GM standard

(B) Dynamical stability standard

(C) GZ_{max} standard

Ships to which these Regulations applied are classified according to the following plying limits.

I. Smooth water

II. Coasting II

III. Coasting I

IV. Ocean going

The application of the regulations according to the classification of ships is specified as shown in the following table 6.1.

Regulation B specifies different wind velocities, according to the plying limit of the ship, which are shown in ( ).

(1) GM-Standard.

Table 6.1

Classification	Regulations to be applied		
	A	B	C
I. Smooth water	○	—	—
II. Coasting II	○	○ (15 m/sec)	○
III. Coasting I	○	○ (19 m/sec)	○
IV. Ocean going	○	○ (26 m/sec)	○

GM in the service condition of a ship is required to comply with the following formula.

$$GM \geqq \left[1.07AH + 0.134\sum\left(7-\frac{n}{a}\right)n\bar{B}\right]B/100fW \quad \text{(m)}$$

Where: A=Projected lateral ares of the ship above water line (m^2)

H=Vertical distance from the centre of gravity of the area A to the centre of gravity of the projected lateral area of the ship below water line (m)

n=Number of passengers in each accommodation space

a=Floor area of each accommodation space (m^2)

$\bar{B}$=Mean breadth of each accommodation space in which passengers are free to move (m)

B=Breadth of the ship (m)

f=Freeboard (m): where f exceeds $B/5.5$, it is taken as $B/5.5$

This standard specifies that, where a ship is subjected to steady wind of 15 m/sec from athwartship direction and where passengers move to ship's side, the ship will not heel beyond 80 per cent of the freeboard (where f exceeds $1/2\,B\tan 20°$, it is taken as $1/2\,B\tan 20°$).

(2) Dynamical Stability Standard.

In Fig. 6.2, which indicates the stability curve, draw moment lever D_w parallel to the base line, take rolling angle θ_0 to the windward (left side) from K, the intersection of D_w with the stability curve, and then draw moment lever due to gust, 1.5 D_w, parallel to the base line. It is then required that the ship complies with the following formula in service condition.

$$\text{Area } AK'C > \text{Area } K'FG'$$

Where: $D_w = kAH/W$

A, H, W=As specified in the preceding paragraph.

k=0.0514 Ocean going

$=0.0274$ Coasting I

$=0.0171$ Coasting II

$\theta_0 = \sqrt{138}\,rs/N$

$$r = 0.73 + 0.60\frac{OG}{d}$$

OG=Vertical distance to the centre of gravity of the ship above water line (m). (It is taken negative, where the centre of gravity is below the water line.)

d=Draught (m)

$s = p - qT$: Where s exceeds 0.10, it is taken as 0.10, and where less than 0.035, it is taken as 0.035.

$p=0.151$ $q=0.0072$ Ocean going

$=0.153$ $=0.0100$ Coasting I

$=0.135$ $=0.0130$ Coasting II

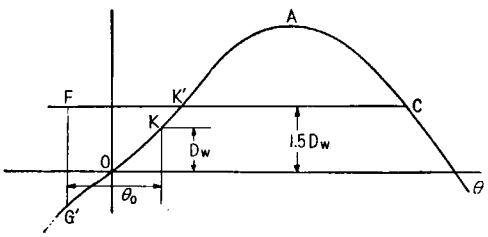

Fig. 6.2

This standard specifies that a ship will be safe under the condition that, when rolling with the amplitude equal to 70% of the synchronous rolling angle in regular seas, about an angle of heel due to steady wind of the velocity as indicated in the aforementioned Table, the ship is subjected to a gust (50% in excess of the steady wind pressure) when she is at the maximum angle of roll windward.

(3) GZ_m-Standard.

GZ_m of a ship in service condition is required to comply with either of the following formulae.

$$GZ_m \geqq 0.0215B$$

or $\geqq 0.275$ (m)

Where: B=Breadth of the ship (m)

This standard specifies that the ship will be safe against the shift of weights aboard, shipping of sea water, steering, etc.

Chapter 2 Some Information regarding Stability which is considered Useful in the Design of Ships

2.1 Approximate Formula to Assess the Stability.

In order to examine the stability of a ship in the stage of basic design, it is necessary to develop an approximate method available in that stage.

The method to obtain the approximate stability curve by presuming the position of the centre of buoyancy at the heeling angle of 90° corresponding to the centre of buoyancy in upright position has been studied by Imai, Watanabe, etc. In this investigation, a more accurate method has been developed based on the above method.

In Fig. 6.3 a) and b) are the coordinates indicating the position of the centre of gravity at the heeling angle of 90°, when the centre of gravity in upright position is taken as the origin.

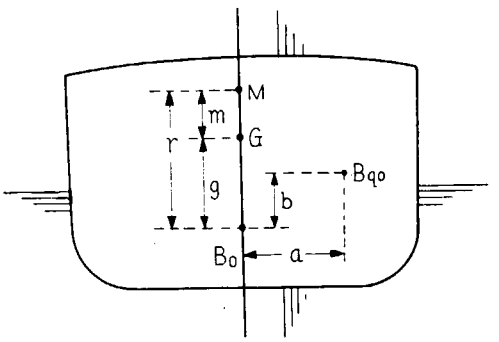

Fig. 6.3

Let $r=B_0M$ and $m=GM$, then GZ is expressed by

$$GZ=F_1a+F_2b+F_3r+F_4m$$

where F_1, F_2, F_3 and F_4 are the coefficients given below (Table 6.2).

Table 6.2

	15°	30°	45°	60°	75°	90°
F_1	—	0.5458	1.2221	1.2835	0.7174	0
F_2	—	−0.2190	−0.4021	−0.1967	0.3462	1
F_3	0.0093	−0.3148	−0.8248	−1.0980	−1.0877	−1
F_4	0.2588	0.5000	0.7071	0.8660	0.9659	1

The values of a and b are as shown in Figs. 6.4 and 6.5, drawn with the parameters of Cb and Cw; that is, in Fig. 6.11, b/d is drawn on the basis of $1+F/d$ with the variation of Cb/Cw from 0.60 to 0.95, and in Fig. 6.5, a/B is drawn on the basis of $1+f/d$ when Cb/Cw is 0.85, where d=draught, f=freeboard, F=effective freeboard and B=breadth.

2.2 Simple Method to Examine the Safety Criteria in a Very Early Stage of Design.

Investigations into the safety criteria as to small ships less than 3,000 gross tons have indicated that satisfaction and dissatisfaction of the safety

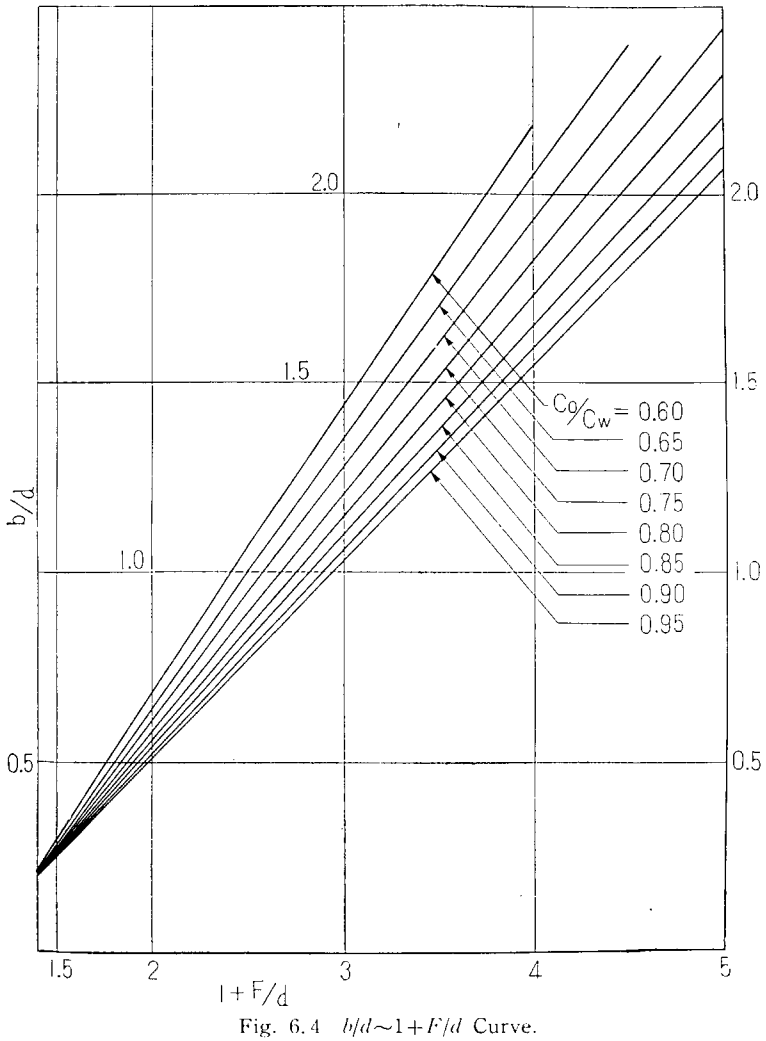

Fig. 6.4 $b/d \sim 1+F/d$ Curve.

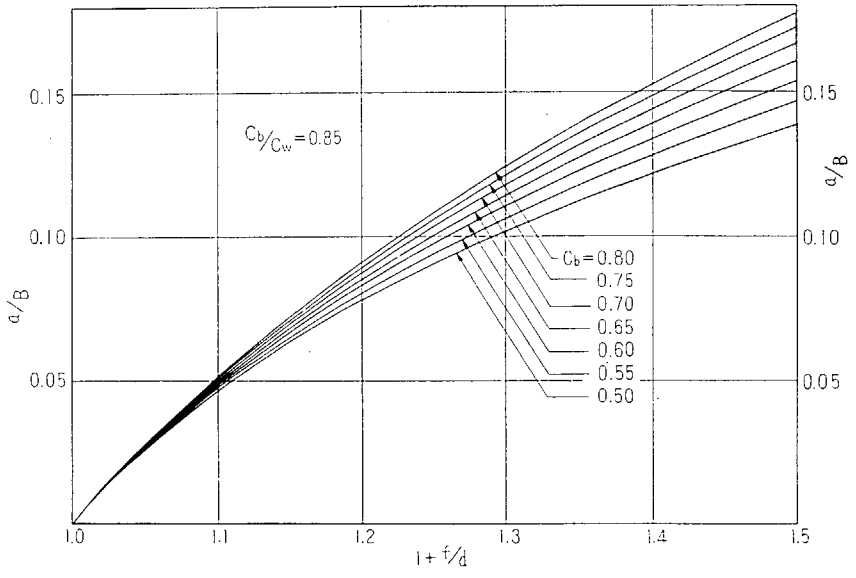

Fig. 6.5

OCEAN-GOING

No.	3	5	31	47
C_0	△	×	×	○
C_1	△	○	○	×
C_2	△	○	△	○
C 丙	○			
	○			

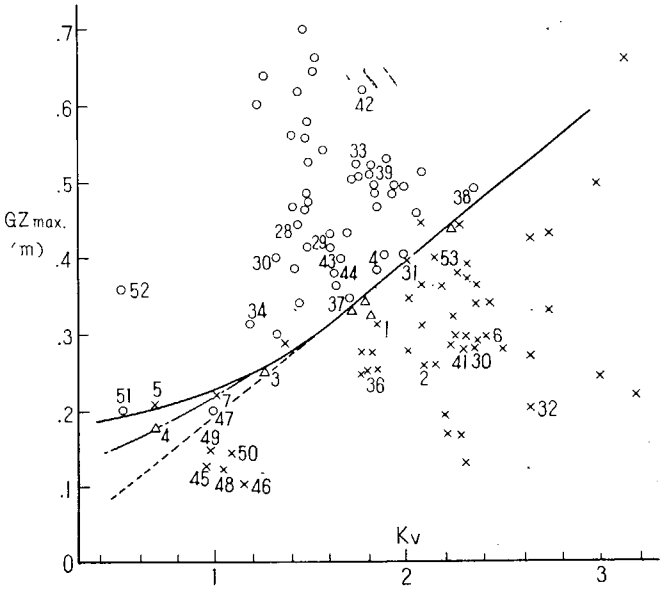

Fig. 6.6

criteria can be discriminated by a demarcation curve, when GZ_{max} are plotted against K_v=volume above water line / volume under water line.

In computing the safety criteria, Watanabe and Kato's method was applied in addition to the standard of the Ministry of Transportation, and these results have indicated that, except in very seldom occasions, the criteria are discriminated by the same demarcation curve, as illustrated in Figs. 6.6 and 6.7.

In Fig. 6.6, GZ_{max} are plotted against Kw, in which points marked × represent that the safety criterion has been proved dissatisfactory. From this figure, limits of required GZ_{max} for a given Kw can be obtained.

In Fig. 6.7, GM/B are plotted against Kw so that whether or not the safety criterion is satisfactory may be checked in such a stage that GZ_{max} is yet unknown and only GM is known. The judgement of the safety criterion may also be available from this figure with satisfactory accuracy.

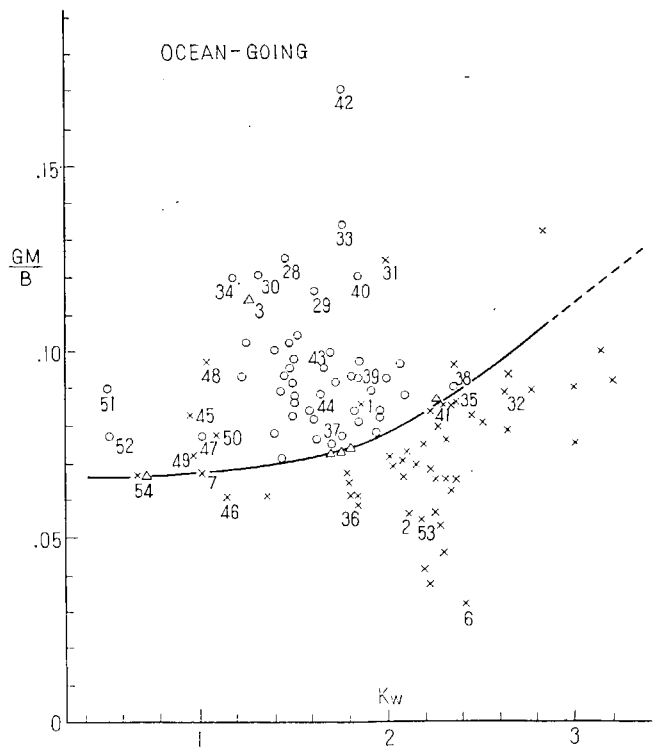

Fig. 6.7

2.3 Determination of the Upper Limits of *GM* from the View Point of Acceleration.

Whilst it will be needless to emphasise the necessity of keeping *GM* above certain standard, the excessive *GM* will cause various troubles. In this investigation, the acceleration was taken up as a factor which should give the greatest adverse effect upon the comfortable feeling of persons on board, tumbling down of cargoes, etc., and an attempt was made to place the upper limit of *GM* with a view to keeping the acceleration under certain standard.

Fig. 6.8 illustrates the limits of acceleration as to machineries or vehecles with very short period of vibration as well as elevators which represent machines having long period of oscillation. From this figure, the limit of acceleration for ships having rolling period of 5 to 20 seconds can be presumed.

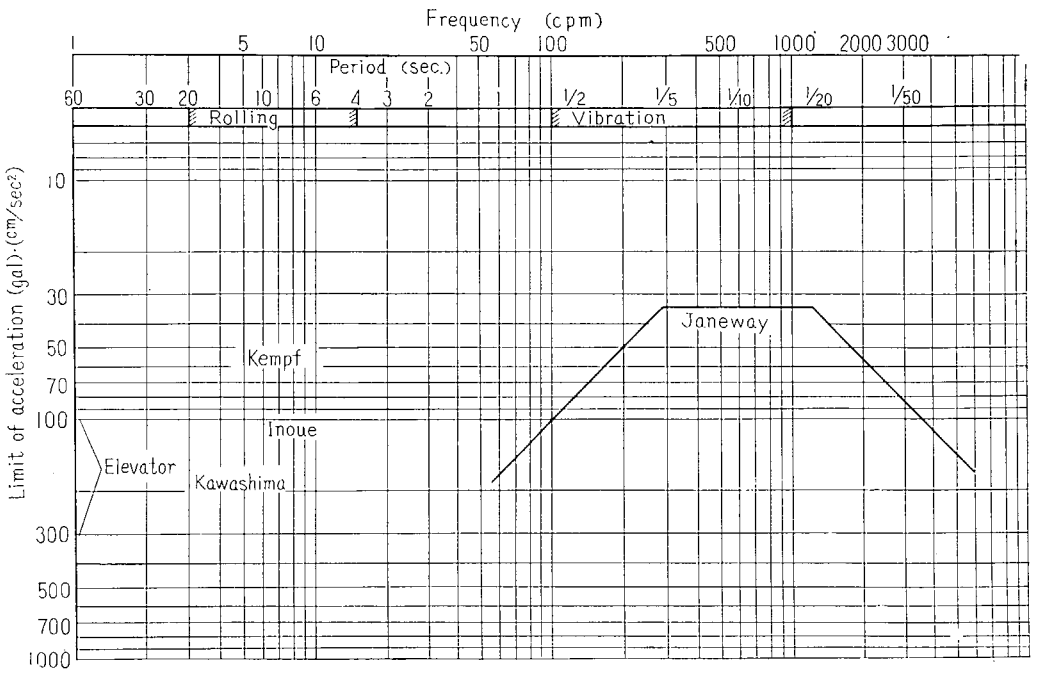

Fig. 6.8 Limit Value of Acceleration.

Fig. 6.9 indicates the correlation between Kempf's Rollzahl and the acceleration at $B/4$ from the centre line of the ship obtained from the data of service experience. The acceleration can be obtained from the period of rolling actually measured, if the measurement is available, or from this figure, if not available.

To determine the upper limit of acceleration from the view point of comfortable feeling of persons on board is after all to determine the upper limit of GM, which implies that it is not preferable to let the ship have unnecessarily large GM from the safety view point only.

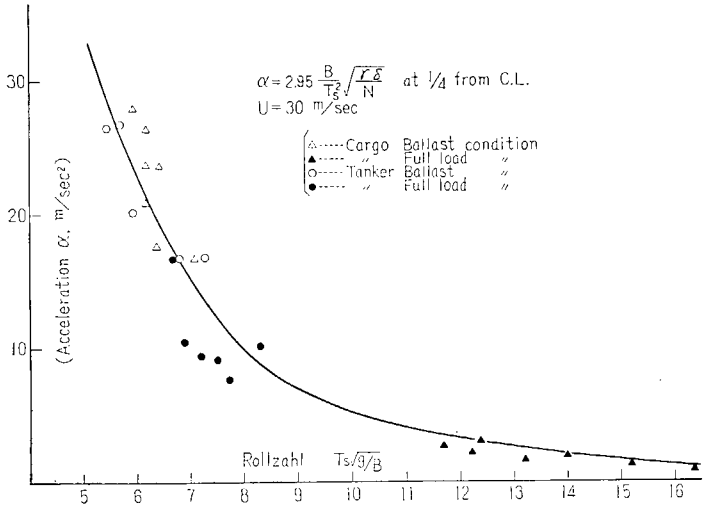

Fig. 6.9 Acceleration due to Rolling.

昭和34年3月20日　印刷
昭和34年3月25日　発行

日本造船研究協会報告 第25号

発行人　出　淵　巽

発行所　社団法人日本造船研究協会
東京都中央区京橋1ノ2
セントラルビル
電話（28）1409

印刷所　松本印刷所
電話（34）4853